Role of Epoxyeicosanoids in Protecting Mitochondria during Cellular Stress

by

Haitham El-Sayed El-Sikhry

A thesis submitted in partial fulfillment of the requirements for the degree of

Doctor of Philosophy

in

Pharmaceutical Sciences

Faculty of Pharmacy and Pharmaceutical Sciences
University of Alberta

ABSTRACT

Mitochondria are at the center of cardiac health and disease. These vital organelles provide most of the energy to the contractile apparatus and play a strategic role in cardiomyocyte survival during cellular stress. Cardiovascular diseases and many aging related diseases are often associated with a decline in mitochondrial function. Recent studies suggested that epoxyeicosanoids protect cardiac mitochondria against ischemia and reperfusion-induced damage. Although epoxyeicosatrienoic acids (EETs) have acknowledged cytoprotective and anti-apoptotic properties in several tissues, little is known about their mitochondrial protective effects. Studies presented in this thesis investigated the mechanisms by which EETs influence mitochondrial function and dynamics during different types of cellular stress. Both natural EETs and their synthetic mimetics have been used to examine their effect on mitochondria. Several models of cellular stress, including serum starvation and photodynamic oxidative stress, have been applied to study mitochondrial responses. Live cell microscopy has been utilized to monitor changes in mitochondrial membrane potential and mitochondrial morphological dynamics. Mitochondrial energetic functions have been assessed with respirometry techniques as well as measurement of catalytic activity of key mitochondrial enzymes. DNA-binding experiments were used to assess mitochondrial biogenesis signaling and immunoblotting methods were used to assess expression levels of mitochondrial proteins. Negative control

experiments were conducted using the putative EET receptor antagonist 14, 15-EEZE to confirm EET-mediated effects. We found that EETs delayed the collapse of mitochondrial membrane potential and attenuated their fragmentation following acute photodynamic stress. Prolonged serum starvation induced a sustained mitochondrial hyperfusion and a relative increase in mitochondrial protein expression but with a progressive decline in mitochondrial energetic function. EET-treatment induced preservation of mitochondrial function against starvation-induced dysfunction. This was associated with balanced mitochondrial morphological dynamics, enhanced OPA1-dependent stress response, and stimulated mitochondrial biogenesis. Together, studies presented here support a mitochondrial protective effect of EET signaling and provide insight into the strategic role of mitochondria during acute and chronic cellular stress. We discuss the molecular mechanisms that promote mitochondrial quality which can offer a promising therapeutic approach to improve organ function in cardiovascular diseases as well as several other age-related diseases.

PREFACE

This thesis is an original work by Haitham El-Sikhry. All data were collected and analyzed by Haitham unless otherwise indicated.

A version of chapter II has been published: El-Sikhry, H.E., Miller, G.G., Madiyalakan, M.R. & Seubert, J.M. Sonodynamic and photodynamic mechanisms of action of the novel hypocrellin sonosensitizer, SL017: mitochondrial cell death is attenuated by 11, 12-epoxyeicosatrienoic acid. *Invest New Drugs* **29**, 1328-1336 (2011). Dr. Miller G.G. analyzed cellular uptake of the photosensitizer SL017, while Madiyalakan, M.R. provided the chemicals and the cell lines for the study.

A version of chapter IV has been submitted for publication in the Public Library of Science One Journal: El-Sikhry, H.E., Alsaleh, N., Dakarapu, R., Falck J.R., & Seubert, J.M. Novel Roles of Epoxyeicosanoids in Regulating Cardiac Mitochondria. *PLoS One*. Alsaleh, N. provided help with immunodetection of the mitochondrial dynamics proteins. Dakarapu, R. and Dr. Falck J.R. provided the dual EET mimetic UA-8. Dr. Victor Samokhvalov helped with conducting the following experiments: mitochondrial respiration, ADP/ATP analysis, enzymatic activity of aconitase and SIRT1, and DNA binding experiments.

"Whoever follows a path to seek knowledge therein,
Allah will make easy for him a path to Paradise"

Prophet Muhammad (peace be upon him)

ACKNOWLEDGEMENT

I would like to thank my supervisor, Dr. John Seubert for his guidance, patience and support through my program. I learned a lot from his knowledge and scientific judgement, which helped me design my studies and present my work. I am thankful and grateful for his great mentorship.

My next appreciation goes to my supervisory committee members, Dr. Thomas Simmen and Dr. Paul Jurasz for their kindness, guidance, support, and valuable suggestions. I also thank Dr. Ayman El-Kadi for all his advice and support.

My gratitude also goes to all members in Dr. Seubert's lab for their help during my studies. I would like to thank Dr. Ketul Chaudhary and Dr. Sri Nagarjun Batchu for their valuable assistance while starting my program. My appreciation goes to Dr. Victor Samokhvalov and Nasser Alsaleh for their help conducting the starvation studies. I also thank Mohamed Abukhashim, Rawabi Qadhi, Maria Akhnokh, Igor Zlobine and Lokchart Jamieson for their support and nice compuny through my journey in graduate studies.

I am deeply thankful to my parents, Dr. Sayed El-Sikhry and Mrs. Amina El-Hamahmy for their ongoing prayers, support and encouragement. Their care and passion were fundamental in making me the kind of person I am. There is nothing I can say or do to adequately acknowledge your role my dear parents.

My deepest gratitude goes to my life companion, my beloved wife Yasmeen for always being by my side all through my study years. This success is a coronation for her dedication and hard work supporting my cause and taking care of our family.

Finally, all the praises and thanks are to Allah, the Lord of all that exists. I pray that my efforts and time working on my PhD were in what pleases his Almighty

TABLE OF CONTENTS

LIST OF TABLES

LIST OF FIGURES

LIST OF ABBREVIATIONS

11,12-EET	11(12)-epoxy-5Z,8Z,14Z-eicosatrienoic acid
14,15-EET	14(15)-epoxy-5Z,8Z,11Z-eicosatrienoic acid
14,15-EEZE	14,15-epoxyeicosa-5(Z)-enoic acid
AA	Arachidonic acid
Akt	Protein Kinase B
AMPK	5' AMP-activated protein kinase
ATP	Adenosine triphospate
BAD	Bcl-2-associated death promoter
Bak	Bcl-2 homologous antagonist/killer
Bax	Bcl-2-associated X protein
Bcl-2	B-cell lymphoma 2
Bcl-xL	B-cell lymphoma-extra large
BID	BH3 interacting-domain death agonist
Bim	Bcl-2-like protein 11
CaMK1α	Ca^{2+}/calmodulin-dependent protein kinase 1α
COX	Cyclooxygenases
COX IV	Cytochrome c oxidase subunit 4
CREB	Camp-response element binding protein
CS	Citrate synthase
CYP	Cytochrome P450
cyt.c	Cytochrome c

DCF	CM-H2-DCFDA (5-(and-6)-chloromethyl-2',7'-dichlorodihydrofluorescein diacetate acetyl ester)
DHET	Dihydroxyeicosatrienoic acid
DMSO	Dimethyl sulphoxide
DNA	Deoxyribonucleic acid
DRP1	Dynamin related protein 1
DTT	Dithiothreitol
EET	Epoxyeicosatrienoic acid
EM	Electron microscopy
ER	Endoplasmic reticulum
ETC	Electron transport chain
FBS	Fetal bovine serum
Fis1	Mitochondrial fission protein 1
GAPDH	Glyceraldehyde 3-phosphate dehydrogenase
GTP	Guanosine triphosphate
GTPase	Guanosine triphosphate phosphohydrolase
HB	Hypocrellin-B
HBSS	Hanks' balanced salts solution
HETE	Hydroxyeicosatrienoic acids
HR	Hypoxia-reoxygenation
HRP	Horse radish peroxidase
IHD	Ischemic heart disease
IMS	Intermembrane space

IPC	Ischemic preconditioning
IR	Ischemia-reperfusion
K_{ATP}	ATP-sensitive potassium channel
kDa	Kilodalton
L-OPA1	Long isoforms of OPA1
LOX	Lipoxygenases
MAPK	Mitogen-activated protein kinases
Mff	Mitochondrial fission factor
Mfn	Mitofusin
MI	Myocardial ischemic
MiD49	Mitochondrial dynamics proteins of 49 kDa
MiD51	Mitochondrial dynamics proteins of 51 kDa
MIM	Mitochondrial inner membrane
MitoTG	Mitotracker Green FM
MOM	Mitochondrial outer membrane
MOMP	Mitochondrial outer membrane permeabilization
mPTP	Mitochondrial permeability transition pore
mRNA	Messenger RNA
mtDNA	Mitochondrial DNA
mtRNA	Mitochondrial RNA
MTT	Methylthiazolyldiphenyl-tetrazolium bromide
NF-κB	Nuclear factor kappa-light-chain-enhancer of activated B cells

NRF	Nuclear respiratory factor
OPA1	Optic atrophy 1
OxPhos	Oxidative phosphorylation
PD	Photodynamic
PDT	Photodynamic therapy
PGC1	Peroxisome proliferator-activated receptor gamma coactivator 1
PI3K	Phosphoinositide 3-kinase
PKA	Protein kinase a
PKC	Protein kinase c
PKCδ	Protein Kinase C delta
PPAR	Peroxisome proliferator-activated receptor
RCR	Respiratory control ratio
ROS	Reactive oxygen species
S616	Serine 616
S637	Serine 637
SDH	Succinate dehydrogenase
SDS	Sodium dodecyl sulfate
SDS-PAGE	Sodium dodecyl sulfate-polyacrylamide gel electrophoresis
SDT	Sonodynamic therapy
sEH	Soluble epoxide hydrolase
SEM	Standard error of mean

SIMH	Stress induced mitochondrial hyperfusion
SIRT1	NAD-dependent deacetylase sirtuin-1
SIRT3	NAD-dependent deacetylase sirtuin-3
SL017	(2-(N,N-dimethylaminopropyl)amino-15-acetyl-3,10-dihydroxy-6,7,11-trimethoxy-14-methyl-15-H-cyclohepta(ghi)perylene-4,9-dione)
S-OPA1	Short isoforms of OPA1
TCA	Tricarboxylic acid cycle
TMB	3, 3', 5, 5'-Tetramethylbenzidine
TMRE	Tetramethylrhodamine ethyl ester
TNF-α	Tumour necrosis factor alpha
TTC	2, 3, 5-Triphenyltetrazolium chloride
UA-8	13-(3-propylureido)tridec-8-enoic acid
VCAM-1	Vascular cell adhesion molecule
VDAC	Voltage-dependent anion channel
WI-38	Human lung fibroblast cells
WT	Wild type
ΔΨm	Mitochondrial membrane potential

CHAPTER I

Introduction

1.1. General Background

Despite decades of scientific research, cardiovascular diseases remain a major challenge to human health. It has been suggested that our model of understanding of the progression of the disease might be lacking some essential elements, making us unable to aim therapeutic interventions for the right targets. I believe mitochondrial research is the way to fill this gap. In this thesis, I investigated mitochondria and their dynamics as key elements of cell survival and death. Results presented here shed some light on critical roles of mitochondria during cellular stress conditions and improved our understating of the mechanism of action of the promising cardioprotective epoxyeicosatrienoic acids (EETs)

EETs are CYP450-depended metabolites of arachidonic acid (AA)[1]. Free AA can be released from the cell membrane as a response to cellular stress or hormonal signals[2]. Cytochrome P450 epoxygenases metabolize AA into the lipid mediators epoxyeicosatrienoic acids[3]. EETs act as autocrine and paracrine signaling molecules regulating key cellular processes such as inflammation, proliferation and apoptosis[4]. EETs are abundant in the heart playing robust cardioprotective roles[5]. However, the molecular mechanism of action of EETs remains unclear.

Mitochondria are key organelles in the heart cell. They provide almost all the energy required for the contractile apparatus, regulate calcium signaling, control reactive oxygen species (ROS), and participate in making strategic death or survival decisions[6]. The quality and efficiency of

mitochondria is critical to cardiac health, both at the cellular and at the organ level[7]. Active mitochondrial fusion and fission dynamics are required for effective maintenance of mitochondrial quality, which is essential to the long-living and energy demanding cardiomyocyte[8].

Interestingly, there is little work relating the cardioprotective role of EETs to mitochondria. Mitochondria are damaged after ischemia-reperfusion (IR) events and progress to be defective and fragmented in heart failure[9]. EET treatment limited the IR-induced mitochondrial damage[10] and preserved mitochondrial functions against other forms of cellular stress[11]. Studies in this thesis looked at the role of EETs in protecting mitochondrial functions and dynamics and investigated the molecular mechanisms involved in this effect. In the following introduction, I will start with a brief background about EETs and their cardioprotective properties. I will then discuss the current understanding of mitochondrial dynamics processes and their role in maintaining mitochondrial health. Finally, I will summarize the rational and the objectives of my studies introducing the reader to the latter chapters of this thesis.

1.2. EPOXYEICOSATRIENOIC ACIDS

Epoxyeicosatrienoic acids (EETs) are signaling molecules that belong to the eicosanoid family of lipid mediators. The omega-6 polyunsaturated fatty acid AA serves as the parent precursor for the biosynthesis of EETs as well as other eicosanoids[1]. Three metabolic pathways are known to metabolize AA into three subclasses of eicosanoids[12]. The first is the cyclooxygenase (COX) pathway that produces prostaglandins and thromboxane which are important mediators in controlling the vascular tone, platelet aggregation, pain reception and several other physiological processes[13]. The second is the lipoxygenase (LOX) pathway that produces leukotrienes and lipoxins which act as regulatory signals in the inflammation and immune response[14]. The third is the cytochrome P450 pathway that produces hydroxyeicosatetrienoic acids and epoxyeicosatrienoic acids (EETs)[3]. Similar to other eicosanoids, EETs possess hormone-like functions that convey signals to the same cell that produced them (autocrine signaling) or the neighboring cells (paracrine signaling)[4, 15, 16]. However, unlike other eicosanoids, the biological roles and the mechanism of signal transduction of EETs is not fully characterized.

The biosynthesis of EETs involves the addition of an epoxy group on one of the double bonds of the AA. AA, which is a 20:4(N-6) fatty acid also known as eicosatetraenoic acid, is a 20-carbon chain fatty acid containing 4 double bonds, as the name indicates. Oxidation of one of the double bonds by cytochrome P450 epoxygenases produces epoxyeicosatrienoic

acid (EET). According to which double bond of AA molecule is being oxidized, four regioisomers of EETs can be produced 5,6-, 8,9-, 11,12-, and 14,15-EET[15]. Several CYP epoxygenases have been identified to catalyze this reaction. Among them, CYP2J and CYP2C subfamilies are the major contributors to EET synthesis in the cardiovascular system producing mainly 11,12- and 14,15-EET[17-19]

Elimination of EETs occurs mainly by hydrolysis of the epoxy group into the dihydroxy derivative. This is catalyzed by the soluble epoxide hydrolase (sHE) to produce the corresponding dihydroxyeicosatrienoic acid (DHET)[20]. EETs can also be incorporated into membrane phospholipids, undergo β-oxidation, or glutathione conjugation. However, hydrolysis by sEH remains the main metabolic pathway for EETs[19, 21].

Experimentally, cellular levels of EETs can be increased by improving their synthesis as in genetically modified animal models that overexpress CYP2J2 enzyme[22, 23], or by the external addition of EETs. Also, blocking the sEH-dependent removal of EETs increases EET levels as has been reported in animals deficient in sEH[24-26]. Further, pharmacological inhibition of sEH provides a convenient approach to augment EET signaling in various experimental and clinical settings[27-29].

1.3. BIOLOGICAL ROLES OF EET

1.3.1. EET roles in the cardiovascular system

Perhaps the most studied function of the EETs is their role in regulating vascular tone. EETs have been identified as an endothelial-derived hyperpolarizing factor (EDHF) causing potent relaxation of vascular smooth muscles[16]. Addition of any of the EET regioisomers to coronary artery induced vasodilatation[16, 30] as did sEH inhibitors[31, 32]. It has been suggested that the hypertensive effect of angiotensin II is actually mediated by sEH-dependent degradation of EETs[31, 33]. In fact, a number of sEH inhibitors have been under intensive studies as a promising new class of antihypertensive drugs[34, 35].

The vasodilatation effect of EET is mediated through the activation of outward potassium channels, specifically the large-conductance Ca^2-activated K channels (BK_{Ca}) and ATP sensitive K channels (K_{ATP}), resulting in increased K efflux from the smooth muscle cell, hyperpolarization and relaxation of vascular smooth muscles[36-38]. However, the signaling mechanism by which EETs activate potassium channels is less clear[19]. This was partially due to the limited information about the direct binding target of EETs that would initiate downstream signaling cascade leading to the activation of potassium channels. The majority of the evidence support the involvement of guanine nucleotide binding protein (G protein) receptor signaling. EETs have been demonstrated to induce $G\alpha_s$ activity, activate adenyl cyclase, increase cAMP levels and activate protein kinase A (PKA)

which phosphorylates and activates potassium channels[38-42], all support the existence of an EET receptor coupled to G protein. However, such a receptor have not been characterized and remains hypothetical[19], although there has been success in designing EET surrogate molecules that antagonize their effect on this putative receptor[43].

In addition to the PKA-dependent activation of K_{ATP} channels, Lu *et al.* have demonstrated that EETs directly bind and activate cardiac $K_{(ATP)}$ channels identifying the binding site in the channel molecule[44, 45]. This added an important direct target for EET signaling in addition to the possible G-protein coupled receptor (GPCR).

Apart from their vasodilatation effect, EETs also promote angiogenesis. EETs induce proliferation of vascular endothelial cells in vitro[46-48] and promote capillary density in skeletal muscles in vivo[49, 50]. Several signaling pathways have been reported to mediate this function including the phosphatidylinositol 3-kinase (PI3K)/Akt pathway[51, 52], the mitogen-activated protein kinase (MAPK) pathway[49, 53] and the aforementioned cAMP/PKA pathway[54, 55]. All are known to activate transcription factors like CREB and FOXO and are typically activated downstream to cell membrane receptors which also supports the theory of a specific EET receptor. Importantly, this added another level of EET activity regulating gene expression and cell proliferation.

Further, EETs have strong anti-inflammatory properties. This has been demonstrated in endothelial cells[56, 57] as well as various other

tissues[58-60]. Inflammation is a major factor in vascular function and cardiovascular diseases, which indicates an additional significance of EETs in vascular homeostasis. The mechanism of action of EET anti-inflammatory function involves inhibition of nuclear factor kappa B (NFκB)[56, 61]. Importantly, EETs and their metabolites DHETs have been identified as potent agonists of the peroxisome proliferator-activated nuclear receptors (PPARs)[62-64] which regulate the expression of several important cellular pathways including inflammation. PPARs are significant direct binding targets for EETs in addition to K_{ATP} channels and the putative EET receptor, which adds to the complexity of EET signaling mechanisms

Furthermore, EETs also significantly participate in regulation of hemostasis. EETs inhibit platelet aggregation and adhesion to vascular walls by a mechanism involving activation of the platelet large conductance K_{Ca} channels, hyperpolarization of platelet membrane and attenuation of their activation[65-67]. Also, EETs induce the release of fibrinolytic enzymes from endothelial cells which appears to be mediated by cAMP/PKA pathway[39]. Thus, EET signaling may attenuate blood clotting and promote fibrinolysis.

There is no doubt that EETs play a significant role in the regulation of the cardiovascular system. They are produced in cardiomyocytes, endothelial cells, vascular smooth muscles, as well as circulating white blood cells, red blood cells and platelets[19]. In fact, EETs increase blood flow in the coronary artery and improve cardiac function at normal conditions[68,

[69]. However, there is another aspect of EETs effects in the cardiovascular system that is not less interesting than the previously mentioned functions. It is their cardioprotective effect during cardiac pathologies, which I will discuss in section 1.4 below.

1.3.2. EETs anti-apoptotic effect and cancer

Apart from EET functions in the cardiovascular system, EETs demonstrated significant anti-apoptotic and cytoprotective effects in a wider range of tissues. For example, inhibition of sEH in brain and neuronal tissues provided protection against ischemic injury[25, 70, 71]. Also, overexpression of CYP450 epoxygenases attenuated TNF-induced cell death in endothelial cells[72]. Similar cytoprotective role has been reported in kidney, lung, as well as cardiac tissues[59, 73-76]. This anti-apoptotic effect was suggested to be mainly mediated by activation of the survival PI3K/Akt pathway, but also required MAPK and K_{ATP} channels activity[72, 75, 77]. Furthermore, EETs induced several changes in gene expression that promote the cellular resistance against apoptosis. This includes upregulation of PI3K expression[72] and anti-apoptotic proteins of the Bcl2 family[70, 76], as well as downregulation of pro-apoptotic proteins Bax, Bad and TNF receptors[70, 76]. This indicates that EET signaling is protective against apoptosis, both acutely and progressively.

The cytoprotective role of EETs opened the gate for a new potential for their therapeutic value. They are proven to be beneficial in several human diseases that are marked by loss of organ function due to cell death

in post-mitotic tissues (more about this in section 1.4). In contrast, cell death is the precious target in cancer treatment. The cytoprotective effect of EETs can increase the chances of cancer cells to survive cytotoxic effect of antineoplastic drugs, especially when combined with EET-mediated anti-inflammatory, proliferative and angiogenic properties. Indeed, addition of exogenous EETs or upregulation of CYP450 epoxygenases significantly enhanced proliferation of cancer cells[78]. In addition, EETs evidently induced angiogenesis in cancer tumors[79]. Other evidence suggested that EET induce cancer cell motility and metastasis (the spread of cancer cells into other tissues) as well[79-81]. In fact, CYP450 epoxygenases were found highly expressed in human cancer tissues but not in the adjacent normal tissues[82-84] indicating that EETs are actually employed by cancer cells to promote their growth and survival. Therefore, inhibition of EETs' production or stimulation of their removal offer promising therapeutic targets for anticancer therapy[85-87]

Although most reports suggested that EET only support already established malignancies rather than initiating new ones, the pro-cancer properties of EETs warrant a careful design for any proposed therapeutic use of them. This might be achieved by targeted drug delivery approaches, or by using organ-specific pharmacological agents. Importantly, the role of EETs in the resistance of cancer cells to cytotoxic treatments should also be accounted for[88, 89].

1.4. EET-MEDIATED CARDIOPROTECTION

The first indication that EETs might be involved in the protection against cardiovascular disease came from epidemiological studies that looked at the correlation between genetic variations in CYP450 epoxygenases and the cardiovascular health of their carriers. A single nucleotide polymorphism (SNP) in the human cardiac epoxygenase CYP2J2 gene was associated with a significant increase in the risk of developing coronary heart disease[90]. The same SNP was reported to be significantly more frequent in myocardial infarction patients[91]. Several other studies reported an association between polymorphisms in CYP450 epoxygenases and hypertension[92, 93]. These observations suggested a cardioprotective role of CYP450 epoxygenases and their products EETs.

This cardioprotective role of EETs seemed attributed to their general anti-inflammatory and fibrinolytic activity and their vasodilatory effect on coronary arteries. However, a key study by Seubert et al[94] provided the first evidence for EET-mediated cardiopotection independent from their effect on the vasculature. In this study, a mouse genetic model was generated which overexpressed the human CYP2J2 enzyme specifically in the cardiomyocytes. These transgenic mice were resistant to cardiac ischemic injury, which was evident by the decrease in the size of the infarct tissues following ex-vivo no-flow ischemia and reperfusion[94]. This was combined with a significant improvement in the post ischemic contractile function of the heart as reported by the left ventricular developed pressure[94].

Interestingly, another mouse model lacking the sEH gene demonstrated similar cardiopotection[95]. Further, exogenous EETs[94, 96], or its mimetic UA-8[97], as well as pharmacological inhibition of sEH[98] reproduced this cardiopotection against ischemia-reperfusion injury, while inhibition of CYP450 epoxygenases[94] or antagonizing the EET putative receptor with 14,15-EEZE[95, 98, 99] blocked this effect. Collectively, these studies confirmed the cardioprotective role of EETs against ischemia-reperfusion injury, which correlated with the reported increased risk of ischemic heart disease in humans deficient in EET biosynthesis[90, 91].

In addition to protection against the acute damage of ischemia and reperfusion, EETs attenuated cardiac remodeling following myocardial infarction[32, 100, 101] and prevented cardiac hypertrophy induced by pressure overload[102] or angiotensin II[103]. These are major contributors in clinical cardiac hypertrophy and heart failure. In fact, induction of sEH (the main removal pathway for EETs) mediates hypertensive effect of angiotensin II[27, 31] as well as its role in cardiac hypertrophy[103]. Knocking down the sEH gene protected from pressure overload-induced heart failure and cardiac arrhythmias in mouse models[104]. Interestingly, pharmacological inhibition of sEH improved cardiac function even when administered one week after the myocardial infarction event[105], and was able to reverse a pre-established cardiac hypertrophy[102]. Collectively, there is strong evidence supporting the role of sEH in the development of hypertrophy and heart failure, where preserving EETs with sEH inhibitors represents a promising therapeutic

approach[32, 34]. Thus the cardioprotective role of EETs is not restricted to the anti-apoptotic effect towards acute stress, but also against chronic cardiac stress leading to cardiac hypertrophy and heart failure.

Moreover, EETs showed cardioprotective effect against doxorubicin-induced cardiotoxicity. My colleagues and I reported that mice overexpressing cardiac CYP2J2 exhibited preserved cardiac function compared to wild type mice following doxorubicin treatment[74]. As well, exogenous EETs attenuated apoptotic caspase activation in cardiomyobalsts treated with doxorubicin[74].

Several studies investigated the mechanism of EET cardiopotection. Initial evidence suggested a role of K_{ATP} channels and p42/p44 MAPK pathway in the EET-dependent improvement in post-ischemic cardiac function[94]. Later studies also pointed out the involvement of PI3K/Akt prosurvival pathway as inhibiting PI3K blunted the EET-cardioprotective effects[95, 106]. Another study from our laboratory suggested that EETs actually induce the cardiac expression of B-type natriuretic peptide (BNP) which then mediates cardioprotection[107]. Inhibiting BNP effect by natriuretic peptide receptor antagonists also inhibited the protective effect of EETs against ischemia and reperfusion injury in sEH null mice[107]. Although the previously mentioned pathways are known effectors in EET signaling, understanding how these multiple pathways interact together is elusive, and it remains unclear why inhibiting one pathway is enough to block EET-mediated protection towards ischemic stress.

In terms of protection against long term stress, studies that reported EET-cardioprotection against cardiac remodeling suggested a major role for EET inhibitory effect on the NFκB inflammatory pathway[102]. Cardiac hypertrophy is associated with elevation of NFκB activity and suppressing this pathway with EET interfered with hypertrophy and the progression of the cardiac remolding cascade. An important addition to this field was presented recently by my colleagues and myself. We reported that EETs induce autophagy in cardiomyocytes during starvation stress[11]. Autophagy is an important cellular response to stress in order to avoid cell death. It is considered a major survival program that inhibits several steps in the apoptotic pathway during cellular stress[108]. The EET-stimulatory effect on autophagy relied on K_{ATP} channels and the subsequent activation of AMP activated protein kinase (AMPK). Blocking K_{ATP} channels attenuated the EET-induced autophagy[11]. Importantly, autophagy has been demonstrated to be protective against cardiac remodeling following myocardial infarction[109]. Thus, the discovery that EETs induce autophagy improved our understanding of the EET-mediated cardioprotection.

1.5. MITOCHONDRIA AND EET-CARDIOPROTECTION

Mitochondria are critical organelles in the heart playing key roles in cardiac health and disease. The heart relies on mitochondria to supply ATP for its continuous mechanical and electrophysiological activity. Mitochondria occupy 20-30% of the cardiomyocyte volume and they are essential for the cardiomyocyte in many ways in the addition to providing energy for the contractile apparatus[110]. Mitochondria play a central role in the cellular response to stress and in making the strategic decision of survival or death[111]. Cardiomyocytes are terminally differentiated cells that have almost no capacity to proliferate[112]. Cell death in such tissue is typically not compensated for, and naturally scales up to disturb organ function. As such, mitochondrial fitness is critical to cardiac health[113].

Cardiac ischemia and reperfusion (IR) injury is a clear example of how mitochondrial damage can severely affect cardiac physiology and human health. Briefly, the lack of oxygen during ischemia suppresses mitochondrial oxidative phosphorylation (OxPhos) and ATP production causing a sharp decline in cellular energy which disrupt contractile function and deactivates ATP-dependent ion pumps[114]. Anaerobic glycolysis is activated to supply ATP for survival but this causes a drop in cytosolic pH which aggravates ionic imbalance leading to elevated levels of cytosolic calcium[115]. Such stressful conditions promote apoptotic cell death which proceeds by the mitochondrial outer membrane permeabilization (MOMP) and the release of cytochrome c and other mitochondria-contained

apoptotic factors[116]. Survival of the cardiomyocyte relies on early restoration of blood flow to the ischemic tissue. However, reintroduction of oxygen to the injured mitochondria results in a significant release of ROS and related free radicals[117]. Such elevated ROS in addition to calcium overload induce an unregulated opening of the mitochondrial permeability transition pore (mPTP), a nonselective channel of the mitochondrial inner membrane[118]. Sustained opening of mPTP is destructive to the mitochondrion as it dissipates the mitochondrial membrane potential ($\Delta\Psi m$), and allows the passage of water from the cytosol to the mitochondrial matrix leading to mitochondria swilling, collapse of the cristae structure and rupture of the mitochondrial outer membrane (MOM) releasing cell death mediators[119]. Such mitochondrial damage irreversibly disrupts cellular energy and commits the cell to necrosis. In fact, generalized opening of mPTP is believed to be the leading cause of cardiomyocyte death during reperfusion injury[115].

The notion that IR injury targets mitochondria encouraged the development of therapeutic strategies aiming to protect cardiac mitochondria as a way to limit cardiomyocyte loss in IR events. An example of these mitochondrial-protective approaches is the pharmacological inhibition of mPTP to improve mitochondrial resistance to calcium overload and oxidative stress during reperfusion[120, 121]. Approaches to strengthen mitochondrial antioxidant capacity also show promising results[122, 123]. Interestingly, Ischemic Preconditioning, which is a robust cardioprotective

technique, has been reported to be mediated by enhancing mitochondrial quality control processes resulting in a healthier mitochondrial population more capable to withstand ischemia and reperfusion stress[124, 125]. While all of these strategies have their practical limitations[126], it is fair to agree with the saying that in cardioprotective signaling “all roads lead to mitochondria”[127].

This inspired the question whether EETs protect cardiac mitochondria against IR injury. Our group was the first to investigate the effects of EETs on mitochondria and the results were interesting. We found that EETs inhibited mPTP opening induced either by IR or laser stress[10]. This was probably downstream of EET-mediated activation of potassium channels as blocking either the BKca or the K_{ATP} attenuated this effect[10]. Although the precise signaling cascade leading to mPTP inhibition is debatable, these results provided the first evidence for EET-induced mitochondrial protection.

In addition, IR stress induced a clear mitochondrial fragmentation apparent in the smaller size of mitochondria and the increase of their numbers in electron microscopy examination of post-ischemic hearts of wild type mice[10]. Interestingly, transgenic mice that overexpress CYP2J2 had significantly less mitochondrial fragmentation following IR stress. Intriguingly, similar protection against mitochondrial fragmentation induced by doxorubicin was observed in cardiomyoblasts treated with 11,12-EET[74]. Mitochondrial morphological dynamics are closely linked to mitochondrial

health and cellular response to stress[128-130]. As mitochondrial fragmentation has also been reported in failing hearts[131], the protective effects of EETs against mitochondrial fragmentation warranted more investigation to explore the role of mitochondrial dynamics in the EET-induced cardioprotection.

1.6. MITOCHONDRIAL DYNAMICS

The morphological diversity of mitochondria was described since they were first discovered by Rudolph Kölliker in 1857. It is also reflected in the name mitochondrion which was coined by Carl Benda in 1898 from the Greek words mitos (thread) and chondrion (grain)[132]. However, the ability of the mitochondrion to change its morphology, divide, or fuse with other mitochondria was not reported until late in the 20th century. By the 1990s, the advancement in microscopical technology and the use of mitochondrial specific fluorescent stains enabled the detailed visualization of mitochondrial morphological dynamic processes. After two decades of research, a lot is now known about mitochondrial dynamics and their importance in various cellular processes.

Mitochondria actively undergo continuous fusion and fission processes. In fusion, two or more mitochondria join together to form a longer or branched mitochondrion. On the other hand, in fission a mitochondrion divides into two or more smaller mitochondria. These opposing processes are carefully balanced. Increased fusion or decreased fission leads to elongation of mitochondria and forming of an interconnected mitochondrial network, while inhibition of fusion or enhancement of fission result in mitochondrial fragmentation[133]. Several cellular conditions influence the mitochondrial dynamics balance. For example, mitotic cell division induces mitochondrial fission [134], while autophagy promote mitochondrial elongation[135]. This makes mitochondrial morphology an indicator for a

number of cellular conditions and stress level. Importantly, both mitochondrial fusion and fission play important roles in the process of mitochondrial quality control[8]. Disruption of the mitochondrial dynamic balance result in accumulation of dysfunctional mitochondria leading to failure in organ function and increases susceptibility to cellular stress[136]. In fact, defects in mitochondrial dynamics proteins are the cause for several human diseases[137]. Thus, the significance of mitochondrial dynamics is certainly more than random changes in the organelle shape. Rather, mitochondrial dynamics are inter-related with many important cellular activities that scale up to affect human health.

1.6.1. Mitochondrial Fusion

In mitochondrial fusion, two adjacent mitochondria share their membranes and matrix components into a bigger mitochondrion. It involves two distinct steps; tethering and fusion of MOMs from the two mitochondria, which carried out by the MOM guanosine triphosphatases (GTPases) Mitofusin 1 (Mfn1) and Mitofusin 2 (Mfn2), followed by fusion of mitochondrial inner membranes (MIMs) which is controlled by the MIM GTPase Optic Atrophy 1 (OPA1). The energy required for the fusion process is provided by hydrolyzing GTP molecules by these GTPases[138]. Following the completion of the fusion process, proteins, mtDNA and other matrix components are mixed together as well as membrane proteins in a slower rate[139]. Fusion is then important to maintain the homogeneity of the mitochondrial population in the cell[140]. If a mitochondrion is partially

defective or have accumulated a relatively higher levels of mtDNA mutations, it can be recovered by fusing with other functional mitochondria to complement its defect and repair mtDNA. However, if the mitochondrion is severely dysfunctional, fusion is blocked to isolate this defective member from the functional network[141, 142]. Fusion also plays an important role in the development and differentiation of several tissues. For example, the development of myoblasts into adult cardiomyocytes requires a significant increase in mitochondrial fusion which if blocked will prevent this developmental stage[143]. Knocking down any of the mitochondrial fusion proteins Mfn1, Mfn2, or OPA1 is embryonically lethal[144, 145] which indicates an essential role of mitochondrial fusion. Importantly, several other functions of mitochondrial fusion proteins have been discovered in addition to their role in mitochondrial fusion (discussed below).

1.6.2. Mitochondrial Fission

Similar to mitochondrial fusion, the molecular mechanism of mitochondrial fission is not precisely defined. Several proteins have been recognized to participate in the process. The cytosolic Dynamin Related Protein 1 (DRP1), which is also a GTPase, is translocated into the MOM at the fission site[146, 147]. Several MOM proteins; Mitochondrial Fission protein 1 (Fis1)[148] and Mitochondrial Fission Factor (Mff)[149], participate the recruitment of DRP1 on the MOM. Visual evidence highlights the role of Endoplasmic Reticulum (ER) in wrapping around the mitochondrial tubule marking the fission site and initiating the fission process[150, 151]. Once at the

MOM, DRP1 molecules self-assemble into a ring around the mitochondrial tubule[152, 153]. This activates the GTPase function of DRP1 which provides the energy used to constrict the DRP1 ring causing the mitochondrial tube to divide into two segments[154, 155]. Thus, DRP1 is thought to provide the mechanical power to complete mitochondrial fission.

Excessive mitochondrial fission was first associated with apoptotic cell death and it was since considered a sign of severe mitochondrial stress[156]. However, fission has other significant roles in normal mitochondrial physiology. Mitochondria cannot be synthesized *de novo*, they are generated by division of other mitochondria[157]. In other words, mitochondrial fission is the only way for mitochondria to multiply. Also, mitochondrial fission is required during cell division to disintegrate the mitochondrial network into smaller bodies in order to be distributed among daughter cells[134]. In addition, evidence suggest that mitochondrial fission is the way by which mitochondria get rid of their defective components by segregating them into one end of the mitochondrion which can then be chipped off leaving the functional part intact in a healthier daughter mitochondrion[142]. Further, the elimination of defective mitochondria through autophagy, which is a major component of the mitochondrial quality control system, is dependent on mitochondrial fission[158].

1.7. REGULATION OF MITOCHONDRIAL DYNAMICS

Mitochondrial morphological dynamics respond to several cellular parameters such as cytosolic calcium concentration, oxidative stress levels, availability of amino acids and metabolic substrates, and the stage of the cell cycle[159]. The regulation of mitochondrial dynamic processes to work in harmony with other cellular activities depends primarily on the expression levels of the mitochondrial dynamics machinery proteins and their post-translational modifications[160]. It is worth mentioning that mitochondrial dynamics proteins participate in other important mitochondrial and cellular functions which suggested their value as therapeutic targets for several health conditions[161, 162]. In the following section, I will discuss the main proteins that compose the mitochondrial dynamics machinery and their role in mitochondrial dynamics and other cellular activity.

1.7.1. OPA1

The fusion protein OPA1 was first identified in 2000 for its role in autosomal dominant optic atrophy, a genetic progressive loss of vision due to degeneration of the optic nerve that was linked to a mutation in *Opa1* gene. OPA1 is a large dynamin related protein (100 kDa) with one trans-membrane domain anchoring it to the MIM facing the inter-membrane space (IMS), one GTPase domain and two coil-coil domains that participate in interaction of OPA1 with other molecules[163-165].

Opa1 is a ubiquitously expressed and highly conserved gene with homologues in yeast and all higher metazoans. Like other major mitochondrial dynamics genes, mutations in *Opa1* gene resulting in complete ablation of the protein are embryonically lethal. Though, haplo-insufficiency mutations cause a wide range of conditions with common loss of vision due to optic nerve atrophy[166-169].

Several OPA1 isoforms are constitutively expressed. OPA1 mRNA undergoes complex pattern of alternative splicing in the cytosol resulting in 8 splice variants. Upon arrival of the mature OPA1 to MIM, a subset of OPA1 splice variants is then further processed by several mitochondrial proteases to cleave the trans-membrane domain leaving a shorter soluble form of OPA1 isoforms[170, 171]. The result is two main groups of OPA1 isoforms; long isoforms (L-OPA1) anchored to the MIM, and short isoforms (S-OPA1) soluble in the inter-membrane space (IMS). Thus, OPA1 appears as 5 distinct bands in SDS-PAGE blots between 80-100 kDa. Importantly, both forms are required for normal OPA1 function in mitochondrial fusion.

Functions of OPA1

The first recognized role for OPA1 was its function as a mitochondrial fusion dynamin. Knocking down OPA1 in cellular models caused mitochondrial fragmentation, while upregulating its levels caused a long interconnected mitochondrial network[172]. OPA1 controls the fusion of MIMs from two mitochondria, the second step of the fusion process after fusion of MOMs[173]. The profusion function of OPA1 requires its GTPase activity, as

mutant OPA1 forms that lack an active GTPase domain are incapable of executing mitochondrial fusion[165, 174]. Importantly, if a mitochondrion loses its membrane potential, usually as a result of a severe dysfunction, OPA1 undergoes proteolytic degradation which blocks the ability of this mitochondrion to fuse with other healthy mitochondria[175, 176]. This quarantine strategy is important to maintain the quality of the mitochondrial population in the cell.

In addition to mitochondrial fusion, OPA1 plays a chief role in the MIM organization and cristae structure which is fundamental to mitochondrial functions. The majority of mitochondrial activities, such as oxidative phosphorylation (OxPhos), ionic balance, as well as mitochondrial fusion, rely on their ultrastructure and polarized membranes. Mounting evidence support a significant, role of OPA1 in several mitochondrial functions through regulation of cristae structure.

OPA1 participates in several forms of protein and membrane interactions. S-OPA1 molecules dimerize to make a homodimer (184 kDa) that acts as a building block for higher order complexes[170, 177]. One S-OPA1 molecule interacts with two L-OPA1 molecules from two opposing parts of the MIM forming a detectable trimer at 285 kDa[170, 178]. These oligomers are thought to play a central role in forming cristae invaginations and controlling their junction with the boundary MIM[178-180]. OPA1 also interacts with Mitofusin 1 from the MOM, which may regulate the interaction between the two membranes[172].

While L-OPA1 is firmly inserted into the MIM, S-OPA1 can also associate with the MIM. Recent studies visualized S-OPA1 dimers forming a lattice-like layer over cardiolipin-rich membranes resembling the MIM[177, 181]. This association dramatically increased OPA1 GPAsae activity and forced the membrane to form tubules with specific diameter[182].

OPA1 has a major role in mitochondrial respiration and energetic function. Electron Transport Chain (ETC) complexes reside in the MIM and pump protons from the matrix to the IMS to build an electrochemical gradient which is then used by ATP synthase to generate ATP molecules. The folds in the MIM, which are called cristae, were originally thought to increase the surface area of the MIM to enhance the respiratory capacity of the mitochondrion. It has been confirmed that the majority of the oxidative phosphorylation (OxPhos) takes place in cristae rather than the boundary part of the MIM[139, 183, 184]. ETC complexes concentrated on cristae membrane and pump protons in the intra-cristal space where they are trapped within the impermeable folded MIM. OPA1 is playing the critical role of holding the cristae junction tight to close this circle. Short and long OPA1 oligomerize to bring MIM together and to make a diffusion barrier for solutes of the intracristal space[184-186].

Moreover, S-OPA1 that is usually considered freely soluble in the IMS has been confirmed to associate on the outer surface of the MIM, covering the membrane with a lattice-like organization[177, 181]. This organization, together with oligomers at cristae junctions, regulates MIM

structure and has a potentially significant role in regulating protein association and other important reactions on the MIM. For example, intact OPA1 is necessary to maintain the supercomplex organization of respiratory chain complexes[187] and to improve the assembly and stability of ATP synthase[174, 188]. Indeed, silencing OPA1 expression causes aberrant cristae structure, reduction of mitochondria membrane potential, and dysfunctional mitochondrial respiration[188, 189]

Furthermore, recent studies demonstrated that OPA1 regulates mitochondrial respiratory activity in response to the availability of metabolic substrates[174, 190]. In times of nutrient restriction or at higher metabolic demand, OPA1 oligomers increase leading to increased cristae number and improved mitochondrial efficiency and ATP production[174]. The ability of OPA1 to respond to starvation and other forms of cellular stress[191, 192] regulating mitochondrial function accordingly indicated a role of OPA1 in mitochondrial response to stress.

OPA1 has another key role in cell death. Mitochondrial outer membrane permeabilization (MOMP) and release of IMS proteins ignites the caspase machinery executing apoptotic cell death, while the irreversible opening of the permeability transition pore commits the cell to necrotic death[193]. It has been stated that it is mitochondria where cell death decision is made, and that mitochondrial membranes are the battle ground for pro- and anti-apoptotic effectors[116]. Importantly, OPA1 has a recognized key role in MOMP. The MOMP process is composed of two sequential but

independent steps; formation of permeabilizing pores in the MOM, and mobilization of IMS apoptotic factors, notably cytochrome c (cyt.c), from their stores inside the intracristal space to be available for release through the newly formed pores on MOM[116, 194, 195]. Approximately 85% of cyt.c is trapped inside cristae participating in the OxPhos. As OPA1 oligomers are the gatekeeper of cristae junctions insuring their tightness, disruption of these oligomers is necessary to open these junctions allowing the release of cyt.c and the progression of the apoptotic process[178, 186, 196]. Pro-apoptotic factors of the Bcl-2 family proteins like tBid and Bnip3 are able to disassemble OPA1 oligomers releasing cyt.c[178, 180, 197]. Of note, overexpression of OPA1 has anti-apoptotic effect by stabilizing cristae junctions[198, 199]

In addition, evidence supports a role of OPA1 in the regulation of mitochondrial calcium uptake. Recent studies indicated that matrix $Ca^{2}+$ increases if cristae junctions open when OPA1 is defective[200]. As most $Ca^{2}+$ channels are concentrated on cristae membranes rather than boundary membrane, these findings suggest that OPA1 oligomers restrict access of $Ca^{2}+$ ions into intracristal space by tightening cristae junction. Thus, knocking down OPA1 enhances both rate and amplitude of mitochondrial $Ca^{2}+$ uptake[200]

To summarize, OPA1 molecular functions can be categorized into two distinct roles; executing mitochondrial fusion and organizing MIM into cristae. Importantly, evidence suggest that these two roles of OPA1 are

somewhat independent in many cases[174, 178]. While the GTPase catalytic activity of OPA1 is required for its role in mitochondrial fusion, it is not required for OPA1 oligomerization and holding the cristae junction tight. In fact, a mutation in the OPA1 GTPase domain that blunts its catalytic activity and fusion function favored its oligomerization and was resistant to disruption by apoptotic stimuli[180]. Similar observations have been reported about the requirement of L-OPA1 expression for the fusion function of OPA1[192], while it is not necessary for forming OPA1 oligomers, at least the first order of these oligomers[170, 174, 177].

Regulation of OPA1

Due to the several splice variations of OPA1 molecule both at the mRNA and the protein levels, the regulation of OPA1 expression and functions is a complex process that still requires further investigation. Levels of OPA1 are regulated during the cell cycle via transcription and proteolytic removal[159, 201]. Tissue specific splice variation of OPA1 mRNA regulates expression of different OPA1 variants with limited variability among organs and organisms[170].

In terms of post translational modifications, proteolytic processing appears to be the main mode of regulating OPA1 function. Mitochondrial peptidases constitutively cleave a subset of mature L-OPA1 isoforms to yield enough S-OPA1 necessary for its function[171, 202]. Thus, this proteolytic processing is required to activate OPA1. However, extensive processing of L-OPA1 that depletes its levels deactivate its fusion function. Thus, the

extent of this process, and the resultant ratio between L-OPA1 and S-OPA1, is carefully controlled by several mitochondrial proteases. Also, other forms of OPA1 proteolysis have also been reported resulting in general degradation of OPA1 molecules into inactive fragments[202-204]. Importantly, OPA1 proteolytic processing is regulated by multiple factors to activate or deactivate OPA1 accordingly. For example, high mitochondrial ATP and OxPhos activity induces stimulatory OPA1 processing[205], as does mild cellular stress[191]. Conversely, inhibitory OPA1 proteolysis is induced by mitochondrial depolarization[141, 175, 206], during apoptosis[178, 186, 189, 207] and in a lesser extent in response to postprandial changes in nutrient levels[190]. It is worth mentioning that the proteolytic processing of OPA1 can have different outcomes in terms of OPA1 functions. Extensive cleavage of L-OPA1 to form S-OPA1 will affect OPA1's profusion function more that its ability to form oligomers[174]. However, general proteolytic degradation of OPA1, as seen during apoptosis, suppress all OPA1 functions.

In addition to the irreversible proteolytic control of OPA1, reversible acetylation and deacetylation regulate the GTPase activity of OPA1. OPA1 is reported to be highly acetylated in cardiac pathological stress resulting in inhibited mitochondrial fusion. Deacetylation with the mitochondrial SIRT3 deacetylase restored OPA1 activity and mitochondrial fusion[208].

Another distinct level of OPA1 regulation is the manipulation of its ability to oligomerize. Not much is known about the physiological control of OPA1 oligomerization. Proapoptotic factors such as tBid and Bnip3 disrupt

OPA1 oligomers allowing the release of cytochrome c during apoptotic cell death[178, 207]. On the other hand, the conditions that promote OPA1 oligomerization are less clear. Mild oxidative stress has been shown to induce OPA1 oligomerization[209, 210]. In support for the role of the redox state in OPA1 oligomerization, a recent study showed that the process of OPA1 oligomerization requires the redox sensor ROMO1 which promoted OPA1 oligomers during mild oxidative stress[211]. Importantly, high levels of oxidative stress induced disruption of OPA1 oligomers probably as a part of the cell death cascade[178]. Interestingly, levels of OPA1 oligomers have been shown to respond to the availability of mitochondrial respiratory substrates such as malate, glutamate and succinate[174]. Higher levels of mitochondrial substrates inhibited OPA1 oligomerization leading to relaxed cristae organization and slower mitochondrial respiration. In contrast, low levels of these substrates, which indicates metabolic demand or starvation state, induced a prompt increase in OPA1 oligomerization[174]. This was mediated by OPA1 interaction with mitochondrial solute carriers that facilitate the transfer of these substrates across the MIM[174]. With this mechanism, OPA1 senses the availability of nutrients and reversibly regulates mitochondrial ultrastructure and respiration accordingly.

1.7.2. DRP1

Dynamin Related Protein 1 (DRP1) is considered the main executer and regulator of mitochondrial fission. Like OPA1, DRP1 is a big (~80kDa) GTPase related to the dynamin family of membrane-pinching mechano-

enzymes[212]. DRP1 can also homo-oligomerize but into higher orders compared to OPA1 oligomers. However, unlike OPA1, DRP1 is primarily expressed in the cytosol and translocate to MOM at the fission site upon activation, which is an important step in the regulation of mitochondrial fission[213]. Several splice variant isoforms of DRP1 have been identified in human and murine tissues some with organ specific distribution[214]. DRP1 has multiple forms of posttranslational modifications that affect its ability to translocate to mitochondria and its GTPase activity which significantly regulate mitochondrial dynamic balance[215]. Thus, DRP1 is considered as an important link between cytosolic signaling and mitochondrial dynamics[133]. In addition to its fundamental role in mitochondrial fission, accumulating evidence suggest its importance for other important cellular processes such as apoptosis and cell proliferation[216, 217]. In the following sections, I will briefly discuss the different functions of DRP1 and the major ways of regulating these functions.

Functions of DRP1

The most recognized function of DRP1 is its role in mitochondrial fission. Following recruitment of DRP1 from the cytosol to MOM, DRP1 self-assembles forming a ring surrounding the mitochondrion at the fission site[152, 155, 218]. This activates the GTPase activity of DRP1 which then hydrolyze GTP molecules to provide energy to constrict the DRP1 ring around the mitochondria dividing it into two daughter segments[153].

Inhibition of DRP1 translocation or GTPase activity suppresses mitochondrial fission and affects the dynamic balance towards longer mitochondria[148, 213]. Interestingly, DRP1 inhibition also attenuates apoptotic cell death[146]. This leads to the concept that mitochondrial fission is required for apoptosis which was supported with the obvious mitochondrial fragmentation that preceded apoptosis[156, 219]. Further investigation revealed that translocation of DRP1 to MOM facilitates the recruitment of pro-apoptotic factor Bax at the fission site to form the permeabilization pore in the MOM, a significant step in the intrinsic pathway of apoptosis[147]. As a result, inhibition of DRP1 emerged as a new promising therapeutic approach to attenuate cardiomyocyte death in cardiac IR[220, 221]. Indeed, a pharmacological inhibitor has been designed to bind to and inhibit DRP1[222] which led to a significant decrease in infarct size following IR in experimental mice[223].

Another benefit of inhibiting DRP1 was revealed from studies that investigated the cellular response to starvation stress. Restriction of amino acid supply or activation of autophagy induced a notable change in mitochondrial morphology towards longer more branched mitochondria[135, 224, 225]. Similar results were seen in cardiomyocyte mitochondria in mice undergone 12 hours fasting[135]. This was mediated by a phosphorylation-dependent inhibition of DRP1 that suppressed mitochondrial fission and allowed unopposed mitochondrial fusion[135]. Mitochondrial elongation is

believed to be an important survival response to cellular stress to improve cellular energy levels[135].

Considering the role of DRP1 in apoptosis and response to stress, scientific community believed that inhibiting DRP1 could be the solution for several cardiac conditions. As a result, animal models have been designed to genetically suppress DRP1 in cardiomyocytes[226-228]. Unexpectedly, long term outcomes of inhibition of DRP1 were quite detrimental in contrast to the short term benefits. Mitochondria became longer and bigger but with defective respiratory activity and with fragile resistance to starvation or IR stress[226]. These recent reports of time-dependent detrimental outcome of DRP1 suppression strongly support a role of DRP1 and mitochondrial fission in the maintenance of mitochondrial health[229].

Regulation of DRP1

DRP1 is regulated mainly by post-translational modifications. Phosphorylation and dephosphorylation by cytosolic kinases and phosphatases play the major role in regulating DRP1 activity[133]. Several serine residues have been identified as phosphorylation sites but with different outcomes on DRP1 translocation to mitochondrial membranes. According to the amino acid sequence of human DRP1 splice variant 1 (brain isoform), serine 616 (S616) and serine 637 (S637) are the most studied phosphorylation sites of DRP1. Phosphorylation at S616 by cyclin-dependent kinase 1 (Cdk1/cyclin B) activates DRP1 during mitotic cell division[134]. This induces mitochondrial fission to transform the mitochondrial

network into smaller individuals prior to their distribution among daughter cells[134]. S616 is also phosphorylated by protein kinase C delta (PKCδ) in response to oxidative stress which contributes to the mitochondrial fragmentation observed in such model of cellular stress[230].

In contrast, several studies demonstrated that phosphorylation of DRP1 at S637 by PKA inhibit its GTPase activity and translocation to mitochondria[231-233]. The calcium dependent phosphatase calcineurin dephosphorylates this serine regaining DRP1 activity[233, 234]. This contributes to the activation of DRP1 and mitochondrial fission during apoptosis and calcium overload. Interestingly, both PKA and cacineurin have been reported to be targeted by EET signaling. EETs activated PKA in cardiomyocytes [235] and inhibited calcineurin following ex-vivo IR stress[106]. This suggests that EETs might promote DRP inhibition during stress which may explain their protective effect against stress-induced mitochondrial fragmentation. However, EETs also induce calcium influx through the cell membrane into the cytosol during normal condition[23], which may contradict their effect on calcineurin.

In addition, one study reported that Ca2+/calmodulin-dependent protein kinase 1α (CaMK1α) also phosphorylates S637 but with stimulatory effect on DRP1-dependent mitochondrial fission[236]. It is not clear how phosphorylation of the same site can have opposing effects[133]. As DRP1 interacts and binds to several cytosolic proteins such as PKCδ[236], calcineurin[233], and microtubules[237], one can speculate that DRP1's

interaction with other proteins might influence the activity outcome of DRP1 phosphorylation. As such a theory has not been investigated, it is common to conclude, considering the majority of supporting evidence, that pDRP1 S637 is the inhibited form of DRP1.

Other forms of DRP1 posttranslational modification include inhibition by S-nitrosylation which is required for mitochondrial elongation during myogenic differentiation[238]. DRP1 also undergoes ubiquitination but with controversial outcomes on DRP1 stability and mitochondrial morphology[215, 239]. In addition, SUMOylation also regulates DRP1 by stabilization on mitochondrial membrane enhancing mitochondrial fission during mitotic cell division[240, 241] and apoptosis[242]. It remains unclear how these multiple forms of DRP1 modification coordinate to regulate its activity in mitochondrial fission and other DRP1 functions.

1.7.3. Other mitochondrial dynamics proteins

Mitofusins

Mitofusin 1 and 2 are fusion GTPases attached to the MOM. Both are about 85kDa proteins with high similarity in amino acid sequence and function[243]. Each has two transmembrane domains and a small loop facing the intermembrane-space with both terminals facing the cytosolic side of the membrane. Both Mfn1 and Mfn2 have two cytosolic hydrophilic coiled-coil domains which are important for homotypic or heterotypic interaction with mitofusin molecules from the opposing mitochondrion during mitochondrial fusion[133]. Thus, Mfn1 and Mfn2 tether adjacent mitochondria

together by the interaction of the coiled-coil domains while the GTPase activity is required to complete the fusion of MOMs. Cells with mutant non-functional GTPase domain have tethered but not fused mitochondria[244].

Mfn2 is also expressed in the endoplasmic reticulum (ER) where it plays an important role in the association between ER and mitochondria[245]. Mfn2 is also important in the recruitment of the cytosolic ubiquitin ligase Parkin during mitochondrial depolarization preparing the mitochondrion for removal by autophagy[246]. In addition, Mfn2 is required for mitochondrial transport along microtubules[247] which is important for mitochondrial distribution among the cell especially in neurons. Indeed, human mutation in Mfn2 is the cause of Charcot-Marie-Tooth disease which is characterized by degeneration of long peripheral neuronal axons[248].

Fis1, Mff, MiD49 and MiD51

Mitochondrial fission protein 1 (Fis1), mitochondrial fission factor (Mff), mitochondrial dynamics proteins of 49 and 51 kDa (MiD49 and MiD51) are MOM proteins that participate in the recruitment and activation of DRP1 at the fission site[249]. Fis1 was the first to be identified as a DRP1 receptor on MOM[148], however later studies demonstrated that DRP1 can be recruited in absence of Fis1[250]. More recent studies identified Mff as a necessary protein for DRP1 recruitment[149]. However, other studies demonstrated that MiD49 and MiD51 are able to mediate DRP1 recruitment and mitochondrial fission in absence of both Fis1 and Mff[249]. Recent attempts to understand how these proteins regulate DRP1 hypothesized that Mff functions as a

dominant receptor for DRP1 while MiD51 regulates its GTPase activity[251]. However, such theory are yet to be proved.

1.8. THESIS OVERVIEW

1.8.1. Rationale and Hypothesis

As discussed earlier, EETs are bioactive lipids that exert interesting cytoprotective properties albeit through undefined mechanisms. The few studies that reported protection of cardiac mitochondria with EETs (reviewed in section 1.5) warrant more investigation on how EETs preserve mitochondria during cellular stress. This would provide new insight on the mechanism of EET cardioprotection, and would also explore whether EETs participate in the regulation of mitochondrial activities. Mitochondria are very interesting organelles with profound influence on human health and disease. The main interest of my studies was to explore the effect of EETs on mitochondria during cellular stress with particular emphasis on mitochondrial dynamics. The **general hypothesis** was:

"EETs participate in the regulation of mitochondrial function and dynamics and limit mitochondrial injury following cellular stress"

To test this hypothesis, I studied the mitochondrial response to various types of cellular stress including ischemia-reperfusion[97, 106], serum starvation[11], doxorubicin toxicity[74], and photodynamic stress[252] (studies have been published in the referred articles). I am particularly interested in starvation and photodynamic stress. In serum starvation stress, the lake of amino acids, lipids, and growth hormones in the media induces both autophagy and apoptosis[253, 254], which provides the opportunity to study the interplay between pathways of cell survival and death where mitochondria

play a chief role. Photodynamic stress resembles an easy model to study the effect of abrupt oxidative stress on mitochondria which is an important component of IR injury. It also allows studying the role of EETs on resisting this model of cancer therapy. In this thesis, I am presenting my studies regarding these two models of cellular stress.

1.8.2. Objectives

The objectives of my studies were to answer the following questions:

1. Do EETs preserve mitochondrial function during photodynamic induced stress (addressed in chapter II)
2. Do EETs protect mitochondrial dynamic balance against photodynamic induced stress (addressed in chapter III)
3. Do EETs protect mitochondrial quality following serum starvation induced stress, and how? (addressed in chapter IV)

CHAPTER II

Sonodynamic and Photodynamic Mechanisms of Action of the Novel Hypocrellin Sonosensitizer, SL017: Mitochondrial Damage is attenuated by Epoxyeicosatrienoic Acid

A version of this chapter has been published: El-Sikhry, H.E., Miller, G.G., Madiyalakan, M.R. & Seubert, J.M. Sonodynamic and photodynamic mechanisms of action of the novel hypocrellin sonosensitizer, SL017: mitochondrial cell death is attenuated by 11, 12-epoxyeicosatrienoic acid. Invest New Drugs29, 1328-1336 (2011).

2.1. INTRODUCTION

Sonodynamic therapy (SDT) involves utilization of ultrasound energy for the activation of drugs in target tissues. While conceptually analogous to photodynamic therapy (PDT), SDT exerts therapeutic effects by sound energy instead of light energy. Photoactivation of therapeutic agents is limited by the poor transmission of light energy at effective wavelengths in the visible spectrum, through tissues and endoluminal blood[255]. SDT has the distinct advantage of the ability to focus ultrasound energy to target sites buried deep within tissues and locally activate the sonosensitizing compound[256, 257]. Thus, ultrasound energy overcomes a major limitation of PDT.

Many compounds under investigation as potential PDT and SDT sensitizers are activated by either light or ultrasound; however precise mechanisms of activation and cytotoxicity remain complex and warrant further study. In both PDT and SDT, mechanisms of cell death depend largely on the subcellular localization of the sensitizer. Mechanisms of action involved in SDT are governed by ultrasound parameters, the type of biological system being insonated and the type of sonosensitizing compound[256, 258]. Suggested mechanisms include cavitation, pyrolysis and generation of ROS or a combination of more than one mechanism[259].

Hypocrellin-B (HB) derivatives are low molecular weight compounds which belong to the non-toxic perylenequinone family of photosensitizing and sonosensitizing compounds. HB derivatives exert cytotoxic effects by

mediating singlet oxygen-induced apoptotic cell death when exposed to light energy[260, 261]. SL017 is a novel HB compound with both sono- and photosensitizing properties but the mechanisms of action remain largely unexplored.

AA is a polyunsaturated fatty acid normally found esterified to cell membranes, which can be released in response to several stimuli including hormones[2]. Free AA can then be metabolized by cytochrome P450 epoxygenases, CYP2J2 and CYP2C9, to epoxyeicosatrienoic acids (EET's), which act as potent cellular signaling molecules. We and others have demonstrated that EET's protect tissue and cells from toxic injury[69, 75, 95, 96]. Although the precise mechanisms remain elusive, EET-mediated anti-apoptotic properties are thought to involve mitochondrial pathways[10, 74]. Interestingly, CYP2J2 has been found to be significantly up-regulated in cancer cells, suggesting a role for EET's in the development and survival of malignant tumors[79, 83].

We investigated the intracellular distribution and mechanism of action of SL017 following light and ultrasound activation. We found that SL017 was rapidly taken up by cells and preferentially targeted mitochondria. Activation of SL017 triggered significant ROS production and mitochondrial damage resulting in loss of membrane potential and increased fragmentation. Moreover, our data suggest increased levels of EET's attenuated the mitochondrial damage. Taken together, these data

provide mechanistic information regarding the cytotoxic effects for the novel HB-derivative, SL017.

2.2. MATERIALS AND METHODS

2.2.1. Materials

SL017 (2-(N,N-dimethylaminopropyl)amino-15-acetyl-3,10-dihydroxy-6,7,11-trimethoxy-14-methyl-15-H-cyclohepta(ghi)perylene-4,9-dione) was provided by Quest Pharmatech Inc. (Edmonton, AB) and was stored in the dark at -20°C. Fluorescent stains CM-H2-DCFDA (5-(and-6)-chloromethyl-2',7'-dichlorodihydrofluorescein diacetate acetyl ester), TMRE (tetramethylrhodamine ethyl ester) and MitoTG (MitoTracker Green FM) were obtained from Molecular Probes, Invitrogen (Carlsbad, CA), dissolved in DMSO (dimethylsulfoxide) and stored in the dark at -20°C. The 11,12-epoxyeicosatrienoic acid was obtained from Cayman Chemicals (Ann Arbor, MI). L-Ascorbic acid was obtained from Sigma-Aldrich (Oakville, ON).

2.2.2. Cell Culture

Human lung fibroblast cells (WI-38) and Eagle's Minimum Essential Medium (E-MEM) were obtained from the American Type Culture Collection ATCC (Manassas, VA). They were maintained in antibiotic-free E-MEM supplemented with 10% (v/v) fetal bovine serum under a humid atmosphere of 5% CO_2 in air at 37°C. One day prior to experiments, cells were plated on 35mm glass bottom slides (Lab-Tek), 6- or 96-well microtitre plates with E-MEM containing 1% penicillin-streptomycin (Gibco, Invitrogen, Carlsbad, CA).

2.2.3. Estimating cellular uptake and intracellular distribution of SL017

Cellular uptake and intracellular distribution are important properties of sensitizers. Fluorescence properties of SL017 facilitated intracellular uptake kinetics and biodistribution studies using epifluorescence microscopy. WI-38 cells were grown as monloayers on glass bottom slide chambers and treated with SL017 (0.1-10 μM) dissolved in 1% DMSO. A Zeiss Axio Observer Z1 epifluorescence microscope was used to capture single images for specific SL017 fluorescence at 0.25, 0.5, 1, 2, 4, and 8 hours' incubation. Semiquantitative estimates of SL017 fluorescence were determined from ten randomly selected fields with AxioVision software to determine cellular uptake and sub-cellular distribution.

2.2.4. Photodynamic and Ultrasound treatment

Two light sources were used to stimulate the cytotoxic properties of SL017. Cells cultured on 96 well microplates were placed 15 cm directly beneath a 50 W halogen lamp for 5, 10 and 15 min, or cells cultured on LabTek slides were illuminated with the microscope's monochromatic beam from an LED lamp at wavelengths of 470 and 555nm. Cells were exposed to ultrasound using an Excel Ultra Max SX ultrasound generator (Excel Tech Inc, Oakville, Ontario) configured to deliver 2 W/cm^2 power at a frequency of 1 MHz for 30 seconds, 2 in total. The 5 cm^2 transducer was placed below individual culture wells with a coupling gel and allowed to cool

to room temperature between insonations. Experiments were carried out in low-level light to minimize any confounding influence of photoactivation.

2.2.5. ROS Production Following Activation of SL017

CM-H_2-DCFDA was used to assess cellular ROS content following activation of SL017 by either light or ultrasound. WI-38 cells were washed with Hanks' balanced salts solution (HBSS) to remove FBS and pre-loaded with CM-H_2-DCFDA (5 μM). Cells were treated with SL017 (0 or 10 μM) and/or ascorbic acid (0 or 100 μM) in HBSS for 45 minutes at 37°C in the dark prior to PDT or SDT. CM-H_2-DCFDA fluorescence was measured using a BioTek Synergy2 fluorescence microplate reader at excitation of 485±20 nm and detection wavelength range of 528±20 nm. Relative fluorescence values were expressed as percentage of the basal level reading of the same well (F/F_0 %).

2.2.6. Monitoring changes in mitochondrial activity and morphology

Cells were pre-loaded with 100 nM TMRE and 100 nM MitoTG for 30 min at 37°C to record changes in mitochondrial membrane potential ($\Delta\Psi m$) and morphology. TMRE is a cationic dye attracted to polarized mitochondria membranes, a reflection of mitochondrial function. MitoTG was used to observe changes in mitochondrial morphology as it is less sensitive to changes in $\Delta\Psi m$. Changes were recorded in cells treated with SL017 (0.1 μM), ascorbic acid (100 μM) or 11,12-EET (1 μM) for 30 minutes then subjected to time-lapse imaging for 10 min at 37°C and 5% CO_2. A Zeiss

Axio Observer Z1 epifluorescence microscope was used to take z-stack images for two channels every 10 seconds with a 500 ms exposure time. Cells were observed under a 62X objective. TMRE fluorescence was excited at 555 nm and emission was recorded between 575–640nm, and MitoTG was excited at 470 nm and emission was recorded between 500-550 nm.

2.2.7. Statistical analysis

Statistical significance was determined using the unpaired Student's t-test and one-way ANOVA followed by a Duncan's test to assess multiple group comparisons were applicable. Results were considered significant if $p<0.05$.

2.3. RESULTS

2.3.1. SL017 concentrates in mitochondria

SL017, a perylenequinone pigment (hypocrellin) derivative, displays unique spectral absorption and fluorescence emission properties (absorbance max. 657 nm, emission peaks 748, 770, 797 nm) which allow for analysis of cellular uptake and intracellular distribution. Cellular uptake of SL017 by WI-38 human diploid lung fibroblasts was rapid, occurring within 15 min and reaching peak intracellular levels by 30 min (Fig. 2.1A). No further significant uptake was observed over the subsequent 8 hours. SL017 distributed diffusely in the cytosol but bright perinuclear staining suggested a concentrated mitochondrial subcellular localization. Staining mitochondria with the selective TMRE stain revealed a co-localization of TMRE with SL017 indicating a higher concentration of SL017 in mitochondria (Fig. 2.1B).

2.3.2. SL017 Generated ROS

CM-H_2-DCFDA is a non-fluorescent compound until activation by intracellular esterases and oxidation by ROS. WI-38 cells treated with SL017 and subjected to PDT demonstrated a significant increase in ROS levels (Fig. 2.2A). Increased duration of PDT resulted in increasing ROS production. Pretreatment of WI-38 with the anti-oxidant ascorbic acid reduced both initial and treatment-elicited ROS in control and SL017 groups (Fig. 2.2A). Interestingly, in the absence of SDT incubation of WI-38 cells SL017 alone triggered a moderate increase in ROS levels, which was

attributed to minor light exposure. However, a large increase in ROS production was observed in SL017 treated cells following SDT compared to vehicle control. Consistent with PDT, pretreatment with ascorbic acid lowered fluorescence levels confirming generation of ROS.

2.3.3. SL017 Induced Mitochondrial Dysfunction

PDT activated SL017 resulted in the rapid dispersion of TMRE fluorescence from WI-38 cells within 90 seconds (Fig. 2.3, 2.4), indicating dissipation of $\Delta\Psi m$ and suggesting loss of mitochondrial function. Removal of the light source did not restore mitochondrial $\Delta\Psi m$, suggesting that activation of SL017 by PDT triggers irreversible mitochondrial dysfunction. Increasing excitation light intensity (from 5% to 10% of maximum brightness of the LED light source) or the SL017 concentration (from 0.1 to 1 or 10 μM) rapidly accelerated the loss of $\Delta\Psi m$ to less than 20sec (data not shown). Co-treatment with 11,12-EET significantly slowed the SL017-mediated early loss of $\Delta\Psi_m$ (Fig. 2.4B). Conversely, pre-incubation with ascorbic acid failed to inhibit the early SL017 induced mitochondrial dysfunction, partially explained by a limited availability of ascorbic acid in the mitochondrial matrix which suppresses the intra-mitochondrial effect of its elevated cytosolic concentration (Fig. 2.3, 2.4). These data imply that un-activated SL017 accumulates in the mitochondria where it can directly impact membrane potential following activation.

Mitochondria undergo constant fission and fusion processes thought to be critical for normal function; however, dramatic fragmentation and

mitochondrial dysfunction in response to toxicity plays an important role in apoptotic cell death. To determine whether PDT activated SL017 can trigger mitochondrial fragmentation we investigated the mitochondrial morphology in WI-38 cells by real-time imaging. Mitochondria, which exhibit elongated and filamentous morphology in healthy control cells, became dramatically shorter and more spherical following PDT activation of SL017 in WI-38 cells loaded with MitoTG (Fig. 2.5). Initial evidence of mitochondrial fission occurred by 5 min, which transformed long, tubular and interconnected mitochondria into small spherical fragments. After approximately 10 min, clear mitochondrial fragmentation was observed compared to control (Fig. 2.5). Resulting fragments were contracted and swollen to elicit the spherical appearance. Pretreatment with ascorbic acid or 11,12-EET of WI-38 cells treated with SL017 and subjected to PDT, resulted in an moderate attenuation of the mitochondrial fragmentation process (Fig. 2.5).

Figure 2.1

a.

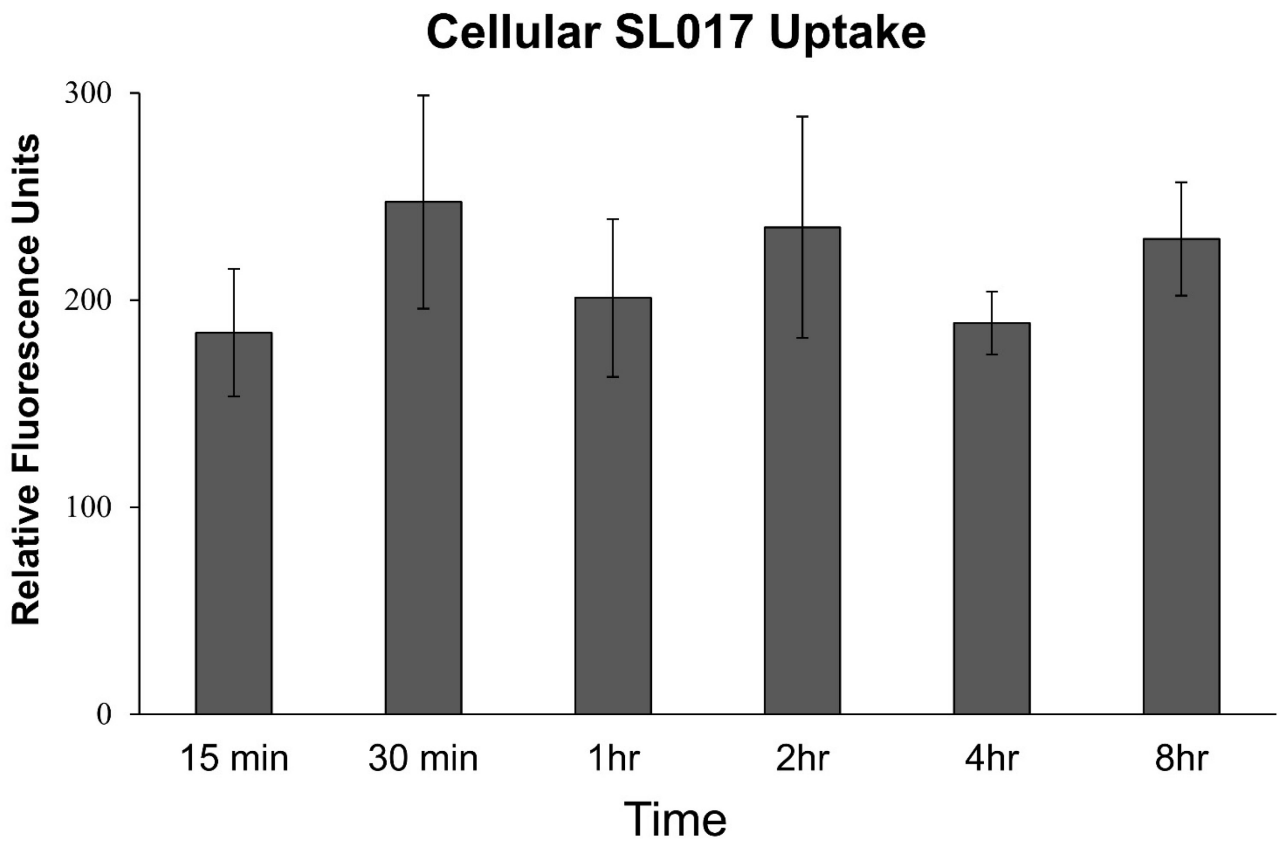
Cellular SL017 Uptake
Relative Fluorescence Units
300
200
100
0
15 min
30 min
1hr
2hr
4hr
8hr
Time

b.

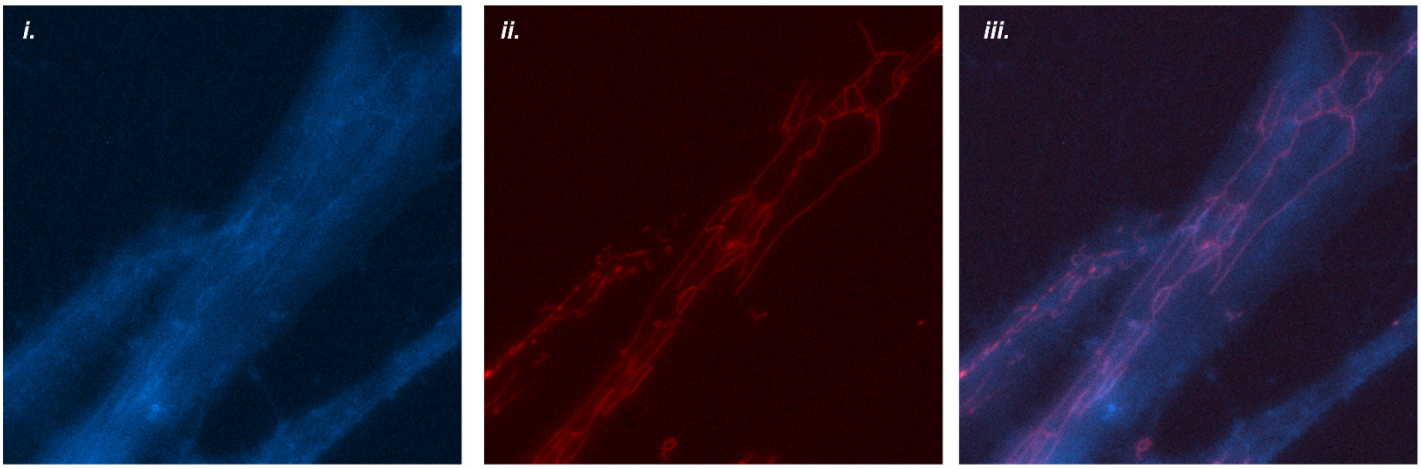
i.
ii.
iii.
SL017
TMRE
Merged Image

Figure 2.1 Cellular Uptake and Distribution of SL017

(a) timecourse of relative intracellular SL017 (10μM) in WI-38 cells. Values represent mean ± SEM, n=4-8. (b) Representative microscope images showing cellular uptake and co-localization of SL017 at 30min. i. SL017 specific fluorescence, ii. Mitochondrial selective dye TMRE, and iii. Overlay of SL017 and TMRE demonstrating mitochondrial co-localization

Figure 2.2

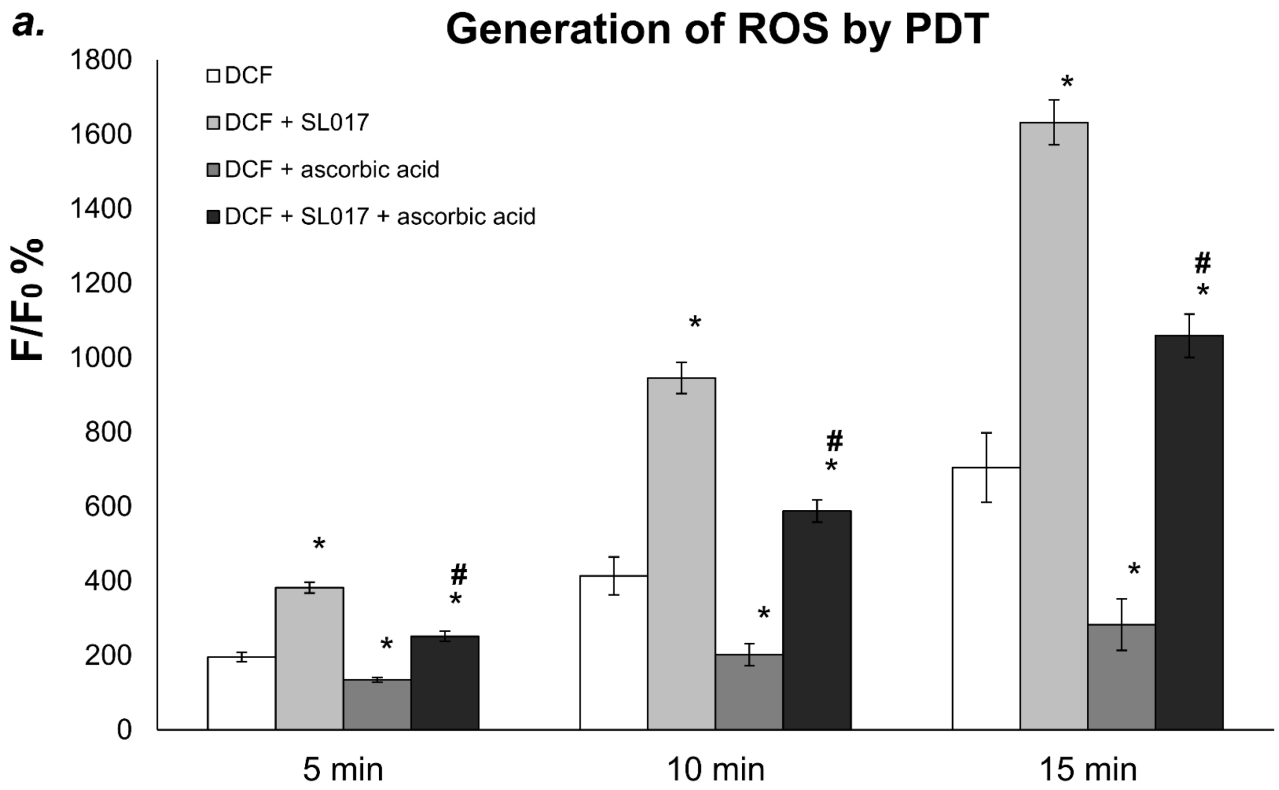
a.
Generation of ROS by PDT
DCF
DCF + SL017
DCF + ascorbic acid
DCF + SL017 + ascorbic acid
F/F0 %
1800
1600
1400
1200
1000
800
600
400
200
0
5 min
10 min
15 min

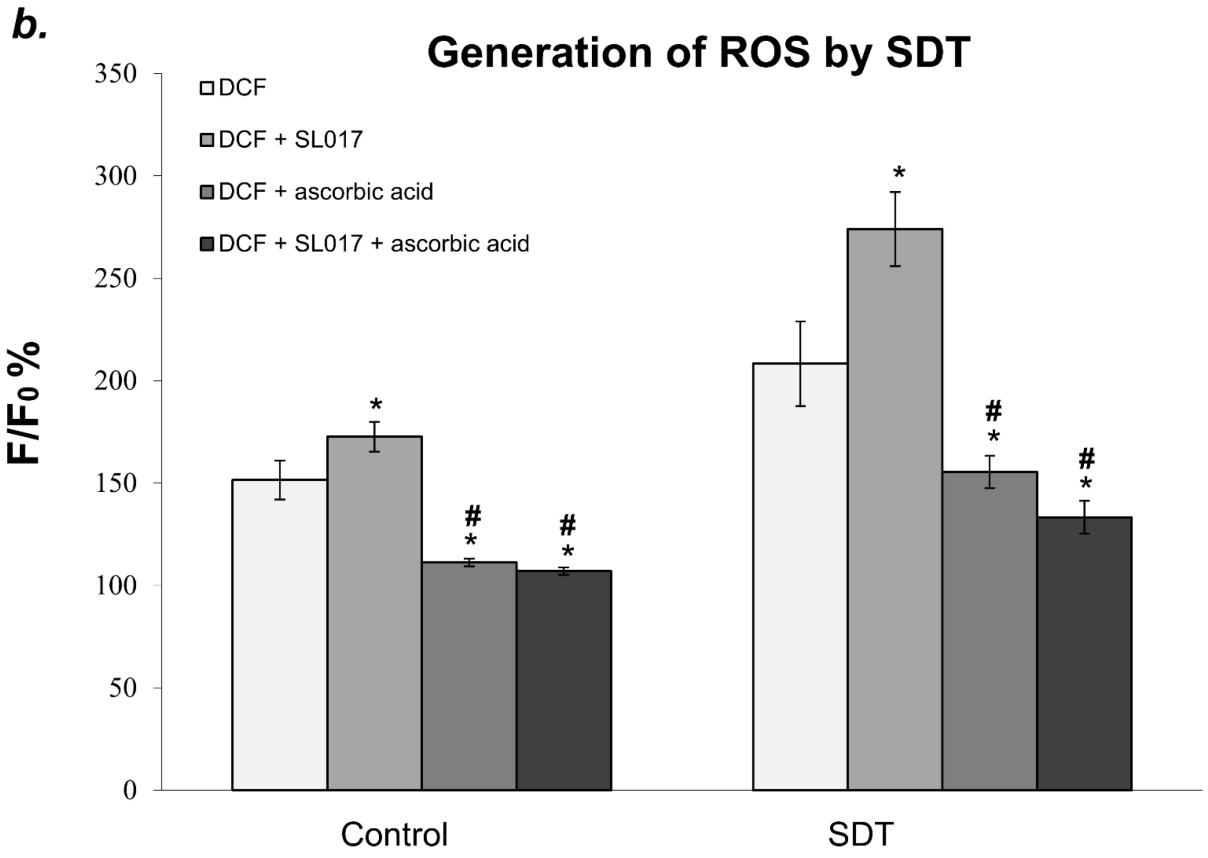
b.
Generation of ROS by SDT
DCF
DCF + SL017
DCF + ascorbic acid
DCF + SL017 + ascorbic acid
F/F0 %
350
300
250
200
150
100
50
0
Control
SDT

Figure 2.2 Increase in cellular ROS by Photo- and Sonodynamic treatment in presence of SL017

Histograms representing the relative ROS production from PDT and SDT induced activation of SL017. WI-38 cells were treated with vehicle, SL017 (10μM) and/or ascorbic acid (100μM) and CM-H2DCFDA (5μM). (a) WI-38 cells exposed to 5, 10 and 15min PDT. Values are percent change in relative fluorescence from baseline, mean ± SD; n≥5; * $p<0.05$ vs. vehicle control, # $p< 0.05$ vs. SL017. (b) WI-38 cells exposed to 2x30sec SDT. Values are percent change in relative fluorescence from baseline, mean ±SD; n≥5; * $p<0.05$ vs. vehicle control, # $p< 0.05$ vs. SL017

Figure 2.3

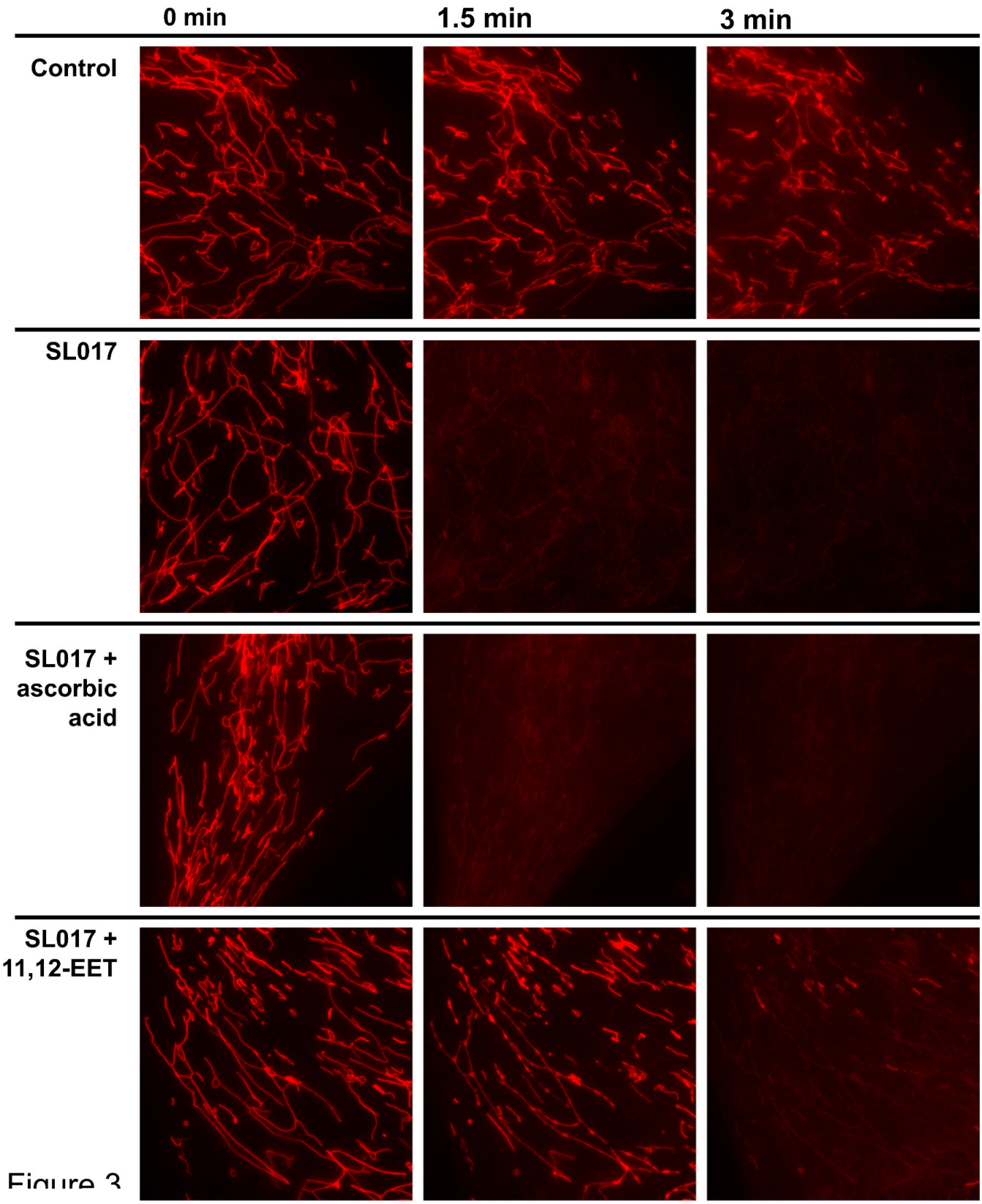

Figure 3

Figure 2.3 SL017 Induced Mediated Mitochondrial Membrane Potential Loss

Dissipation of mitochondrial membrane potential ($\Delta\Psi m$) following PDT activation of SL017. Representative microscopy images showing time-lapse loss of TMRE (100nM) fluorescence in WI-38 cells treated with vehicle, SL017 (0.1μM), ascorbic acid (100μM) and/or 11,12-EET (1μM)

Figure 2.4

a.

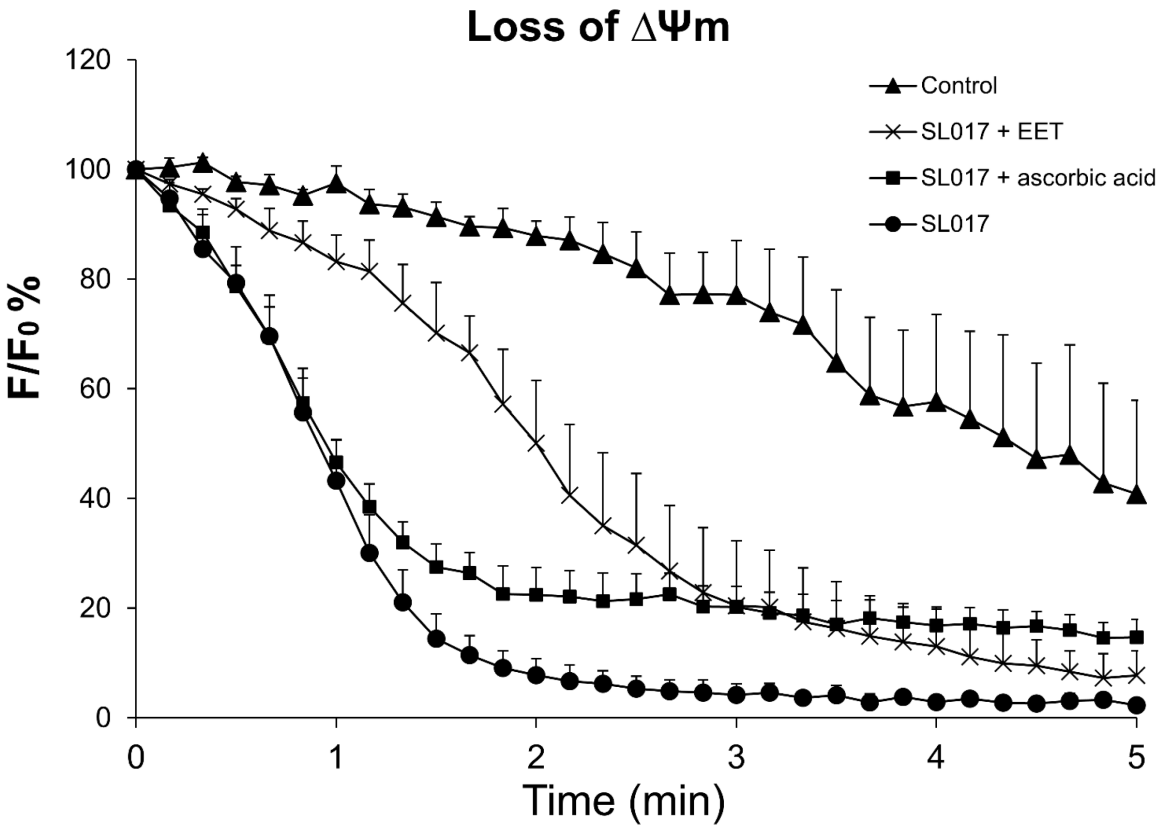
Loss of ΔΨm
Control
SL017 + EET
SL017 + ascorbic acid
SL017
F/F0 %
Time (min)
0
20
40
60
80
100
120
0
1
2
3
4
5

b.

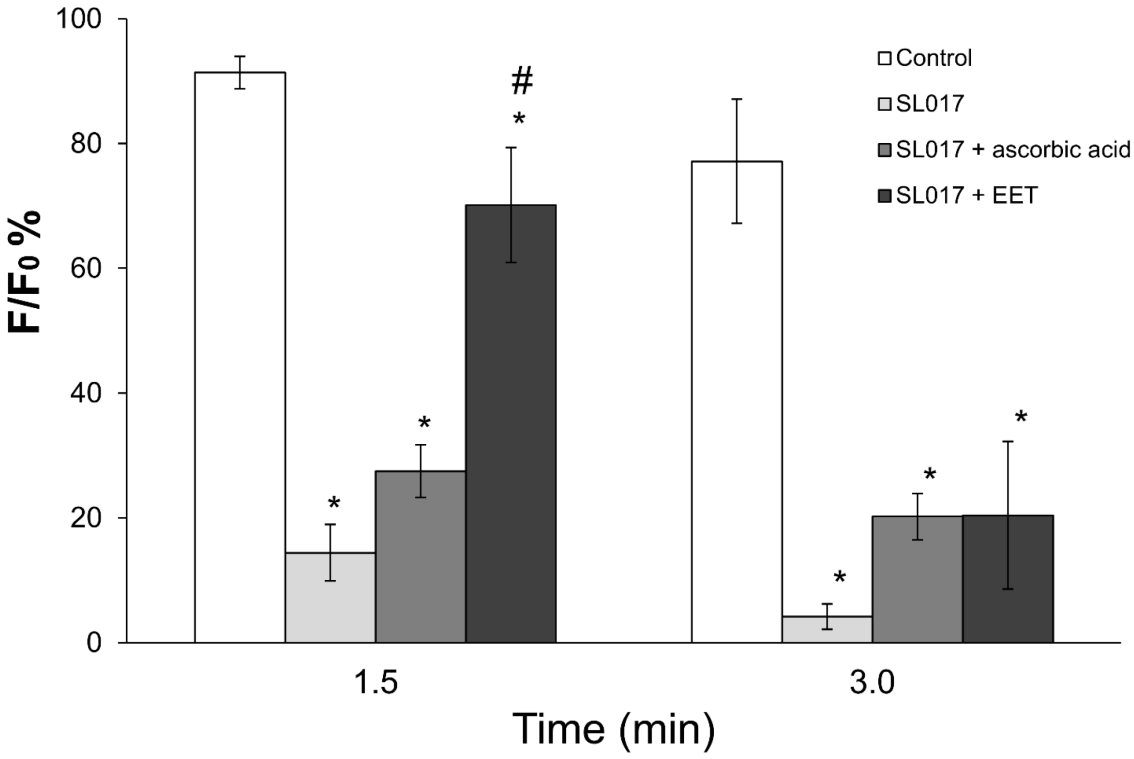
Control
SL017
SL017 + ascorbic acid
SL017 + EET
F/F0 %
Time (min)
1.5
3.0
0
20
40
60
80
100
#
*

Figure 2.4 Timecourse of SL017 Induced Mediated Mitochondrial Membrane Potential Loss

(a) Timecourse of the dissipation of mitochondrial membrane potential in WI-38 cells treated with vehicle, SL017 (0.1μM), ascorbic acid (100μM) and/or 11,12-EET (1μM). (b) Bar graph comparing relative differences in $\Delta\Psi m$ dissipation at 1.5 and 3.0 min of PDT. Values represented as percentage of the fluorescence before photodynamic therapy mean ± SEM, N=3-6, * $p<0.05$ vs. vehicle control, # $p< 0.05$ vs. SL017 treated group at the same time point

Figure **2.5**

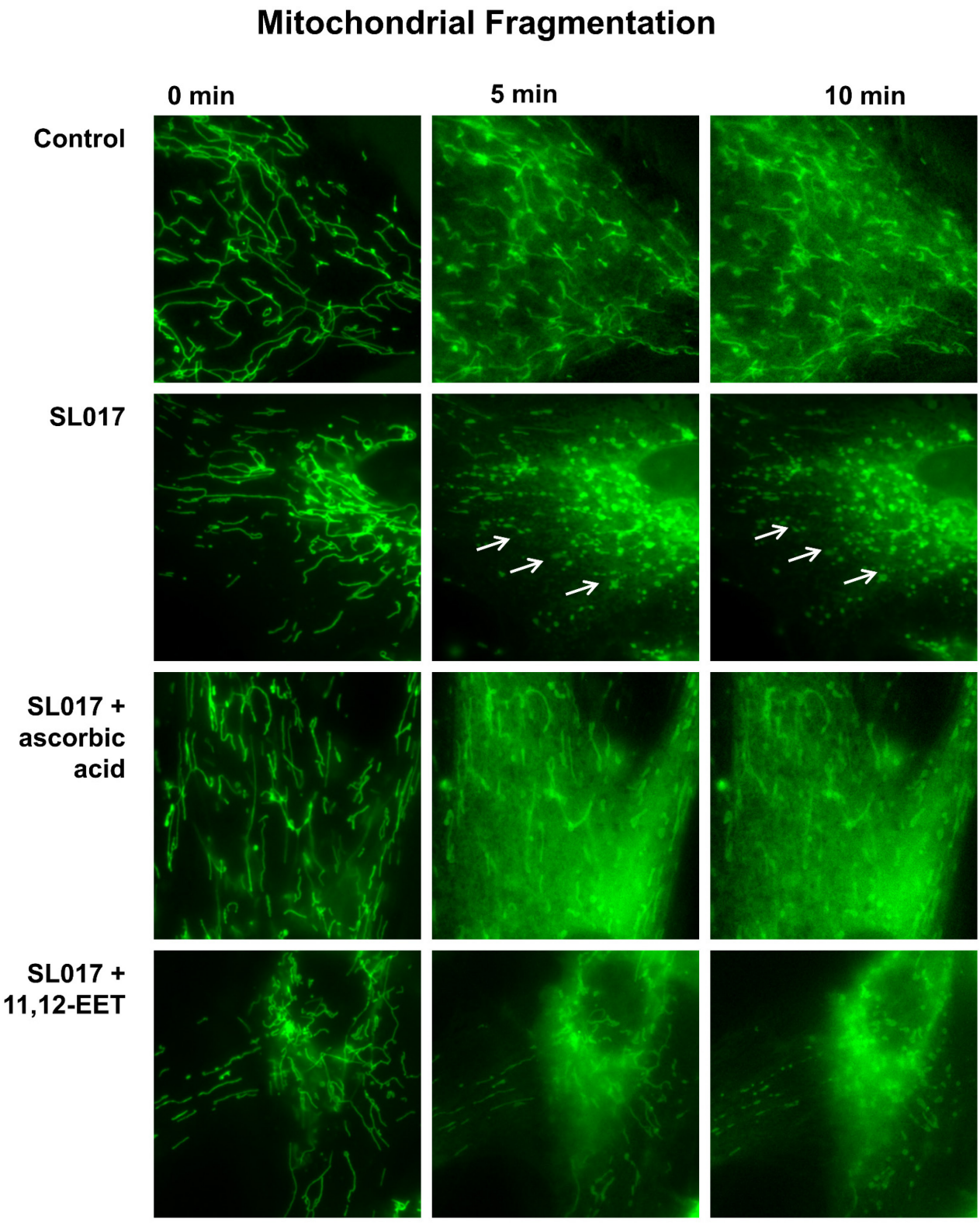
Mitochondrial Fragmentation
0 min
5 min
10 min
Control
SL017
SL017 + ascorbic acid
SL017 + 11,12-EET

Figure 2.5 SL017 Induced Mediated Mitochondrial Fragmentation

Representative frames from time-lapse series show PDT-induced activation of SL017 caused mitochondrial fragmentation in WI-38 cells treated with vehicle, SL017 (0.1μM), ascorbic acid (100μM) and/or 11,12-EET (1μM) and MitoTracker Green FM dye (100nM). Mitochondrial morphology, filamentous and tubular shape, of control cells remains unaltered during this time period. In contrast, SL017 treated cells exhibit significant punctuate and fragmented mitochondrial morphology, marked by arrows

2.4. DISCUSSION

Cellular uptake and mitochondrial localization resulted in a significant mitochondrial dysfunction following activation of SL017. The loss of mitochondrial membrane potential was partially attenuated by the Cytochrome P450 epoxygenase-derived metabolite of AA, 11,12-EET. Furthermore, increases in ROS production induced by PDT or SDT were abolished by the antioxidant, ascorbic acid. These results demonstrate that mitochondria, key organelles involved in regulating cell survival and death, are the central target for SL017 mediated cytotoxicity.

Ultrasound is a well-established tool for medical diagnosis and therapy that can provide significant advantages over PDT, such as being able to reach target sites deep within tissues[259]. PDT involves photo excitation of the photosensitizer molecule, stimulating its transition to a high energy triplet state[259]. The excited photosensitizer can then react directly with cellular substrates to form free radicals, or it can transfer its energy to molecular oxygen converting it to the highly reactive and mobile singlet oxygen. This latter process is the predominant mediator of cytotoxicity. Free radical generation and elevated oxidative stress attack several cellular components leading to apoptotic or necrotic cell death[262]. In contrast, SDT involves a more complex mechanism than PDT. Ultrasound consists of mechanical energy that propagates through tissue in the form of pressure waves. It has the potential to induce biological effects through both thermal and non-thermal mechanisms, depending on the ultrasound parameters

(i.e. frequency, intensity) and the properties of the medium being exposed[258, 259]. Thermal mechanisms arise from a local temperature increase due to absorption of the ultrasound energy. Non-thermal mechanisms consist of a variety of mechanical effects such as acoustic streaming (bulk fluid flow), radiation force, and acoustic cavitation (generation, growth, and collapse of small gas bubbles)[258, 259]. The violent collapse of bubbles during acoustic cavitation can also produce chemical effects such as generation of free radicals and sonoluminescent light[256, 257, 259]. Hypocrellins are photoreactive compounds that have high quantum yields of singlet oxygen following PDT[263]. As a hypocrellin, SL017 was expected to generate ROS upon photosensitization, but how ROS are generated upon activation by ultrasound is unknown. Evidence suggests a ROS-dependent mechanism similar to that for PDT[264-266], while other studies argue that sonosensitizers augment the cavitation effect[267]. Our data clearly demonstrate that both SDT and PDT activation of SL017 generates ROS: the precise mechanism remains to be determined.

Molecular pathways of cellular death are influenced by the intracellular distribution of the cytotoxic agent. Mitochondria are key organelles that regulate both cell survival and death. These organelles migrate through the cell, undergoing continuous fusion (elongation) and fission (fragmentation) processes (dynamics) to maintain proper function and meet cellular energy demands (energetics)[268, 269]. SL017 fluorescence was found to co-localize with the mitochondria-selective fluorescent marker

(Fig. 2.1B) suggesting a key role of mitochondria in its cytotoxic effect. Energy demand during normal function is supplied by ATP, which is generated from the proton motive force ($\Delta\mu_H$) created by proton (ΔpH) and electrochemical gradients ($\Delta\Psi_m$) established by electron movement through the respiratory chain[270-272]. In order to meet the energetic flux during work, cellular function and mitochondrial energetics are tightly regulated. Following PDT, SL017 triggered rapid dissipation of $\Delta\Psi_m$ at low doses, indicating impairment of mitochondrial respiration which reflects interruption of oxidative phosphorylation. The effects of SL017 were partially blocked by co-administration of 11,12-EET, consistent with previous data demonstrating its role in maintaining mitochondrial function following cellular injury[10, 74]. Interestingly, while co-administration of ascorbic acid with SL017 decreased ROS production, it failed to block the loss of $\Delta\Psi_m$. Thus, suggesting that SL017 targets mitochondria prior to an uncontrolled increase in cytosolic ROS production upon activation. This is important for preventing off- target effects and generalized toxicity.

To address whether SL017-mediated dissipation of $\Delta\Psi_m$ is a direct consequence of impaired mitochondrial membrane integrity, we utilized MitoTracker green (MitoTG), a mitochondrial specific probe, which remains in mitochondria regardless of $\Delta\Psi_m$. Our data demonstrated that the loss of TMRE occurred prior to the loss of MitoTG (Fig. 2.5), indicating that SL017 impaired mitochondrial function prior to disturbance of membrane integrity. Depending on the mitochondrial targets of SL017, localization to the inter-

membrane space may result in adverse effects to key proteins involved in maintaining the membrane potential. Alternatively, SL017 may induce opening of the mitochondrial permeability transition pore (mPTP)[273]. Changes to ΔΨm are directly influenced by the mPTP opening which allows passage of molecule <1.5 kDa, thereby initiating adverse effects. Examples include large osmotic pressure changes and uncoupling of oxidative phosphorylation, which ultimately result in cell death[274, 275]. Support for this mechanism of SL017 induced mitochondrial dysfunction stems from evidence that EET-mediated events limiting the loss of ΔΨm and slowing the opening of mPTP [10].

Significant decreases in fusion or increases in fission resulting from toxicity can lead to punctate, fragmented mitochondria which are thought to play a critical role in cellular dysfunction and death[157]. Activation of SL017 triggered formation of distinct mitochondrial spherical fragments well after the loss of ΔΨm, suggesting that dissipation of membrane potential (loss of mitochondrial function) triggered the onset of fragmentation. The precise relationship between mitochondrial membrane potential and mitochondrial dynamics is unknown. Evidence suggests that accelerated mitochondrial fission can be secondary to membrane depolarization[276]. Moreover, dissipation of $\Delta\Psi_m$ has been shown to induce disruption of cristae organization and inhibition of mitochondrial fusion leading to mitochondrial fragmentation[145]. Interestingly, addition of ascorbic acid to the culture medium did not alter the rate of ΔΨm loss, but delayed the rate of

mitochondrial fission. These data suggest that SL017-mediated mitochondrial fission involves both the disruption of membrane potential and the generation of ROS.

The present study demonstrates significant activation of the novel hypocrellin-B derived compound, SL017, by both PDT and SDT. Our data suggest that SL017 cytotoxic mechanisms involve disruption in mitochondrial function and activation of mitochondrial fragmentation which involves generation of ROS. Moreover, the data demonstrate that EET's can attenuate SL017 mitochondrial damage and potentially contribute to cancer therapy resistance. EET's are important lipid mediators that have a variety of cellular activities relevant to cancer pathogenesis and metastasis, such as promoting cell proliferation, enhancing angiogenesis and anti-apoptotic properties[4, 74, 79]. In conclusion, it appears that the mechanism of action of SL017 activated by visible light or ultrasound stems from generation of ROS and the loss of mitochondrial membrane potential.

2.5. LIMITATIONS

In this study, we used WI-38 cells as a cellular model to study the protective effect of 11,12-EET on mitochondria following SL017-induced PD stress. WI-38 cells are human lung fibroblasts[277], thus our results can be useful to understand the cytotoxicity of SL017-induced PD cancer therapy targeted to lung or tracheal tumors. However, other photosensitizers might lack the mitochondrial targeting properties of SL017 leading to a possibly different mechanism of cell toxicity. Our microscopy images revealed that SL017 co-localizes with mitochondria-specific stains indicating its selective concentration inside mitochondria. However, the extent of such accumulation in comparison to other cellular components has not been assessed. Further studies to assess the intracellular distribution of photosensitizers using 3D microcopy and advanced image processing to calculate 3D-colocalization indicators, such as Pearson's correlation coefficient and Manders' correlation coefficient[278], can provide a better insight on the mechanism of PD cytotoxicity.

We report here that 11,12-EET delayed the collapse of mitochondrial membrane potential following PD stress in WI-38 cells. These results correlate with a previous report demonstrated that 14,15-EET protected mitochondrial membrane potential of adult cardiomyocytes following laser induced stress with a mechanism involving inhibition of mPTP opining.[10] This similarity in stress model and protective effect of EETs suggests that 11,12-EET may also inhibit mPTP opening in WI-38 cells following PD

stress. However, we have not investigated such assumption and therefore we cannot confirm that this is the mechanism of EET protective effect described in this chapter. Importantly, these data suggest that protecting mitochondrial polarization during oxidative stress, possibly by inhibition mPTP opening, can be an important mechanism of EET-induced mitochondrial protection.

CHAPTER III

Photodynamic stress activates mitochondrial fission by several pathways

3.1. INTRODUCTION

Photodynamic therapy (PDT) is a promising approach to induce cell death in malignant tissues. It utilizes the ability of visible light to activate a previously administered drug, known as photosensitizer, to exert cytotoxicity within the cancer cell[279]. Once photo-excited, photosensitizer molecules can attack cellular proteins and lipids producing free radicals or transfer their energy to molecular oxygen generating highly ROS[280]. SL017 is a novel photosensitizer that can be activated both with light energy or ultrasound waves, allowing the versatility to be used for topical lesions or deep tumors[252]. In the previous chapter, we demonstrated that activation of SL017 induces a quick and extensive fragmentation of mitochondrial network in the human fibroblasts WI-38. This effect was partially attenuated by the antioxidant ascorbic acid and the epoxyeicosanoid 11,12-EET. As EETs lack antioxidant properties, it is unclear how EETs protect mitochondrial dynamics against photodynamic-induced fragmentation.

The ability of mitochondria to change their morphology has captured the attention of scientists for the last two decades. With the advances in microscopy, it has been verified that a mitochondrion is able not only to change its length and bending angle, but also to fuse together with other mitochondria into a longer or branched mitochondrion. It can also divide into two or more daughter mitochondria. These morphological dynamics turned out to be important for various mitochondrial functions, as well as the general homeostasis of the cellular activities. Currently, mitochondrial

dynamic processes are recognized essential for the development and the survival of animal cells[133, 137]. It has long been thought that mitochondria energetic activity is correlated with mitochondrial fusion, and that short mitochondria is a sign of defective or overstressed mitochondria. This stemmed from the major mitochondrial fragmentation that is observed during apoptosis and in dying cells[156, 219, 281]. Studying the changes in mitochondrial dynamics during apoptosis revealed significant roles of mitochondrial dynamics proteins in cell death pathways.

Dynamin related protein 1 (DRP1) is a cytosolic GTPase that regulates mitochondrial fission. Upon activation, DRP1 translocate to mitochondrial outer membrane where it self-assemble into a ring-like structure around the mitochondrion[152, 153]. It can then constrict the ring dividing the mitochondrion into two separate mitochondria[154, 155, 282]. Importantly, DRP1 activation was found to facilitate Bax dependent mitochondrial outer membrane permeabilization, an important step in apoptosis[222, 283]. Several studies demonstrated that inhibiting DRP1 is protective against apoptosis that result from acute cellular stress[223, 284, 285]. Interestingly, post translational modifications of DRP1 provides an important link between cell signaling pathways and mitochondrial dynamics[215, 231, 232]. For example, during cell division, DRP1 is phosphorylated at serine 616 (S616) which activates its translocation to mitochondria inducing fission[134]. However, during cellular stress such as starvation, DRP1 is inhibited by phosphorylation at serine 637 (S637) which

suppress mitochondrial fission promoting for mitochondrial elongation and cell survival[135, 286]. Importantly, DRP1 phosphorylation at S637 is mediated by protein kinase A (PKA)[231, 232, 287]. Several reports have demonstrated that PKA is activated as a result of EET signaling. External addition of EETs, or stabilizing their endogenous levels by inhibiting the soluble epoxide hydrolase, induced PKA activity in mice hearts[23, 235] and in several cellular models [40, 41]. This provides a possible interaction between EET signaling and regulation of mitochondrial dynamics that might explain the observed protective effect of EET against mitochondrial fragmentation.

Another example for mitochondrial dynamic protein that is important for cell homeostasis is the Optic Atrophy 1 (OPA1). OPA1 facilitates mitochondrial fusion by working on the interaction between mitochondrial inner membranes (MIM)[165, 172]. OPA1 is anchored by a transmembrane domain to MIM facing the intermembrane space (IMS)[163]. Regulation of OPA1 activity is controlled by proteolytic processing of OPA1 molecules. Several mitochondrial proteases cleave the transmembrane domain of OPA1 producing a shorter isoform (S-OPA1) soluble in the IMS[141, 203]. Both OPA1 isoforms, the soluble S-OPA1 and the membrane-bound long isoform (L-OPA1) are required for mitochondrial fusion[164]. Importantly, OPA1 molecules oligomerize in the IMS which is important in bringing the MIM together to form cristae[288, 289]. As cristae is the site where most of the mitochondrial respiration occur, OPA1 is then contributing significantly to mitochondrial function[132, 139, 174]. Upon activation of apoptosis, proapoptotic

signals like tBid interact with and disrupt OPA1 oligomers which remodel mitochondrial cristae and release cytochrome c[178, 180, 186]. This completes the mitochondrial outer membrane permeabilization (MOMP), an important step in the progression of apoptosis[180].

The interesting connection between mitochondrial dynamics and cell death warrants more investigation on the mechanism by which SL017 induced mitochondrial fragmentation. This would help understand the cytotoxic effect of PDT and explain the cytoprotective role of EETs against this promising approach of cancer therapy.

The aim of this study is to investigate the molecular bases of the activation of mitochondrial fission following photodynamic stress, and find out how EETs interfere with these mechanisms. Here we report that photodynamic stress induces mitochondrial fragmentation by activating the fission protein DRP1, and by inhibiting the fusion protein OPA1. 11,12-EET provided protection against SL017 cytotoxicity with a mechanism that did not involve these mitochondrial dynamics regulators.

3.2. MATERIALS AND METHODS

3.2.1. Materials

SL017 (2-(N,N-dimethylaminopropyl)amino-15-acetyl-3,10-dihydroxy-6,7,11-trimethoxy-14-methyl-15-H-cyclohepta(ghi)perylene-4,9-dione) was provided by Quest Pharmatech Inc. (Edmonton, AB) and was stored in the dark at -20°C. The 11,12-epoxyeicosatrienoic acid was obtained from Cayman Chemicals (Ann Arbor, MI). MTT (Methylthiazolyldiphenyl-tetrazolium bromide) and Trypan Blue were obtained from Sigma-Aldrich (St. Louis, MO). Antibodies for OPA1 was obtained from BD Biosciences (Franklin Lakes, NJ), for DRP1, pDRP1 (Ser616), and pDRP1 (Ser637) were obtained from Cell Signaling Technology (Danvers, MA)

3.2.2. Cell culture and Photodynamic treatment

Human lung fibroblast cells (WI-38) and Eagle's Minimum Essential Medium (E-MEM) were obtained from the American Type Culture Collection ATCC (Manassas, VA). Cell were cultured in antibiotic-free E-MEM supplemented with 10% fetal bovine serum under a humid atmosphere of 5% CO_2 in air at 37°C. One day prior to experiments, cells were seeded on experiment microplates at 20,000 cells/cm^2 in E-MEM containing 1% penicillin-streptomycin (Gibco, Invitrogen, Carlsbad, CA). At time of experiment, cells were incubated with 1 uM SL017 and/or 1 uM 11,12-EET for 30 min at 37°C in dark. To activate SL017, the cell monolayer was then placed 15 cm directly beneath a 50 W halogen lamp for 2.5 minutes.

3.2.3. Cytotoxicity determination

WI-38 cells were seeded on 24-well microplates one day before experiment. Following photodynamic treatment, cells were incubated at 37°C in dark for 2 hours to allow the execution of cell death pathways before viability was assessed. For MTT assay, the MTT reagent was added to the cells at final concentration of 3 mg/mL. The plates were incubated for 4 hours at 37°C in the dark to allow viable cells to reduce MTT to the insoluble MTT formazan derivative. The supernatant was carefully withdrawn and the insoluble crystals were dissolved in 400 uL DMSO. After a brief incubation with agitation at room temperature, 100uL aliquots were withdrawn into a 96-well plate and absorbance was read at 594 nm.

For Trypan Blue exclusion assay, cells were grown in 60 mm petri dishes one day before experiment. Following the photodynamic treatment, cells were detached by 0.25% Trypsin/1mM EDTA solution. Trypsin was removed and cells were re-suspended in 0.5 mL EMEM. An equal volume of 0.4% Trypan Blue solution was mixed with the cell suspension. Cells were then counted using a hemocytometer considering the blue stained cells as dead cells while unstained cells were counted as intact viable cells.

3.2.4. Western blot analysis

Following photodynamic treatment, cells were lysed with RIPA buffer and protein content were assayed with Bradford method. Equal protein content (20-30 ug) were denatured in reducing sample buffer at 95°C for 5 minutes and were then loaded on SDS-PAGE gels. Following the

electrophoresis separation, proteins were transferred into 0.2 μm PVDF membranes and probed with antibodies against the indicated proteins. Secondary antibodies linked to horseradish peroxidase were used to assess the amount of the target protein in the cell lysates.

3.2.5. Statistical Analysis

Statistical significance was determined using the unpaired Student's t-test and one-way ANOVA followed by Bonferroni multiple group comparison test were applicable. Results were considered significant if $p<0.05$.

3.3. RESULTS

3.3.1. Dose-dependent toxicity of PDT

To study the toxicity of PDT and the protective effects of EETs, we started by assessing cell viability following increasing doses of PDT treatment. We utilized the MTT assay where the faint yellow MTT reagent is converted intracellularly into a purple derivative only in living cells. The reaction product is then measured colorimetrically indicating cell viability[290]. We exposed WI-38 cells to a range of SL017 concentrations (0.1 – 1 μM) and duration of exposure to activating light (1 – 2.5 minutes). We observed a dramatic decrease in cell activity converting MTT reagent as the PDT dose increases (Fig 3.1A). Treating cells with 1 μM 11,12-EET did not alter these results.

We also assessed cell viability using the Trypan blue exclusion method. In this assay, active cells with intact plasma membranes excludes the blue stain, while dying cells with impaired membrane permeability are stained blue[291]. Applying this method we observed only a slight decrease in cell viability even when treated with the high dose of PDT (1 μM SL017 photoactivated for 2.5 min) (Fig 3.1B). We also recorded that co-treatment with 1 um 11,12-EET protected the cell against PDT-induced cell death..

These results suggested that the MTT viability testing was very sensitive to PDT toxicity in comparison to trypan blue assay. As the MTT reaction is mostly catalyzed by mitochondrial dehydrogenases[292, 293], it is responsive to mitochondrial damage and has been used as an indicator to

mitochondrial enzymatic activity[11]. Therefore, the decrease in MTT reduction can indicate mitochondrial injury following SL017 activation. In addition, being a redox reaction, MTT reduction is naturally sensitive to oxidative conditions[294] as in PDT. These data suggests that SL017-mediated PDT targets mitochondrial enzymes before it escalates to cell death marked by impaired plasma membrane integrity as detected by trypan blue. As 11,12-EET does not have antioxidant properties, it did not block the effect of PDT on mitochondrial dehydrogenases but it helped protect the cell against subsequent damage.

3.3.2. PDT induces phosphorylation of the fission protein DRP1 at S616

DRP1 is regulated by phosphorylation and dephosphorylation at two main sites; S637 and S616[216] (according to the amino acid sequence of human DRP1 isoform 1). To check whether DRP1 is involved in the PDT induced mitochondrial fragmentation, we evaluated the levels of both phosphorylated forms of DRP1 using phospho- specific antibodies. Photoactivation of SL017 led to variable levels of pDRP1 (S637) but with a consistent increase in the active pDRP1 (S616) form (Fig 3.2A-C). These results suggest that DRP1 is being activated as a result of SL017-mediated PDT which can result in mitochondrial fragmentation. Co-treatment with 11,12-EETs did not result in appreciable effect of on DRP1 phosphorylation following PDT stress.

3.3.3. PDT induces the proteolytic degradation of the fusion protein OPA1

Next, we checked the mitochondrial fusion protein OPA1. OPA1 is regulated by proteolysis at 2 levels. First, the cleavage of L-OPA1 into S-OPA1 which is required for normal OPA1 function[202]. Under cellular stress or in mitochondrial dysfunction, this constitutive proteolytic processing of OPA1 is excessively induced disturbing the balance between long and short OPA1 and blocking mitochondrial fusion[175, 204]. Second, the proteolytic degradation of the entire OPA1 molecule into non-functioning fragments. This normally happens during severe cellular stress and preceding apoptosis[180, 197]

Following PDT, we found that both OPA1 inhibitory processes were activated. PDT caused a significant decrease in the ratio of L-OPA1 to S-OPA1 indicating activation of L-OPA1 cleavage (Fig 3.2D). This result is expected considering the destructive effect of SL017 on mitochondrial membrane potential[252]. We also observed decreased expression of all OPA1 isoforms indicative to total degradation of OPA1 (Fig 3.2E). To confirm this and to rule out involvement of mitochondrial autophagy in lowering OPA1 levels, we compared OPA1 to known mitochondrial markers citrate synthase and prohibitin. Citrate synthase is a mitochondrial matrix protein while prohibitin is a MIM protein, both are frequently used to indicate mitochondria content in the cell[107, 295]. Levels of both citrate synthase and prohibitin were not affected by PDT treatment as did OPA1 (Fig 3.3A-C).

The ratio of OPA1 to either mitochondrial marker dropped following PDT treatment (Fig 3.3D,E). These data support a selective proteolytic degradation of OPA1 molecules which explains the observed mitochondrial fragmentation following photoactivation of SL017. Notably, EET treated cells showed no difference in regard to PTD effect on OPA1. This indicates that the protective effect of EET towards mitochondrial dynamics against PDT stress is not mediated through OPA1.

Figure 3.1

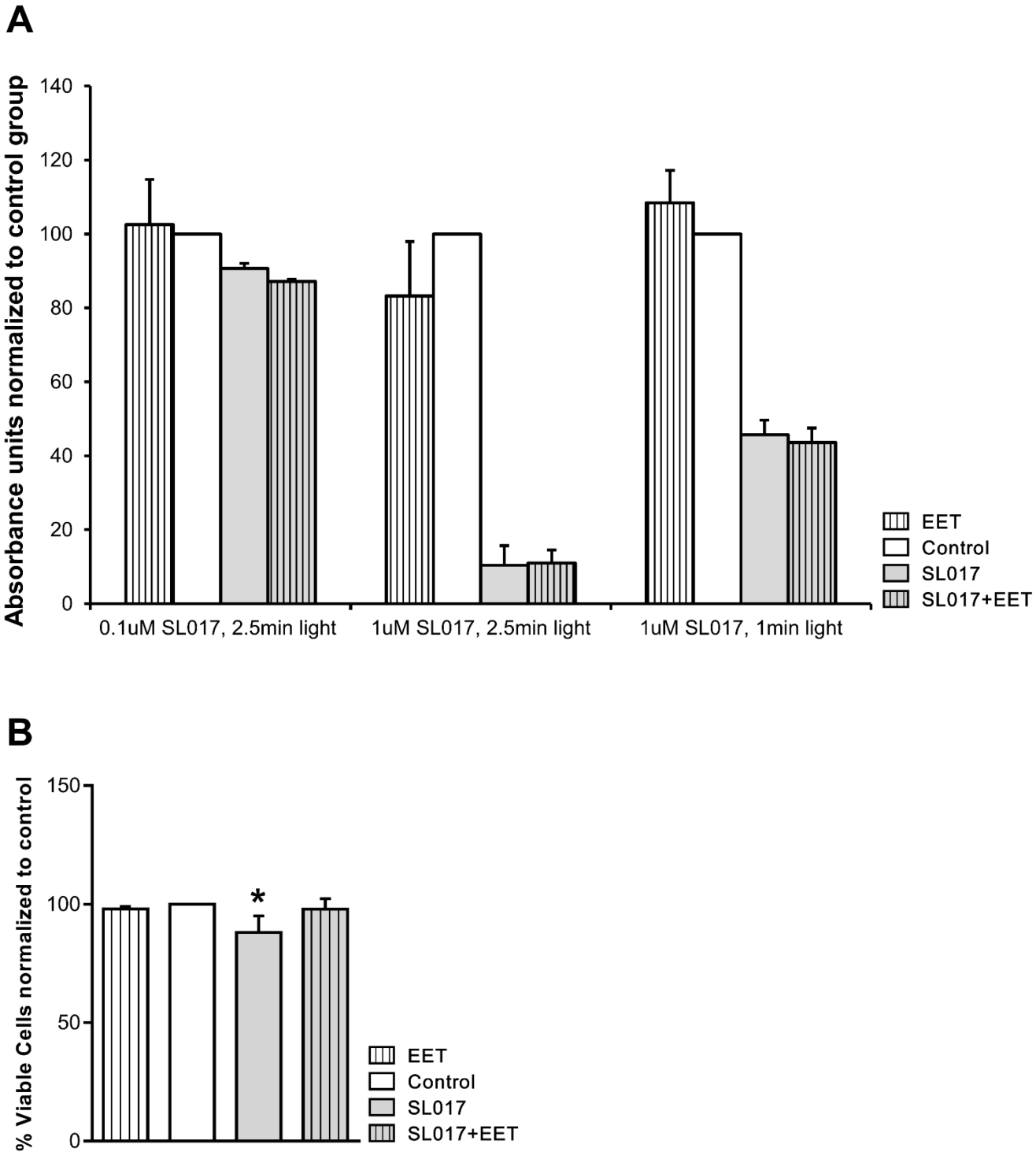
A
Absorbance units normalized to control group
140
120
100
80
60
40
20
0
0.1uM SL017, 2.5min light
1uM SL017, 2.5min light
1uM SL017, 1min light
EET
Control
SL017
SL017+EET
B
% Viable Cells normalized to control
150
100
50
0
*
EET
Control
SL017
SL017+EET

Figure 3.1 Dose-dependent toxicity of PDT

A. Cell viability was assessed with MTT reduction method. WI-38 cells were treated with the indicated concentration of SL017 with or without 1 μM 11,12-EET then subjected to the activating light for the indicated periods. B. Cell viability assessed by Trypan Blue exclusion method following incubation with 1 uM SL017 and 2.5 minutes photoactivation. Values represent means + SEM. n≥3. *=$p<0.05$ compared to corresponding control group

Figure 3.2

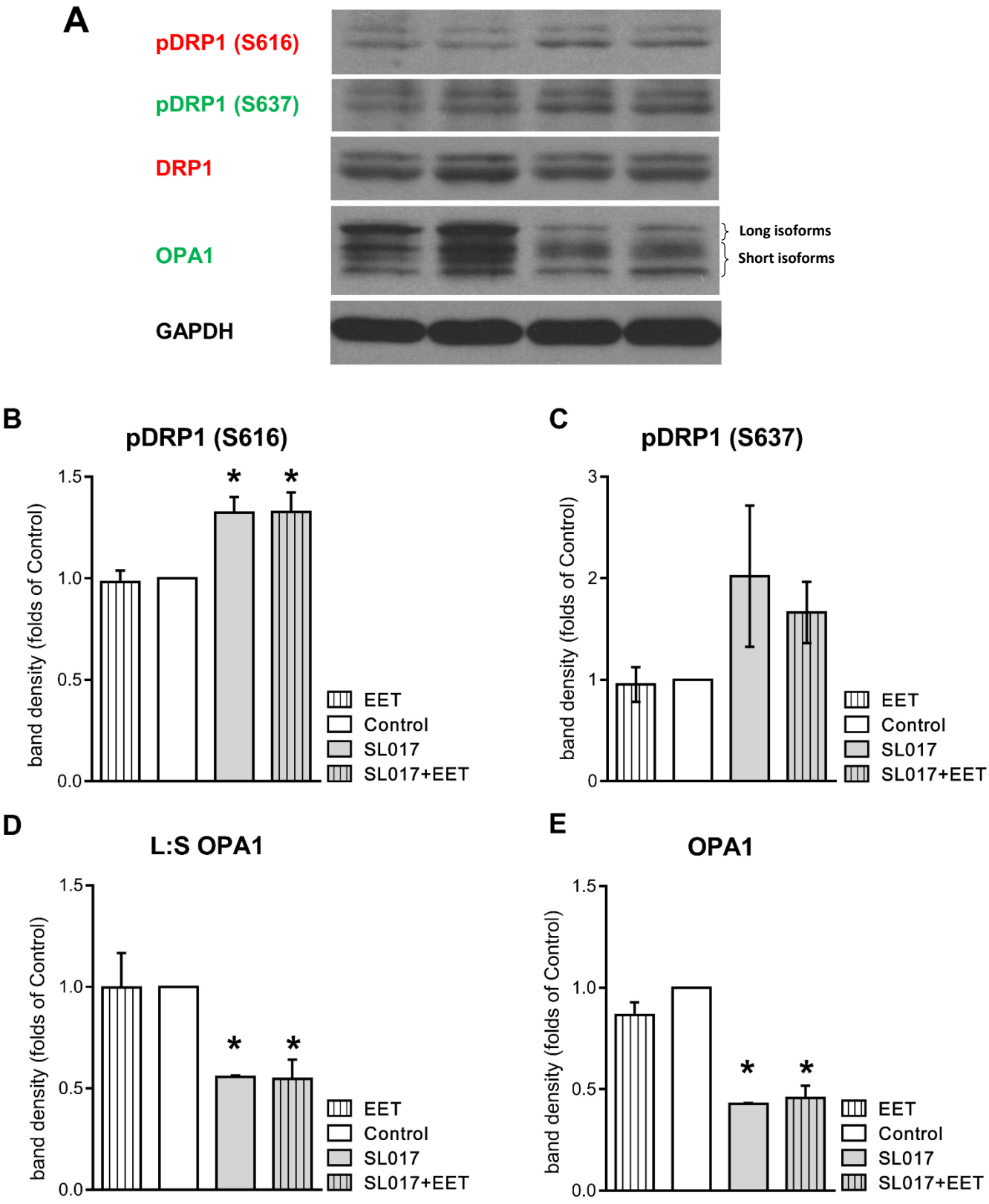
A
pDRP1 (S616)
pDRP1 (S637)
DRP1
OPA1
GAPDH
Long isoforms
Short isoforms
B
pDRP1 (S616)
band density (folds of Control)
1.5
1.0
0.5
0.0
*
*
EET
Control
SL017
SL017+EET
C
pDRP1 (S637)
band density (folds of Control)
3
2
1
0
EET
Control
SL017
SL017+EET
D
L:S OPA1
band density (folds of Control)
1.5
1.0
0.5
0.0
*
*
EET
Control
SL017
SL017+EET
E
OPA1
band density (folds of Control)
1.5
1.0
0.5
0.0
*
*
EET
Control
SL017
SL017+EET

Figure 3.2 PDT affect mitochondrial dynamics protein promoting fission

A, Western blot analysis for WI-38 cells following PDT. Cells were incubated with vehicle with and without 1 μM SL017 and 1 μM 11,12-EET for 30 minutes then subjected to activating light for 2.5 minutes. Proteins promoting mitochondrial fission was marked by the red color, while green denotes proteins promoting fusion. Treatment order is similar to that of B-E. **B, C, and E,** Densitometry and statistical analysis for the indicated proteins' bands. **D.** The ratio between long OPA1 isoforms (the upper two bands) to the short isoforms (the lower 3 bands). Values represent means + SD. n≥3. *=p<0.05 compared to control group.

Figure 3.3

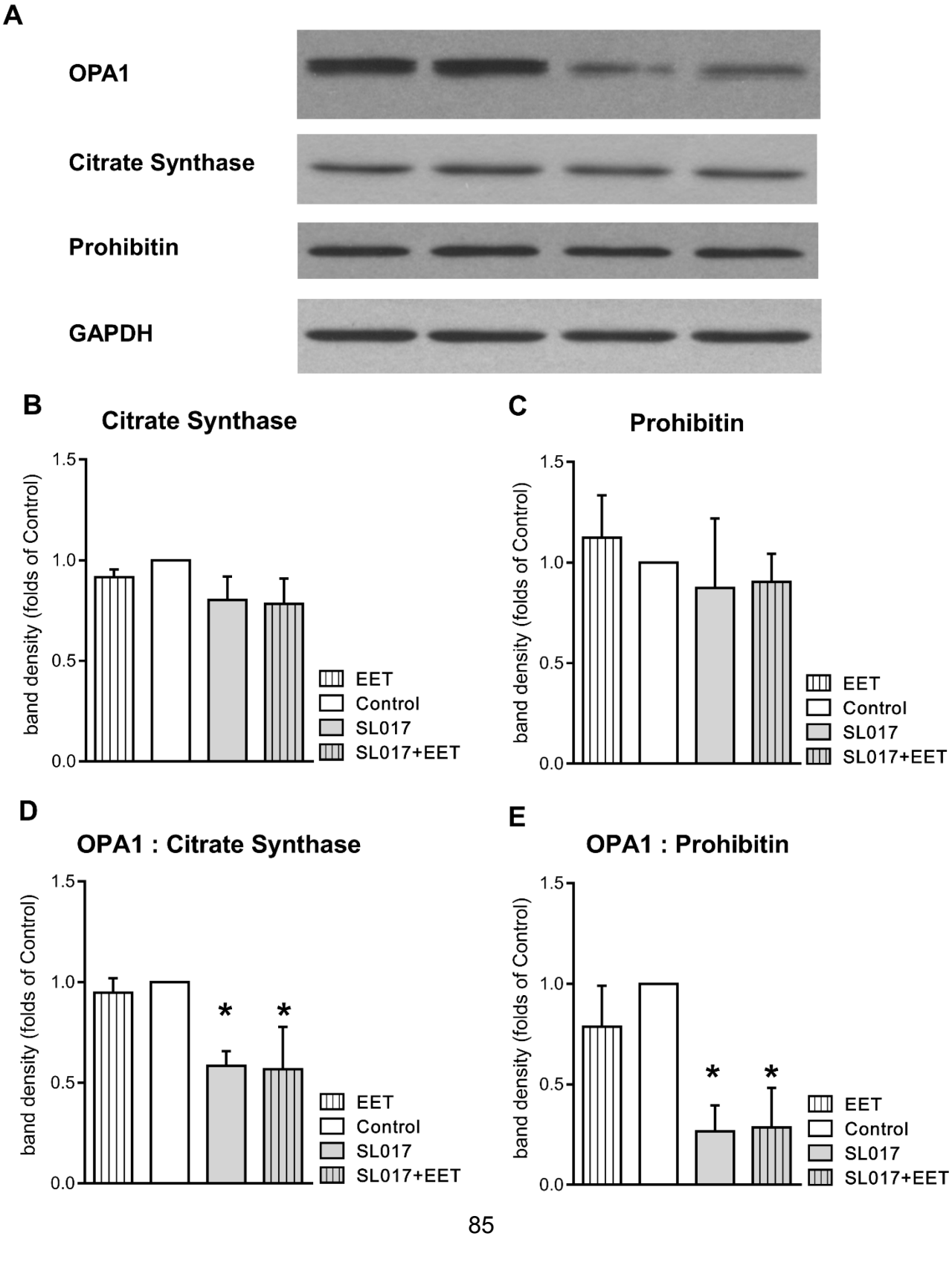
A
OPA1
Citrate Synthase
Prohibitin
GAPDH
B
Citrate Synthase
band density (folds of Control)
1.5
1.0
0.5
0.0
EET
Control
SL017
SL017+EET
C
Prohibitin
band density (folds of Control)
1.5
1.0
0.5
0.0
EET
Control
SL017
SL017+EET
D
OPA1 : Citrate Synthase
band density (folds of Control)
1.5
1.0
0.5
0.0
*
*
EET
Control
SL017
SL017+EET
E
OPA1 : Prohibitin
band density (folds of Control)
1.5
1.0
0.5
0.0
*
*
EET
Control
SL017
SL017+EET

Figure 3.3 Specific proteolytic degradation of OPA1

A, Western blot analysis for mitochondrial proteins in WI-38 cells following PDT. Treatment order is similar to that of B-E. **B, C,** Densitometry and statistical analysis for the indicated proteins' bands. **D, E,** The ratio of OPA1 to mitochondrial markers citrate synthase and prohibitin. Values represent means + SD. n≥3. *=p<0.05 compared to control group.

3.4. DISCUSSION

In this study, we provide further evidence for the mitochondrial toxicity of SL017-dependent PDT. We demonstrated that the PDT simultaneously activates phosphorylation of the fission protein DRP1 at S616 while inducing proteolytic inhibition of the fusion protein OPA1, both leading to the reported extensive mitochondrial fragmentation. Interestingly, we did not detect an appreciable effect for EETs on the PDT-dependent effect on either protein.

The wide use of MTT reagent as an indicator of cell viability has been contested by its specificity to mitochondrial enzymatic activity[293]. We found that MTT reduction is more sensitive to PDT-induced mitochondrial toxicity than other viability reporting methods such as trypan blue exclusion assay. Using both methods together can then provide a useful tool to easily report mitochondrial function in comparison to general cell viability and plasma membrane integrity. Our results suggest that photoactivation of SL017 causes a significant damage to mitochondrial activity followed by cell death marked by loss of plasma membrane selective permeability.

Very little is known about the redox regulation of mitochondria fission. Phosphorylation of fission protein DRP1 at S616 activates its translocation to mitochondrial membranes. Several kinases are reported to mediate phosphorylation of DRP1 at this site[133, 296]. Among them, only protein kinase C delta can be induced by oxidative stress leading to DRP1 activation and mitochondrial fission[230]. This mechanism can explain the stimulation of

DRP1 in PDT-induced oxidative stress. Alternatively, activation of DRP1 can be secondary to collapse of mitochondrial membrane potential. Cereghetti *et. al.* reported that disrupting mitochondrial polarization induces a significant rise in cytosolic calcium leading to activation of DRP1[233]. This was mediated in HeLa cells by the phosphatase calcineurin which dephosphorylates the inhibited pDRP (S637) promoting its activation. However, although we observed mitochondrial fragmentation following collapse of mitochondrial membrane potential (Fig 2.5), we found that pDRP1 (S637) did not drop following PDT stress in WI-38 cells. Therefore, our data suggest that PDT-induced mitochondrial fragmentation involves activation of DRP1 via phosphorylation of S616 but not via dephosphorylation of S637.

Another mechanism by which PDT can induce mitochondria fragmentation is by inhibiting OPA1 dependent mitochondrial fusion. We found that photoactivation of SL017 led to proteolytic degradation of both the long isoform of OPA1 as well as the total molecule. This would block mitochondrial fusion and cause a significant damage to mitochondrial function[297]. OPA1 inhibition have been reported in cells treated with toxic levels of H_2O_2[178], which supports a direct effect of PDT-produced ROS on the degradation of OPA1. As well, the proteolytic control of OPA1 is tightly linked to mitochondrial respiratory activity, membrane potential and mitochondrial ATP levels[171, 298]. Therefore, the observed effect on OPA1 can also be secondary to the collapse in mitochondrial function. Indeed, we

observed mitochondrial fragmentation following the dissipation of mitochondrial membrane potential[252]. Unlike the reversible nature of DRP1 phosphorylation, the proteolytic degradation of OPA1 is irreversible explaining the persistent mitochondrial fragmentation we reported earlier.

In conclusion, our data suggests that the rapid mitochondrial fragmentation following PDT treatment is mediated by activation of the fission protein DRP1, and that this effect is permanent due to the proteolytic degradation of the fusion protein OPA1 (Fig 3.4). These data provide an important insight on the redox regulation of mitochondrial dynamics. While some reports suggests that mild oxidative stress promotes mitochondrial fusion[210, 211], we report that severe oxidative stress, as in PDT treatment, is blocking fusion and activating fission. The level of cellular stress is therefore an important factor shaping the cellular response to photodynamic therapy. In addition, considering the role of DRP1 in apoptosis, our data can help adjust the PDT treatment to levels that induce programmed cell death rather than the inflammatory provoking necrosis, thus decreasing the adverse effects of this promising cancer therapy.

Importantly, although EETs have been protective to mitochondrial function following PDT insult and showed a moderate inhibition of mitochondrial fragmentation[252], our data suggests that this was not mediated through DRP1 or OPA1, at least using our experimental setup. We did not detect an appreciable effect of EETs on the levels of pDRP1 (S637) as we previously hypothesized. This can be due to multiple signaling

pathways activated during the toxic SL017 treatment. We concluded that SL017 with its intense toxicity might not be the best stress model to study the protective role of EETs towards mitochondrial dynamics. We then decided to move on to a more physiological stress model to establish the mitochondrial protective role of EETs. This is what I will discuss in the following chapter.

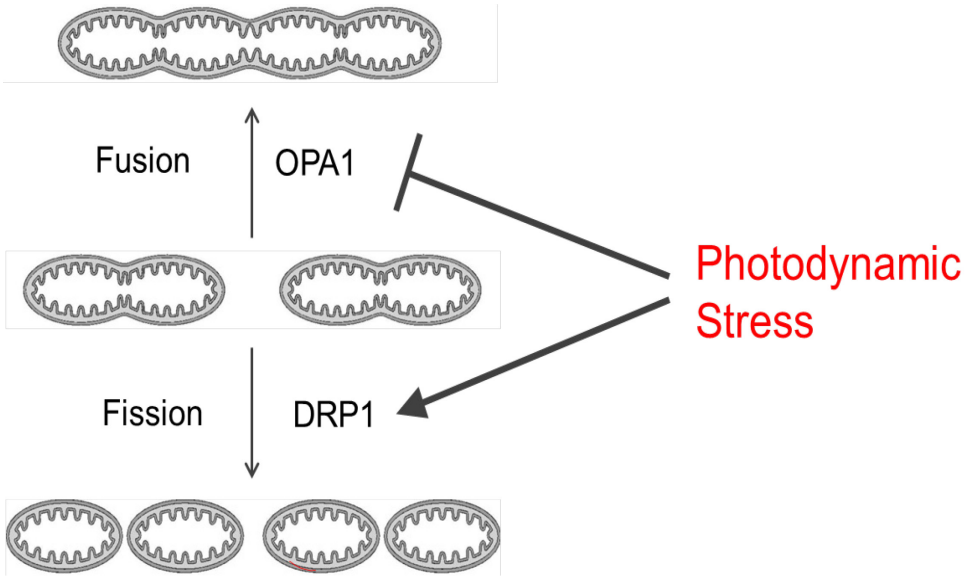

Figure 3.4 A diagram depicting the proposed mechanism of PDT-induced mitochondrial fission

Adapted from Liesa 2009[133]

CHAPTER IV

Novel Roles of Epoxyeicosanoids in Regulating Cardiac Mitochondria

A version of this chapter has been submitted for publication in the Public Library of Science ONE Journal: El-Sikhry, H.E., Alsaleh, N., Dakarapu, R., Falck J.R., & Seubert, J.M. Novel Roles of Epoxyeicosanoids in Regulating Cardiac Mitochondria. PLoS ONE

4.1. INTRODUCTION

Mitochondria provide the primary source of energy that fuels the contractile apparatus within the heart and have a key role in regulating cellular death pathways. These dynamic organelles are closely related to cellular energy demands and stress levels.[268, 269, 299] As cardiomyocytes are post-mitotic cells, maintenance of a healthy pool of mitochondria depends upon a delicate balance between newly generated organelles and efficient turnover of irreversibly damaged ones.[300, 301] Mitochondrial quality control is maintained through precise coordination of a complex interplay between mitobiogenesis and selective degradation through autophagic processes. Dysfunctional mitochondria disturb the energetic balance in the myocardium and can initiate cell death.[124] The removal of dysfunctional mitochondria is an important process to maintain a robust mitochondrial network within the cardiomyocyte.[125, 302] Indeed, compromised mitochondrial quality is linked to major cardiovascular pathologies such as heart failure and ischemic heart disease.[7, 303] Thus, optimum mitochondrial health is vital for cardiomyocyte performance and resistance to stress.

Mitochondria are a major site of interaction between energy metabolism and survival pathways, therefore their response to cellular metabolic stress shapes the cellular fate.[111] During nutrient restriction and other forms of cellular stress, mitochondria fuse into elongated hyperfused network, which is termed Stress Induced Mitochondrial Hyperfusion (SIMH).[192, 210, 304] The transient hyperfused adaptation provides protection

against apoptosis and spares mitochondria from autophagic degradation.[135, 305] However, sustained mitochondrial hyperfusion has been reported to induce inflammatory and apoptotic pathways.[306, 307] Importantly, the majority of reports concerning mitochondrial response to cellular stress have been conducted in non-cardiac cells.

An important regulator of mitochondrial dynamics and function is the Optic Atrophy 1 (OPA1). OPA1 is a large GTPase associated with the mitochondrial inner membrane (MIM) playing key roles in regulating mitochondrial function and quality control by blocking the fusion of dysfunctional mitochondria segregating them for autophagic removal.[176, 178, 186, 308] Recent studies demonstrate that OPA1 regulates mitochondrial reaction to cellular stress.[174, 191] This OPA1-dependent stress response adapts mitochondrial respiration and apoptotic resistance according to the metabolic demand and the cellular stress status. Despite the mounting evidence that OPA1 is a key regulator of mitochondrial function, very little is known about the role it plays in cardiovascular health.

The essential polyunsaturated fatty acid AA serves as the main precursor for the production of eicosanoids via several pathways. Epoxyeicosatrienoic acids (EETs) are cytochrome P450-dependent epoxides of AA that possess autocrine and paracrine signaling activity regulating a wide range of cellular functions.[4, 35] Several reports indicate a protective effect of EETs toward cardiac mitochondria.[10, 74, 252, 309] We recently reported EETs enhance an autophagic response in cardiac cells

promoting their survival during starvation.[11] This was accompanied with preserved mitochondrial function, a key element in cardiac health and resistance to stress. However, it is largely unknown how EETs signaling help enhance mitochondrial resistance to challenging conditions.

In the current study, we further investigate the role of EETs in regulating cardiac mitochondria and improving cellular survival during starvation stress. We report that EETs are actively involved in the regulation of mitochondrial quality and biogenesis. Thus, we provide novel insight into EET-mediated cardioprotective mechanisms that involve maintaining the quality of cardiac mitochondria.

4.2. METHODS

4.2.1. Cell culture and treatment protocol

HL-1 cardiac cells were a kind gift from Dr. Claycomb (New Orleans, LA, USA). Cells were cultivated at 37°C in a humidified atmosphere of 5% CO_2 and 95% air in Claycomb media (Sigma) supplemented with 10% fetal bovine serum (FBS), glutamine (2mM) and norephinephrine (0.1mM).[11] Starvation was modulated by incubating cells in serum and amino acid-free buffer (in mm: 110 NaCl, 4.7 KCl, 1.2 KH_2PO_4, 1.25 $MgSO_4$, 1.2 $CaCl_2$, 25 $NaHCO_3$, 15 glucose, 20 Hepes, pH 7.4) as previously described.[310] In this study, we utilized a novel EET-analogue, UA-8 (13-(3-propylureido)tridec-8-enoic acid, 1μM)) that possesses EET-mimetic and sEH inhibitory properties.[97] In order to block EET-mediated effects, we utilized the antagonist, 14,15-epoxyeicosa-5(Z)-enoic acid (14,15-EEZE, 10μM). Control experiments utilized 14,15-EET (1μM).

4.2.2. Aconitase catalytic activity

Mitochondrial aconitase enzymatic activity were measured spectrophotometrically utilizing MitoSciences kit MS745 (abcam) as previously described.[311] Briefly, mitochondria were isolated from HL-1 cells following starvation protocol and approximately 50μg of mitochondrial preparation were placed in each microplate well. Equal amounts of the substrate isocitrate were added to all wells and the absorbance at 240nm was recorded for 30 minutes. The catalytic activity was measured by the rate of formation of cis-aconitate as detected by the increase in absorbance.

4.2.3. SIRT1 catalytic activity

SIRT1 deacetylation activity was measured by a chemo-luminescence method using SIRT-Glo kit from Promega. Cells were incubated with a proprietary acetylated substrate and 1μM Trichostatine A. Luciferase enzyme is included in the assay medium to convert the deacetylated reagent into a luminescent product. The reaction allowed to equilibrate for 30 minutes and the luminescence was measured reflecting SIRT1 activity.

4.2.4. Mitochondrial Respiration and Cellular energy levels

Mitochondrial oxygen consumption was measured in permeabilized cells as previously described.[312] Approximately 250μg protein of the cell suspension were loaded in the Oxygraph Respirometry chamber in 2mL respiration medium (EGTA 0.5 mM, $MgCl_2.6H_2O$ 3 mM, taurine 20 mM, KH_2PO_4 10 mM, HEPES 20 mM, BSA 0.1%, potassium-lactobionate 60 mM, mannitol 110 mM, dithiothreitol 0.3mM, pH 7.1, adjusted with 5 N KOH) containing 25μg/mL saponin and let to equilibrate for 10 min at 30°C. Complex I substrates glutamate (10mM) and malate (5mM) were then added and oxygen consumption was recorded in the absence of ADP (State 4 respiration). Maximal respiration rate was then activated with the addition of 1mM ADP (State 3 respiration). Respiration rate was represented as nmole O_2 consumed per mg protein per minute. The ratio between respiration rate before and after the addition of ADP (respiratory control ratio, RCR) was also reported.

To measure cellular energy levels, we used a luciferin bioluminescence-based kit (Sigma–Aldrich) to assay the ratio between ATP and ADP in HL-1 cells as described previously[313]. Briefly, cells were cultured on a 96-well plate and treated according to starvation protocol. The culture media was then removed and the ATP assay reagent was added containing D-luciferin substrate and the luciferase enzyme. ATP immediately reacts with the substrate producing light that was measured with a luminometer. ADP assay reagent was then added to enzymatically convert ADP to ATP which then reacted with the substrate and produced additional light reflecting the ADP content.

4.2.5. DNA-Binding activity of pCREB, NRF1, and NRF2

The activity of transcription factors CREB, NRF1, and NRF2 were measured by their ability to bind to their corresponding target DNA sequences. Specified ELISA kits were used for pCREB-Ser133 (Cayman Chemicals), NRF1 (Assay BioTech), and NRF2 (Active Motif). Briefly, following treatment protocol, cells were lysed and the nuclear fraction was extracted according to the assay protocols. Equal protein amounts were incubated on assay plates coated with the corresponding DNA sequence specific to the transcription factor. Only active transcription factors bind to the DNA-coated plates allowing their immunodetection using the provided antibodies. The substrate TMB (3, 3', 5, 5'-Tetramethylbenzidine) was added as a substrate to the HRP-linked secondary antibodies producing a

blue color. The reaction was then stopped by sulfuric acid and absorbance was measured at 450nm indicating the bound transcription factors.

4.2.6. Mitochondrial morphometric analysis

We employed a morphometric analysis approach developed to track filament-like structures to characterize the 3-dimentional morphology of both individual mitochondria and networks.[314] HL-1 cells were grown on glass-bottom 35-mm dishes or 6-well microplates suitable for fluorescent microscopy (MatTek) and treated as outlined above. Next, mitochondria were stained with MitoTracker Red (100nM) or TMRE (100nM) and placed in a micro-incubator installed on the objective stage of a Zeiss AxioObserver epifluorescence microscope. A series of Z-stack images were acquired at optimal z intervals with a Plan-Apochromat 63x / 1.4 oil immersion objective lens. A minimum of 5 random spots, each containing an average of 10 cells, were imaged per treatment group. Experiments were repeated at least 3 independent times and images contained a minimum of 100 cells per treatment group and files were renamed for blind morphometric analysis. Images were first de-convoluted and 3D images of the mitochondrial network were reconstructed using Bitplane Imaris software. The FilamentTracer module was used to track mitochondrial voxels in the 3D space to identify individual mitochondrial bodies and characterize their morphology. The Threshold (loops) algorithm was used to detect mitochondrial fluorescence signal and the approximate diameter was set to ignore signals less than 0.2μm improving signal to noise ratio. Mitochondria

were categorized according to their length into three categories; fragmented mitochondria (0.2-0.5μm), short-to-medium length mitochondria (0.5-5μm) and long-branched mitochondria (>5μm), as reported previously.[314] To better describe the distribution of mitochondria between the categories, the volume of mitochondria were compared to overall total mitochondrial of the population. The ratio between the volume of all long mitochondria to the volume of short and fragmented mitochondria combined was used to compare mitochondrial populations (Fig 4.1A, B). Validation was performed by treating HL-1 cells with positive or negative controls for the DRP1-dependent mitochondrial fission (Fig 4.1C). To activate mitochondrial fission, cells were treated with the PKA inhibitor H89 (1μM) and the calcium ionophore ionomycin (5μM). To inhibit fission and promote mitochondrial elongation, cells were treated with the adenyl cyclase activator forskolin (20μM) and the calcineurin inhibitor cyclosporin A (10μM).

4.2.7. Assessment of OPA1 Oligomers

OPA1 oligomers were stabilized with protein crosslinking and assessed with immunoblotting as previously described,[178, 197] Briefly, following treatment protocol, cells were washed twice with washing buffer (in mM; 120 KCl, 5 KH_2PO_4, 10 HEPES, 1 $MgSO_4$, and 2 EGTA, pH 7.4), then incubated for 30min at 37ºC in the reaction buffer (50 μg/mL digitonin and 20 mM EDC in washing buffer). 1-Ethyl-3-[3-dimethylaminopropyl] carbodiimide hydrochloride (EDC) was used as a cross linker for zero-length, carboxyl-to-amine conjugation to forms stable covalent bonds

between OPA1 molecules in the oligomer enabling their detection with SDS-PAGE analysis[178, 197] Lysis buffer was then added containing 50mM dithiothreitol (DTT) to quench the crosslinking reaction[178]. Cell lysates were gathered for protein assay and SDS-PAGE using 7% gels.

4.2.8. Assessing cristae density

HL-1 cells were grown and treated on glass-bottom dishes (MatTek). Cells were prepared for transmission electron microscopy immediately after experiment as previously described.[11] Briefly, the cell monolayer was fixed with Karnovsky (2% glutharaldehyde and 2% paraformaldehyde), post-fixed in 1% osmium tetroxide and stained in 2% unanyl acetate prior to dehydration and blocking. Electron micrographs were acquired with the Philips 410 electron microscope at 17000x. The experiment was repeated 3 times and electomicrographs were renamed for blind analysis. The density of cristae folds in the mitochondria was assessed by counting number of cristae membranes per perpendicular unit of distance (μm).

4.3. RESULTS

4.3.1. Mitochondria accumulate during starvation

Similar to what we reported in rat neonatal cardiomyocytes, starvation caused a significant increase in levels of mitochondrial proteins in cardiac HL-1 cells.[11] SDS-PAGE western blot analysis revealed a consistent elevation in mitochondrial markers such as cytochrome c oxidase subunit 4 (COX IV), succinate dehydrogenase (SDH) and prohibitin (Fig 4.2A-C) following 24h of starvation. The same effect was observed among all starved groups treated with UA-8 and/or 14,15-EEZE. Normalization of protein levels to cytosolic α-tubulin indicated a relative increase in mitochondrial mass following 24h of starvation.

Previously, we demonstrated the increased mitochondrial mass following 24h of starvation caused a marked decrease in mitochondrial respiratory enzyme activity.[11] In the current report, we assessed aconitase activity, an important tricarboxylic acid cycle enzyme, in the presence of either UA-8 or 14,15-EET in HL-1 cells after 4, 12, and 24h of starvation (Fig 4.2D-F). Due to its redox sensitivity, aconitase activity is commonly utilized to indicate mitochondrial oxidative stress.[315, 316] We observed a significant decrease in aconitase activity following 4h of starvation, whereas UA-8 and 14,15-EET treated cells had preserved activity. UA-8 treated cells continued to show higher aconitase activity compared to starved groups following 24h of starvation. Importantly, addition of the inhibitor 14,15-EEZE abolished the protective effect of UA-8 and 14,15-EET.

The coupling of respiration with generation of ATP, oxidative phosphorylation, is the most essential component of mitochondrial function. The ratio between basal mitochondrial oxygen consumption and ADP-stimulated states indicates the respiratory control ratio (RCR), which reflects mitochondrial bioenergetic efficiency. We measured the effect of starvation on mitochondrial respiration in permeabilized HL-1 cells. Starvation caused a significant decline in RCR, reflecting a collapse in mitochondrial function (Table 1). Importantly, cells treated with UA-8 showed a marked preservation in mitochondrial respiration, which was attenuated by 14,15-EEZE. Consistent with starvation-induced mitochondrial dysfunction, the cellular ratio of ADP/ATP significantly increased over the 24h time course (Fig 4.3). Treatment with UA-8 (Fig 4.3A, B) or 14,15-EET (Fig 4.3C, D) resulted in a significant reduction in the ADP/ATP ratio indicating preserved mitochondrial function.

4.3.2. Starvation-induced mitochondrial hyperfusion

Our results show a starvation-induced increase in mitochondrial mass and decline in function; however, EET-mediated events prevented the loss of function suggesting a preserved pool of mitochondrial quality. It has been shown that starvation stress inhibits mitochondrial fission in non-cardiac cells leading to mitochondrial elongation and formation of hyperfused mitochondrial networks.[135, 317] As mitochondrial fission is required for proper mitochondrial quality control, we assessed mitochondrial dynamics in cardiac HL-1 cells following starvation. We optimized an

automated morphometric analysis to define alterations in mitochondrial dynamic balance. Mitochondrial morphology of starved HL-1 cells confirmed the starvation-induced hyperfusion, which was sustained for 24 hours (Fig. 4.4A). Mitochondrial particles and short tubes of non-starved cells turned into branched interconnected networks composing the majority of the cell's mitochondrial volume. Interestingly, UA-8 treated cells showed significantly less mitochondrial hyperfusion, while co-treatment with 14,15-EEZE abolished the UA-8 effect (Fig. 4.4A). Blind morphometric analysis of microscopical 3D images from three independent starvation experiments confirmed that UA-8 inhibited the starvation-induced mitochondrial hyperfusion (Fig. 4.3B).

Fusion and fission processes are regulated by a group of proteins including DRP1, Fis1 and Mfn2. Immunoblot analysis of the relative levels of these proteins was performed following 24 hours of starvation. We found a significant reduction in mitochondrial pro-fission protein DRP1 in all starved groups (Fig. 4.4C) which correlated with the observed hyperfusion, while Fis1 and Mfn2 did not show a consistent response to either starvation or UA-8 (Fig 4.4E, F).

4.3.3. Starvation effects on OPA1 oligomers and cristae density

OPA1 is a dynamin-like protein found in the inner mitochondrial membrane that regulates both mitochondrial fusion and cristae structure. Following 24h starvation, UA-8 treatment results in a decreased ratio of long isoform of OPA1 (L-OPA1) to short isoforms (S-OPA1, Fig. 4.5A), while the

total expression of all OPA1 isoforms did not significantly change (Fig 4.5B). Since S-OPA1 is the product of proteolytic processing of L-OPA1[170], these data indicate a stimulating effect of UA-8 on the processing of L-OPA1 to S-OPA1 during starvation. Furthermore, co-treatment with 14,15-EEZE attenuated the processing effect of UA-8 treatment toward OPA1 isoforms. L-OPA1 is required for mitochondrial hyperfusion [192]. HL-1 cells treated with UA-8 had reduced levels of L-OPA1 (Fig 4.5A), which correlated with the lower amount of hyperfused mitochondria observed during starvation (Fig 4.3A,B). In addition to a role in mitochondrial fusion, OPA1 molecules assemble into oligomers necessary for cristae organization [184]. Following the results of UA-8 on OPA1 isomers, we then looked at its effect on OPA1 oligomers. We assessed the effects of starvation and UA-8 treatment toward UA-8 oligomer levels. Stabilizing OPA1 oligomers with crosslinking (Fig 4.5D) allowed us to detect increased levels of OPA1 oligomers following starvation and UA-8 treatment. The enhanced level of oligomers following UA-8 was attenuated by co-treatment with 14,15-EEZE (Fig 4.5E).

Mitochondrial ultrastructure was assessed using electron microscopy in non-starved and starved cells following treatment. Mitochondria in non-starved cells had loose cristae arrangement with low number per mitochondrion, which was increased following 24h starvation (Fig 4.5F, G). Mitochondria in UA-8 treated cells had compact cristae structure using most of the space inside the mitochondrion, which was reduced by co-treatment with 14,15-EEZE (Fig 4.5F, G). OPA1 oligomers

are important to cristae organization, which ultimately impacts mitochondrial respiratory efficiency [318]. These data suggest that EET-mediated signaling involves regulation of OPA1 oligomers and cristae density thus contributing to the enhanced mitochondrial function observed in UA-8-treated cells.

4.3.4. EET signaling induce mitochondrial biogenesis

An important element of the mitochondrial quality is the biogenesis of mitochondrial proteins. EETs are recognized agonists for peroxisome proliferator-activated receptors (PPARs) [313, 319], which play a significant role in promoting expression of several mitochondrial proteins [320, 321] Recently, Wang et al. reported that 14,15-EET induced mitochondrial biogenesis in cortical neuronal cells via activation of cAMP-response element binding protein (CREB), which in turn activated the peroxisome proliferator-activated receptor gamma-coactivator 1 (PGC1) [322]. In order to determine the involvement of mitochondrial biogenesis in the protective effect of EETs in HL-1 cardiac cells, we assessed several regulators of mitochondrial biogenesis following 6 and 24 hours of starvation. We measured DNA binding activity of pCREB (Ser133), an upstream activator of PGC1. Starvation induced a marked 6-fold activation of pCREB during the first few hours (Fig 4.6A), which subsided by 24h (Fig 4.6B). However, both 14,15-EET and UA-8 preserved pCREB activity (Fig 4.6B), an effect that was completely abolished with 14,15-EEZE co-treatment. Of note, pCREB in non-starved cells was not as sensitive to 14,15-EET or UA-8.

Next, we assessed the catalytic activity of the nuclear deacetylase SIRT1, which can deacetylate PGC1 resulting in activation of mitochondrial biogenesis [323]. We observed a time-dependent SIRT1 response to starvation-induced stress, with activation at 6h (Fig 4.6C) followed by a drop below non-starvation levels at 24h (Fig 4.6D). Interestingly, 14,15-EET and UA-8 preserved SIRT1 activity at the 24h point, which was attenuated by co-treatment with 14,15-EEZE (Fig. 4.6D). We observed a moderate activation of SIRT1 activity in non-starved cells treated with 14,15-EET.

Downstream targets of PGC1 include transcription factors, nuclear respiratory factor 1 and 2 (NRF1, and NRF2), which promote the expression of mitochondrial respiratory complexes, mitochondrial DNA transcription factors and antioxidant defense genes [324]. We assessed the activity of NRF1 and 2 DNA binding following 6 and 24h of starvation. NRF1 and NRF2 DNA binding activity was significantly increased in HL-1 cells treated with 14,15-EET, under both starvation and non-starvation conditions (Fig 4.7A-D). This effect was sustained for 24h and inhibited with the EET antagonist 14,15-EEZE. Together, these data suggest EET-mediated signaling events are involved in the regulation of mitochondrial biogenesis and energy metabolism.

Table 1. Mitochondrial respiration

The rate of oxygen consumption in different states of mitochondrial respiration. Values represent mean ± SEM, N≥3, *, $p<0.05$ in comparison to non-starvation control, #, $p<0.05$ in comparison to starvation control.

		O_2 Consumption (nmol O_2/min/mg protein)		
		State 4	State 3	RCR
Non Starvation	Control	5.7 ± 1.0	25.2 ± 2.2	4.5 ± 0.3
	UA8	5.5 ± 0.9	32.2 ± 5.6	5.9 ± 0.3
	UA8, EEZE	6.2 ± 1.2	18.7 ± 6.2	3.4 ± 1.4
	EEZE	6.6 ± 1.6	18.7 ± 5.4	3.5 ± 1.4
Starvation	Control	3.7 ± 0.9	4.4 ± 0.7*	1.3 ± 0.2*
	UA8	4.1 ± 0.5	19.8 ± 2.4#	4.8 ± 0.2#
	UA8, EEZE	5.2 ± 1.6	5.0 ± 1.3*	1.0 ± 0.0*
	EEZE	2.9 ± 1.4	2.8 ± 1.4*	0.9 ± 0.1*

Figure 4.1

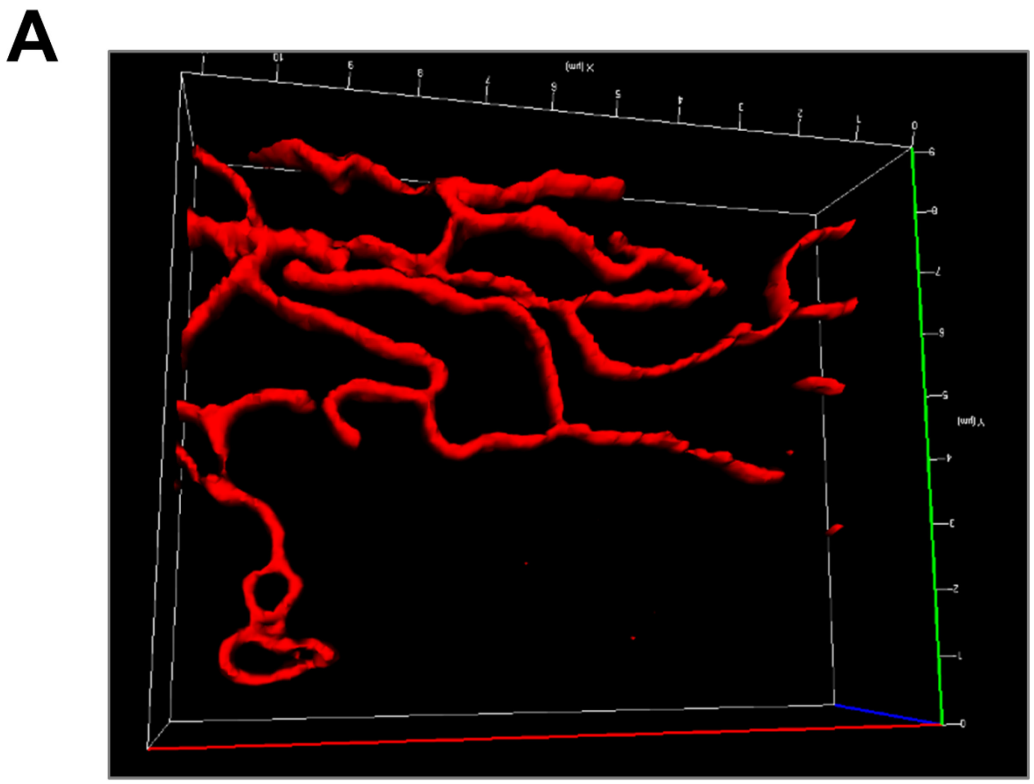
A
B
Long mitochondria
Short mitochondria
Fragmented mitochondria
Distribution of Mitochondrial Length
100%
80%
60%
40%
20%
0
Control
Fission Inhibited
Fission Induced
C
Long : Short Mitochondria
2.5
2.0
1.5
1.0
0.5
0.0
#
*
*
Control
Fission Inhibited
Fission Induced

Figure 4.1 Morphometric analysis of mitochondrial dynamics

A. 3D images of mitochondria were analyzed morphometrically to identify mitochondrial structures and to numerically report their length and size. Mitochondria were stained with MitoTracker Red (100nM) and Z-stacks images were captured with Zeiss AxioObserver Epifluorescence microscope. Image processing was conducted by Zeiss ZEN 12 and Bitplane Imaris software as detailed in the methods section. **B.** Distribution of mitochondria according to their length into long (>5μm), short (<5μm) and fragmented (<0.5μM) mitochondria. To verify the morphometric method in our cells, DRP1-dependent fission was inhibited by forskolin (20μM) and cyclosporine A (10μM) or activated by H89 (1μM) and iononmycin (5μM). **C.** The ratio of long mitochondria to short and fragmented mitochondria provides a single descriptor to mitochondrial length allowing simple statistical analysis between treatment groups. Values represent mean+SEM; *N*=3 independent experiments, *, $p<0.05$ in comparison to control.

Figure 4.2

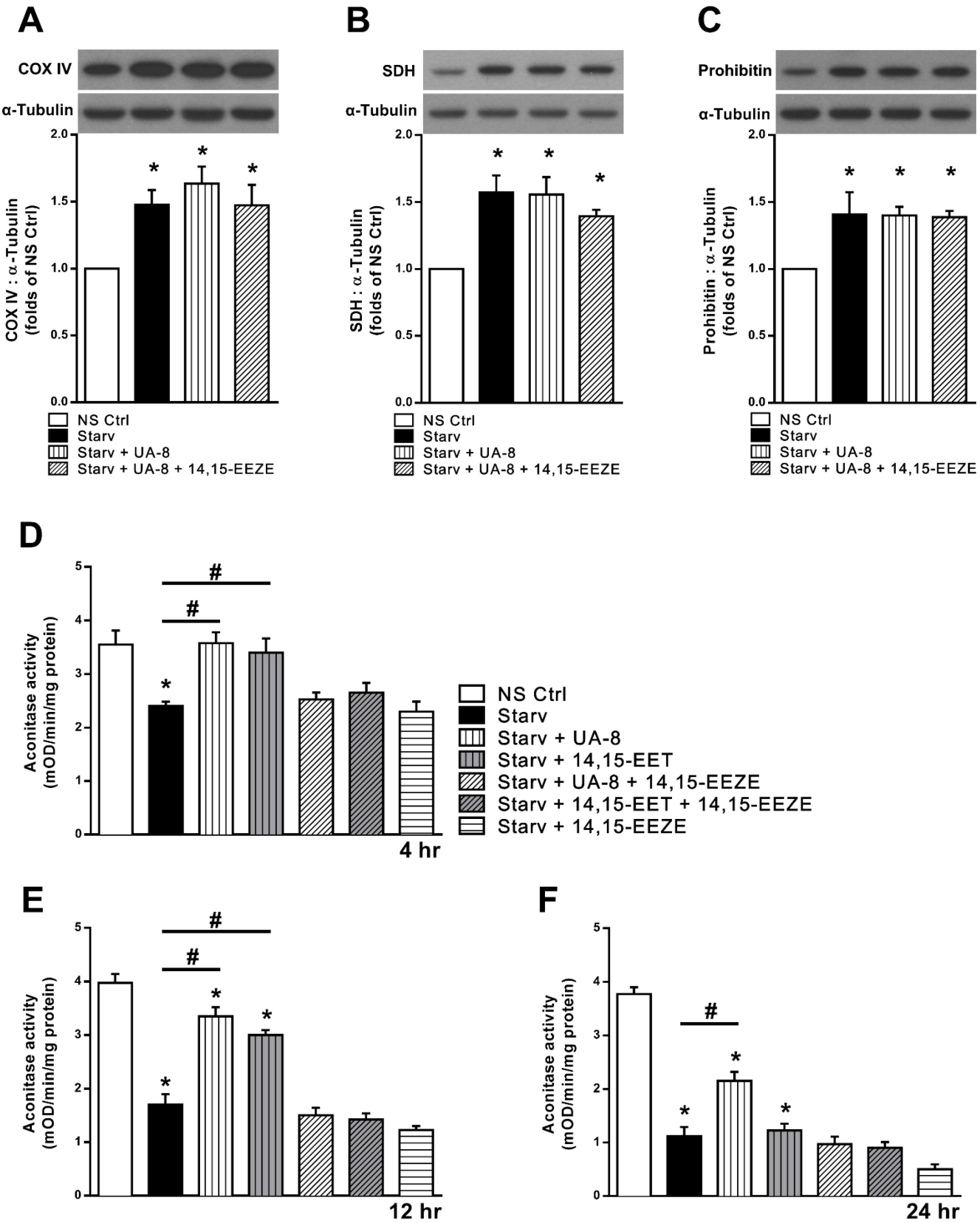
A
COX IV
α-Tubulin
COX IV : α-Tubulin (folds of NS Ctrl)
B
SDH
α-Tubulin
SDH : α-Tubulin (folds of NS Ctrl)
C
Prohibitin
α-Tubulin
Prohibitin : α-Tubulin (folds of NS Ctrl)
NS Ctrl
Starv
Starv + UA-8
Starv + UA-8 + 14,15-EEZE
D
Aconitase activity (mOD/min/mg protein)
4 hr
Starv + 14,15-EET
Starv + 14,15-EET + 14,15-EEZE
Starv + 14,15-EEZE
E
12 hr
F
24 hr

Figure 4.2 Mitochondrial enzyme expression and function following 24h starvation

Cardiac HL-1 cells were incubated either under normal conditions (NS Ctrl) or with an amino acid-free and serum-free starvation buffer (Starv) for 24h with or without UA-8 (1μM) and 14,15-EEZE (10μM). Cells subjected to 24h starvation had increased mitochondrial protein expression of (**A**) cytochrome oxidase IV (COX IV); (**B**), succinate dehydrogenase (SDH); and, (**C**) prohibition as demonstrated in representative immunoblots and quantified in corresponding histograms. Aconitase enzymatic activity was measured in HL-1 cells after (**D**) 4h; (**E**) 12h and (**F**) 24h of starvation. Starvation decreased activity of the mitochondrial enzyme while both 14,15-EET (1μM) and UA-8 (1μM) preserved activity. Co-treatment with the putative antagonist 14,15-EEZE (10μM) abolished the observed effect of 14,15-EET and UA-8. Values represent mean+SEM; N=3 independent experiments, *, p<0.05 in comparison to non-starvation control, and, #, p<0.05 between indicated groups.

Figure 4.3

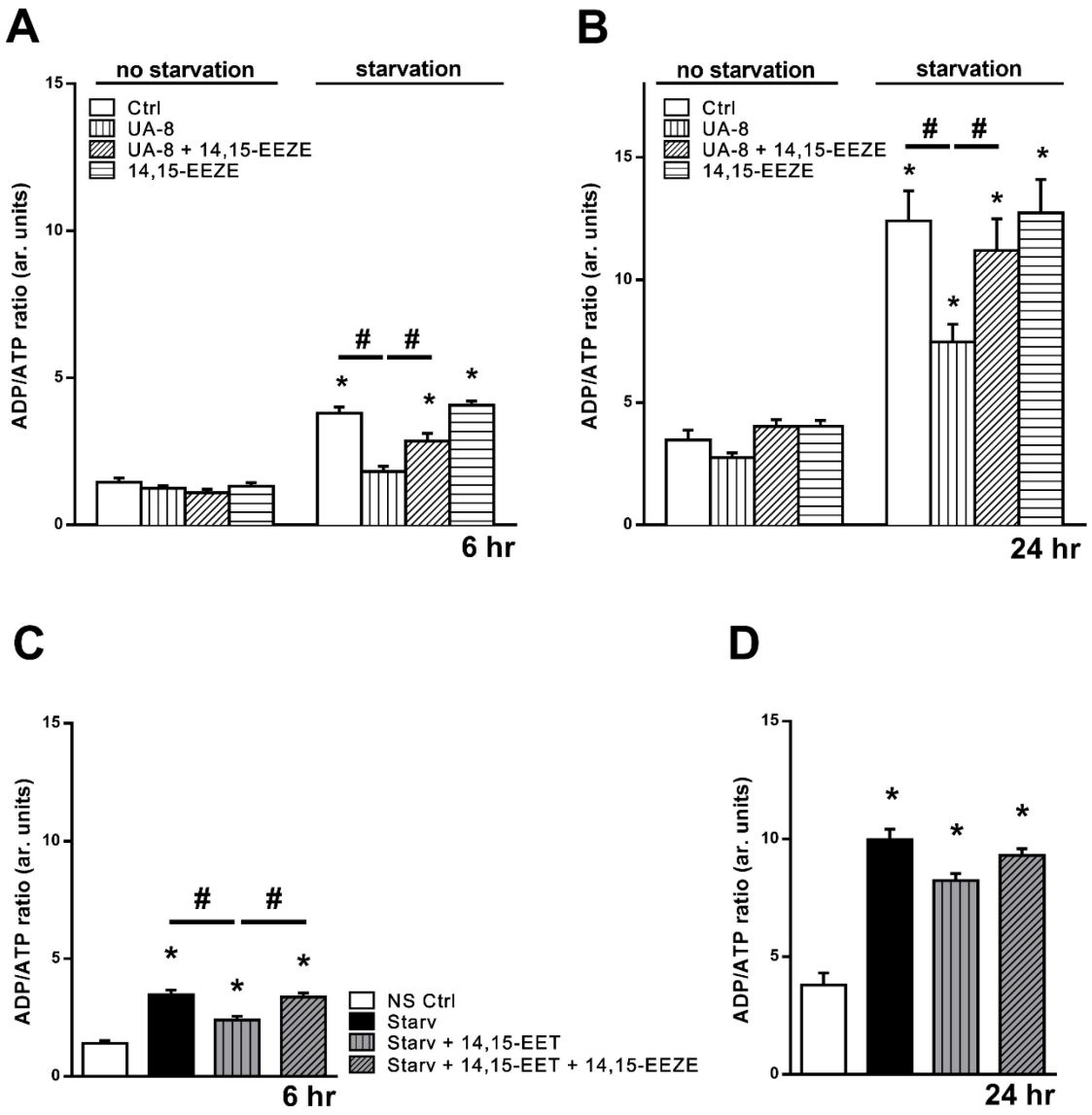
A
no starvation
starvation
Ctrl
UA-8
UA-8 + 14,15-EEZE
14,15-EEZE
ADP/ATP ratio (ar. units)
6 hr
B
24 hr
C
NS Ctrl
Starv
Starv + 14,15-EET
Starv + 14,15-EET + 14,15-EEZE
D

Figure 4.3 Enhanced cellular energy levels in EETs-treated cells

Intracellular levels of ATP and ADP were measured in HL-1 cardiac cells by chemiluminescences. HL-1 cells were incubated in starvation buffer (Starv) with or without UA-8 (1μM) and/or 14,15-EEZE (10μM) for (**A**) 6h and (**B**) 24h. HL-1 cells were incubated in starvation buffer (Starv) with or without 14,15-EET (1μM) and/or 14,15-EEZE (10μM) for (**C**) 6h and (**D**) 24h. Values are expressed as ADP/ATP ratio reflecting the cellular energy demand. Values represent mean+SEM; N=3 independent experiments, *, p<0.05 in comparison to non-starvation control, and, #, p<0.05 between indicated groups.

Figure 4.4

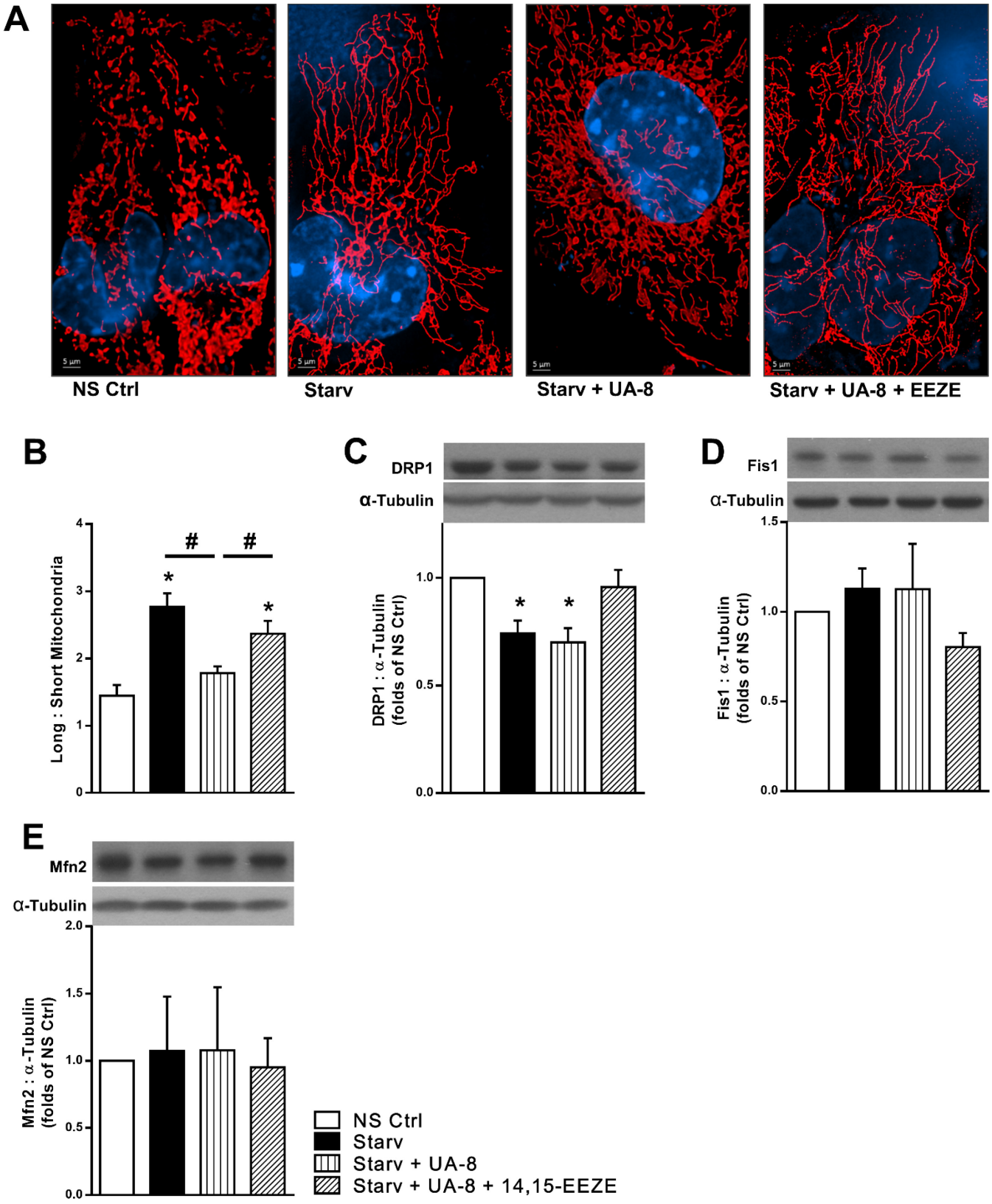
A
NS Ctrl
Starv
Starv + UA-8
Starv + UA-8 + EEZE
B
Long : Short Mitochondria
C
DRP1
α-Tubulin
DRP1 : α-Tubulin (folds of NS Ctrl)
D
Fis1
α-Tubulin
Fis1 : α-Tubulin (folds of NS Ctrl)
E
Mfn2
α-Tubulin
Mfn2 : α-Tubulin (folds of NS Ctrl)
NS Ctrl
Starv
Starv + UA-8
Starv + UA-8 + 14,15-EEZE

Figure 4.4 UA-8 inhibited the starvation-induced mitochondrial hyperfusion

HL-1 cardiac cells were treated under normal cell culture conditions (NS Ctrl) or following 24h starvation (Starv) with or without UA-8 (1μM) and/or 14,15-EEZE (10μM). (**A**) Representative images of mitochondrial morphology demonstrating starvation induced mitochondrial hyperfusion that was inhibited by UA-8. (**B**) The ratio of long:short mitochondria reflecting the starvation-induced hyperfusion and the inhibitory effect of UA-8. (**C**) Relative expression of the mitochondrial fission protein DRP1. (**D**) Relative expression of the mitochondrial fission protein Fis1. (**E**) Relative expression of the mitochondrial fusion protein Mfn2. Legend in E applies also to B-D. Values represent mean+SEM; N≥3 independent experiments, *, $p<0.05$ in comparison to non-starvation control, and, #, $p<0.05$ between indicated groups.

Figure 4.5

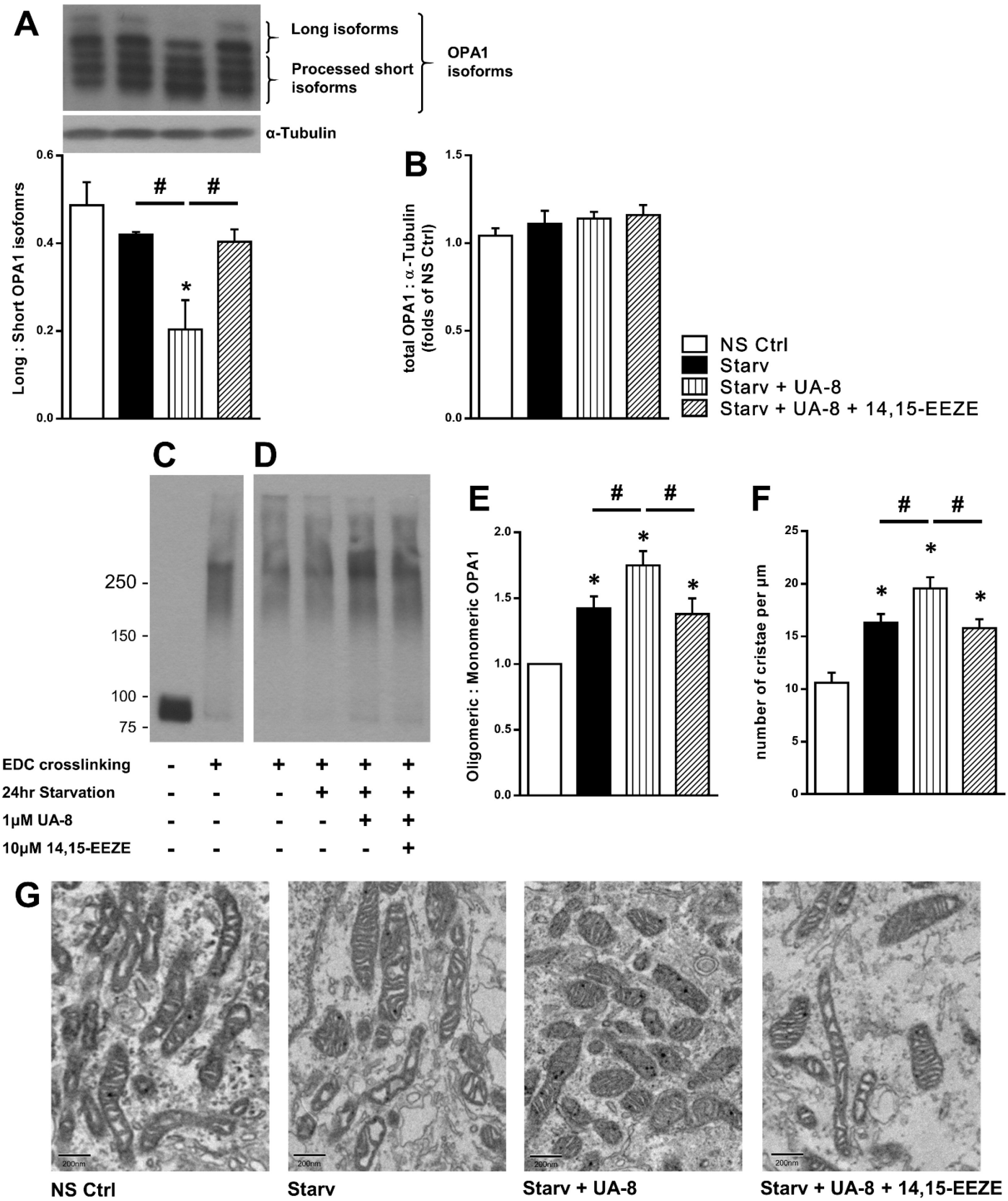
A
Long isoforms
Processed short isoforms
OPA1 isoforms
α-Tubulin
Long : Short OPA1 isofomrs
0.6
0.4
0.2
0.0
#
#
*
B
total OPA1 : α-Tubulin (folds of NS Ctrl)
1.5
1.0
0.5
0.0
NS Ctrl
Starv
Starv + UA-8
Starv + UA-8 + 14,15-EEZE
C
D
250
150
100
75
EDC crosslinking - + + + + +
24hr Starvation - - - + + +
1μM UA-8 - - - - + +
10μM 14,15-EEZE - - - - - +
E
Oligomeric : Monomeric OPA1
2.0
1.5
1.0
0.5
0.0
F
number of cristae per μm
25
20
15
10
5
0
G
200nm
NS Ctrl
Starv
Starv + UA-8
Starv + UA-8 + 14,15-EEZE

Figure 4.5 Effect of starvation and UA-8 treatment on OPA1 and cristae density

HL-1 cardiac cells were treated under normal cell culture conditions (NS Ctrl) or following 24h starvation (Starv) with or without UA-8 (1μM) and/or 14,15-EEZE (10μM). (**A**) UA-8 treated cells had lower levels of L-OPA1 isoforms and higher levels of S-OPA1 isoforms, while 14,15-EEZE inhibited this effect. (**B**) Histogram representing the quantification of total OPA1 expression. (**C**) Crosslinking OPA1 molecules with EDC (20mM) stabilized the oligomers and allowed their detection with SDS-PAGE analysis. (**D**) OPA1 oligomers as detected in HL-1 cells following 24h starvation with the indicated treatments. (**E**) Histogram representing the quantification of the ratio of oligomeric to monomeric OPA1. (**F)** Cristae density, presented by number of cristae per mitochondrial length, showing similar pattern to OPA1 oligomers. (**G**) Representative electromicrographs depicting changes in cristae width and number upon starvation and UA8 treatment. Values represent mean+SEM; *N*=3 independent experiments, *, $p<0.05$ in comparison to non-starvation control, and, #, $p<0.05$ between indicated groups.

Figure 4.6

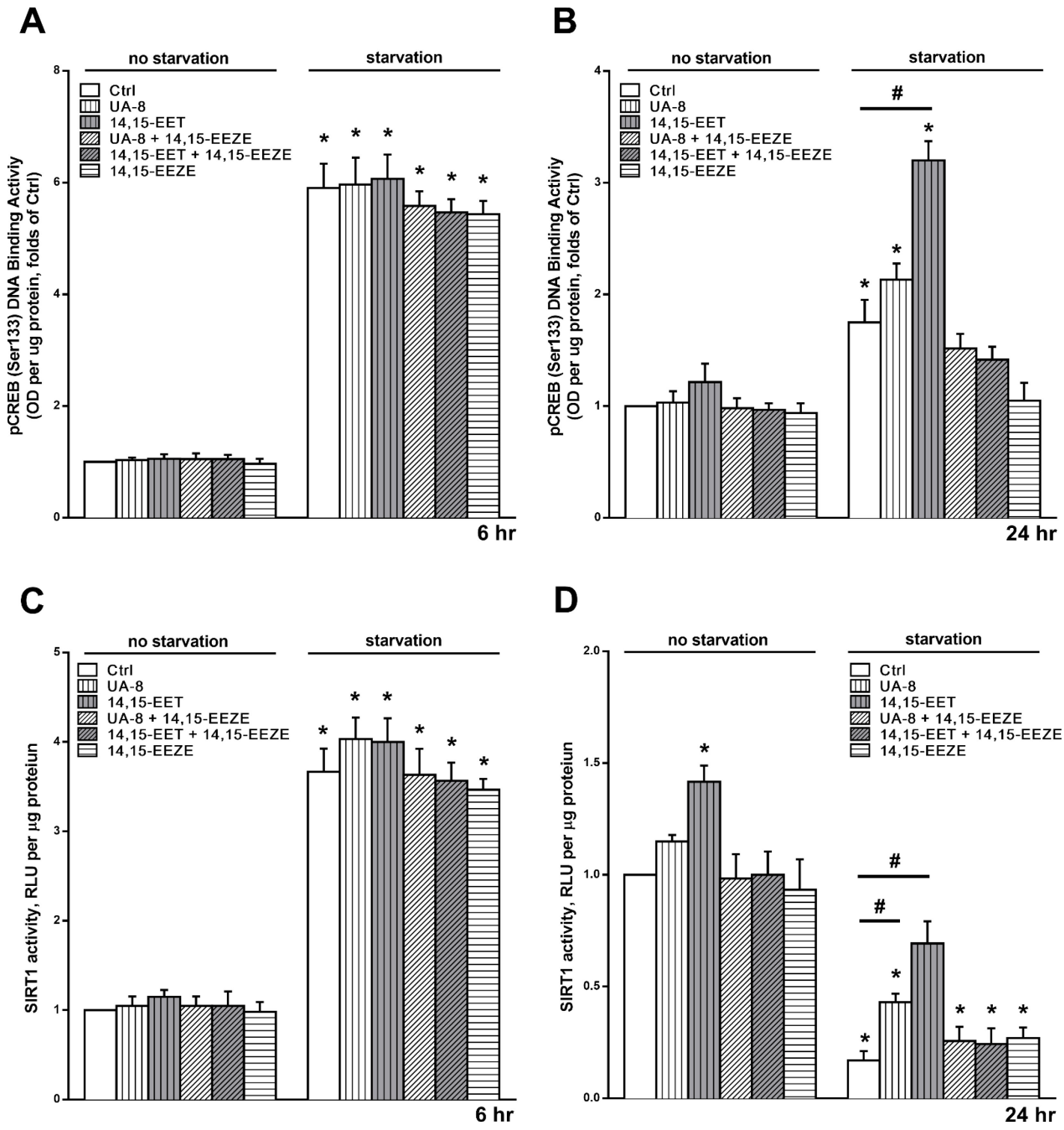
A
no starvation
starvation
Ctrl
UA-8
14,15-EET
UA-8 + 14,15-EEZE
14,15-EET + 14,15-EEZE
14,15-EEZE
pCREB (Ser133) DNA Binding Activiy
(OD per ug protein, folds of Ctrl)
6 hr
B
no starvation
starvation
#
pCREB (Ser133) DNA Binding Activiy
(OD per ug protein, folds of Ctrl)
24 hr
C
no starvation
starvation
SIRT1 activity, RLU per μg proteiun
6 hr
D
no starvation
starvation
#
#
SIRT1 activity, RLU per μg proteiun
24 hr

Figure 4.6 EET preserved the activity of mitochondrial biogenesis regulators upstream of PGC1

HL-1 cardiac cells were treated under normal cell culture conditions (NS Ctrl) or following 24h starvation (Starv) with or without UA-8 (1μM), 14,15-EET(1μM) and/or 14,15-EEZE (10μM). DNA-binding activity of the pCREB (Ser133) in HL-1 cells following (**A**) 6h and (**B**) 24h. The catalytic activity of SIRT1 was measured in whole-cell lysates by bioluminescent assay in the presence of trichostatin A (1μM) in HL-1 cells following (**C**) 6h and (**D**) 24h. EET-treated cells had significantly preserved pCREB and SIRT1 activities following 24h starvation. Values represent mean+SEM; *N*=3 independent experiments, *, $p<0.05$ in comparison to non-starvation control, and, #, $p<0.05$ between indicated groups.

Figure 4.7

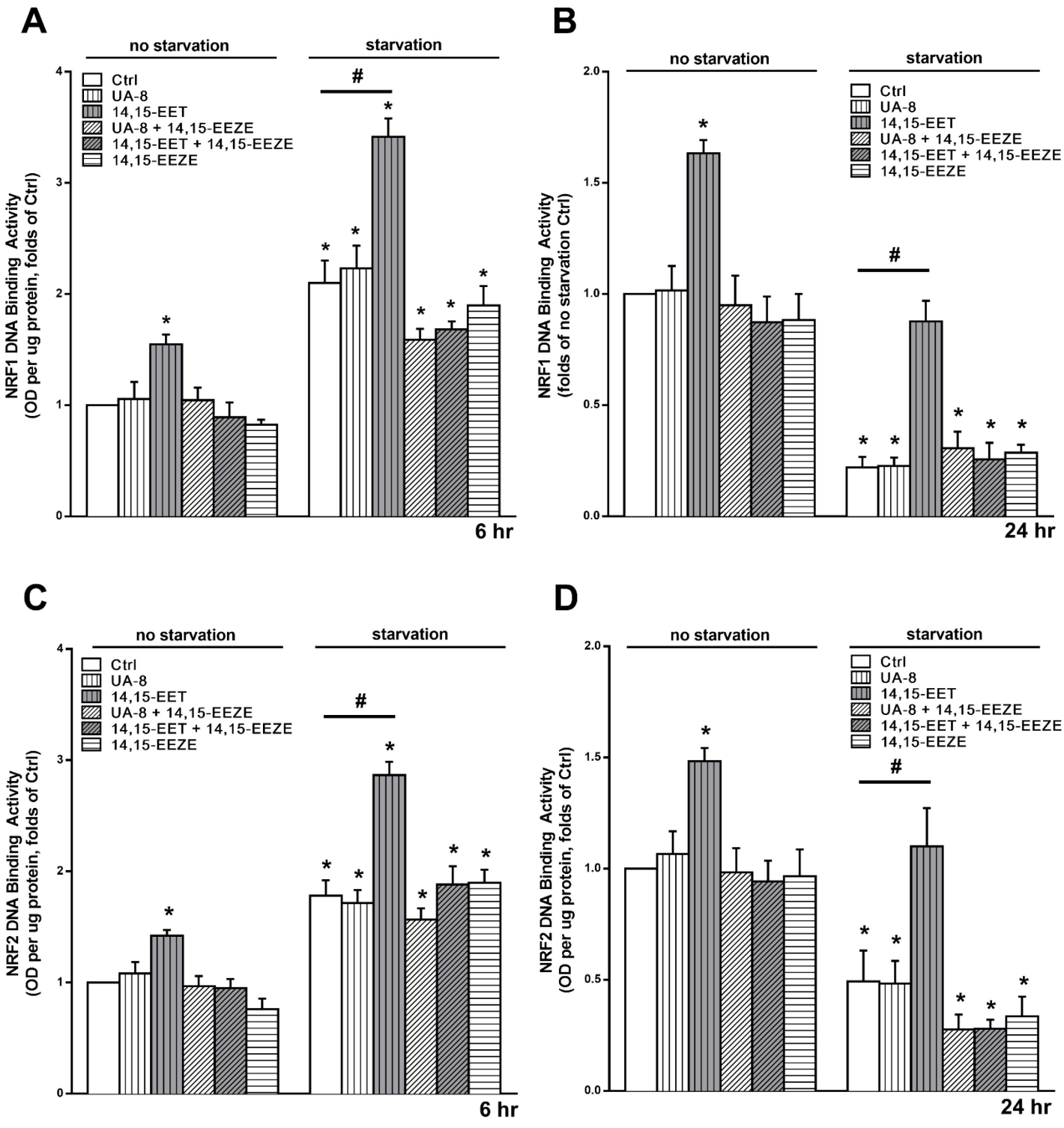
A
no starvation
starvation
Ctrl
UA-8
14,15-EET
UA-8 + 14,15-EEZE
14,15-EET + 14,15-EEZE
14,15-EEZE
NRF1 DNA Binding Activity
(OD per ug protein, folds of Ctrl)
#
6 hr
B
no starvation
starvation
NRF1 DNA Binding Activity
(folds of no starvation Ctrl)
24 hr
C
no starvation
starvation
NRF2 DNA Binding Activity
(OD per ug protein, folds of Ctrl)
6 hr
D
no starvation
starvation
NRF2 DNA Binding Activity
(OD per ug protein, folds of Ctrl)
24 hr

Figure 4.7 EET enhances the activity of mitochondrial biogenesis transcription factors NRF1 and 2

HL-1 cardiac cells were treated under normal cell culture conditions (NS Ctrl) or following 24h starvation (Starv) with or without UA-8 (1μM), 14,15-EET(1μM) and/or 14,15-EEZE (10μM). DNA-binding activity of NRF1 in HL-1 cells following (**A**) 6h and (**B**) 24h and NRF2 in HL-1 cells following (**C**) 6h and (**D**) 24h. EETs enhanced the activity of both transcription factors at all conditions and time points. Values represent mean + SEM. N≥3. *, $p<0.05$ in comparison to non-starvation control. #, $p<0.05$ between the indicated groups.

4.4. DISCUSSION

In this study, we provide evidence that EET-mediated signaling preserves mitochondrial quality during serum starvation. Prolonged serum starvation increases the relative mitochondrial protein content but markedly impairs mitochondrial function indicating the existence of an unhealthy pool of mitochondria. The signs of defective mitochondrial quality were reduced following EET treatment. The protective response improved mitochondrial function as demonstrated by better mitochondrial respiration and mitochondrial enzymatic activity. Mechanistic data suggest that EETs enhance OPA1-dependent responses, which preserve mitochondrial cristae structure. In addition, we provide evidence that EET-mediated actions involve regulation of mitochondrial biogenesis leading to a better mitochondrial health, which eventually promote survival of starved HL-1 cells.

Mitochondria play a crucial role in cellular adaptation during stress by regulating the balance between cell survival and death[325]. The ability of a cell to maintain adequate ATP levels strongly correlates with the ability to avoid necrotic cell death [326]. The relative importance of mitochondria to the cell survival is highlighted by its preservation from autophagic degradation during starvation[225]. Brief starvation induces several responses, such as OPA1 oligomerization, that improve mitochondria energy production[135, 174, 191, 192]. In the current study, upregulation of mitochondrial biogenesis within the first 6h of starvation suggests the cellular strategy to invest in

maintaining mitochondria quality for survival. However, prolonged starvation eventually depletes essential nutrients triggering extensive autophagic and apoptotic responses [108]. Such a switch in survival strategies was observed following 24h of starvation course as mitochondrial function and biogenesis declined. The early improvement in mitochondrial function during starvation is potentially a critical period to increase survival.

Studies investigating mitochondrial response to starvation indicate a quick inhibition of mitochondrial fission shifts the balance of mitochondrial dynamics toward longer and/or branched mitochondria[135]. The hyperfused mitochondria then become resistant to removal by autophagic degradation[135, 225]. Consistent with this idea, our data demonstrating the relative increase in mitochondrial protein content observed following 24h of starvation suggest that cells were attempting to limit loss of mitochondria. Despite the preservation of mitochondrial quantity, there was a marked deterioration in mitochondrial quality as confirmed by lower respiratory capacity and higher oxidative stress. This contrast between mitochondrial amount and function indicated an unhealthy mitochondrial pool.

Mitochondrial quality control is a complex series of coordinated events involving turnover of damaged organelles, generation of new organelles and maintenance of function. Mitochondrial fission segregates defective mitochondria from the functional network [142, 158], while autophagic events eliminate damaged organelles to maintain a healthy population within the cell [327, 328]. Several studies report suppression of mitochondrial

fission leads to a progressive decline in mitochondrial function. For example, inhibition of DRP1 expression in vitro led to impairment of mitochondrial respiratory function, lower levels of cellular ATP and higher levels of ROS, all indicative of degrading mitochondrial quality[329]. Further evidence demonstrates that cardiac-specific down-regulation of DRP1 induces mitochondrial elongation and inhibits mitophagy resulting in the accumulation of damaged mitochondria over time causing cardiac dysfunction and increased susceptibility to starvation or ischemic injury[226, 228]. Excessive mitochondrial fusion or insufficient fission disrupts the balance resulting in the accumulation of compromised mitochondria over time[330]. Indeed, hyperfused mitochondria are linked to the decline in mitochondrial function seen in aging skeletal muscles[209, 331] and have been suggested to contribute to the progression of chronic diseases[304]. In contrast, short term suppression of fission may be protective toward acute apoptotic stimuli[234], cardiac ischemia/reperfusion injury[223] and improve mitochondrial function in early time points of cellular stress[192]. Therefore, we suggest that the outcome of stress-induced mitochondrial hyperfusion is time-dependent, where early benefits come at the expense of a later decline in mitochondrial quality. This understanding concurs with the cellular situation during life-threatening stress, where immediate benefits are given priority over future outcomes.

Previously, we demonstrated that HL-1 cardiac cells treated with EETs had better cell survival following 24h of starvation[11]. Thus, we are

interested in understanding the mechanism(s) of EET-mediated protection, more specifically, how EETs preserve mitochondrial quality. In the current study, EET-mediated effects limited the elongation of mitochondria and decreased the relative levels of L-OPA1. While L-OPA1 is required for hyperfusion, evidence indicates that proteolytic processing of L-OPA1 might be a protective stress response[191]. OPA1 is emerging as a master regulator of mitochondrial structure and function. Originally recognized as a mitochondrial fusion protein, OPA1 is critical in structuring mitochondrial inner membranes into cristae, thereby significantly influencing both mitochondrial integrity and function[165, 332]. OPA1 oligomers stabilize cristae junctions resisting apoptosis-induced disruption and the consequent release of cytochrome c [178, 186, 189]. OPA1-dependent organization of cristae structure was found to positively regulate assembly of respiratory chain complexes promoting OxPhos coupling and directly improving mitochondrial functional efficiency[187, 318]. Mitochondrial dysfunction triggers OPA1 to undergo proteolytic degradation, which prevents defective mitochondria from fusing with healthy organelles and allows for autophagic elimination[176, 297]. L-OPA1 is required for mitochondrial fusion and decreased levels of L-OPA1 lower the threshold required to sense mitochondrial dysfunction resulting in better quality control. Interestingly, recent reports showed that stress-induced processing of L-OPA1 led to enhanced resistance to apoptosis[175, 191]. Our data demonstrating EET-mediated events lead to decreased L-OPA1 levels together with our

previous data indicating EETs promote survival during starvation stress by reducing apoptosis suggesting the importance of OPA1 in the protective response[11].

Metabolic stress or starvation has been shown to promote OPA1 oligomerization and increased cristae density[174]. OPA1 oligomers can regulate mitochondrial inner membrane architecture providing stability for ETC complexes and ATP synthase[174]. However, it is unknown whether the increased processing of L-OPA1 is coupled to the increased oligomerization. Our data demonstrating EET-mediated protection resulting in increased OPA1 oligomers, cristae density and decreased L-OPA levels, suggest a strong correlation and is consistent with other studies[191, 205]. However, the specific mechanisms and pathways by which EET signaling augment OPA1-dependent survival remain unknown. The response improves mitochondrial efficiency and provides a novel mechanism of protection.

EET-mediated cytoprotective effects involve a complex array of pathways that provide protective benefits to mitochondria. A balanced control between mitochondrial biogenesis and elimination help maintain a healthy pool of organelles that provide energy and regulate cell survival/death pathways. Mitochondrial quality is regulated through a complex process coordinating mitochondrial and nuclear genomes through NRF1/2, Tfam, SIRT1/3, CREB and PGC1α pathways.[333] Generation of new organelles will increase the cell's ability to supply ATP. Our results

demonstrated improved ADP/ATP ratio and increased mitochondrial O_2 consumption following EET treatment, which reflect a significant enhancement of mitochondrial function. Moreover, EET treatment stimulated the activity of key factors required for mitobiogenesis suggesting production of new mitochondrial components. Specifically, we showed increased transcriptional activity of CREB and NRF1/2 as well as increased enzymatic activity of SIRT1. Collectively, our data indicate that EET-mediated effects involve activation of mitobiogenesis as an inherent part of the overall protective response against starvation in HL-1 cardiac cells.

Importantly, our new findings expand on previous data demonstrating that EET-mediated events enhance an autophagic response in HL-1 cardiac cells subjected to starvation and provides support for a hypothesis that EETs regulate mitochondrial quality control[11]. Activating autophagy, specifically mitophagy, may be accompanied with concurrent induction of mitochondrial biogenesis to supplement the mitochondrial population with freshly synthesized mitochondrial proteins[334], thereby enhancing overall mitochondrial turn over to maintain higher mitochondrial quality[334]. The early adaptive response observed in control cells was lost as the stress continued but not in EET-treated cells. Thus, these data support the role of EET-mediated signaling extending the survival phase of the cellular response to starvation stress and delaying the apoptotic phase in HL-1 cardiac cells.

In conclusion, we report novel EET-mediated cytoprotective mechanisms involving regulation of mitochondrial quality. These effects enhance cellular survival during periods of starvation-induced stress. Although the precise molecular mechanisms remain unknown, we propose that EET-mediated events promote mitobiogenesis coupled with enhanced autophagic responses. Obtaining a better understanding of the complex cellular responses to stress, which lead to better mitochondrial quality control, will provide insight into novel therapeutic interventions to reduce cell death of post mitotic cells such as the cardiomyocytes. The protective mechanisms activated by EETs involve a cascade of adaptive reactions directed to maintain a healthy pool of mitochondria promoting cell survival. Further elucidation of the mechanism in cardiac cells will provide insight into diseases such as heart failure and offer new targets for therapeutic strategies.

4.5. LIMITATIONS

The use of HL-1 cells as a model for cardiac cells has been criticized due to the differences between these two cell types in terms of structure, beating activity, and metabolic profile.[335] HL-1 cell line is derived from a mouse atrial cardiomyocyte tumor thus continuously proliferating.[336] They consume less fatty acids as energy substrates in comparison to adult cardiomyocytes.[337, 338] Also, energy management in adult cardiomyocytes is much more sophisticated than that in HL-1 cells.[339, 340] However, HL-1 cells retain a functional sarcomere structure, active electrophysiology and contractility.[336] They also retain active expression of cytochrome P450 enzymes[341] making them a valuable tool in studying the protective effects of EETs during cellular stress as has been reported previously.[11, 75] They are particularly useful in studying the response to starvation stress as we demonstrated in a previous study reporting the role of EETs in enhancing the autophagic survival response during starvation stress, in which experiments were conducted in both HL-1 cells and rat neonatal cardiomyocytes in parallel.[11] Indeed, both cell models showed the same response pattern to starvation and EET treatment.[11] Importantly, both cell types responded similarly to starvation and EET treatment in terms of autophagic markers, mitochondrial enzymatic activity, and mitochondrial protein levels which was the foundation of the current study.[11] Therefore, we consider our findings from HL-1 cell described in this chapter as an insight into the response of cardiac cells to similar experimental conditions.

However, further verifying studies using *in vivo* models are required to establish the effect of EETs on cardiac mitochondria in more physiologically-related conditions.

CHAPTER V

General Discussion and Future Directions

5.1. EET-INDUCED MITOCHONDRIAL PROTECTION

Mitochondrial damage following cardiac ischemia and reperfusion is a critical component of the cardiac injury. As mitochondria detain inside their restrictive membranes several cell death mediators, mitochondria injury often commits the cardiomyocyte to apoptotic or necrotic cell death which contributes to the myocardial infarction and progression to cardiac remodeling and heart failure. Thus, improving mitochondrial resistance to cellular stress is a considerable cardioprotective approach. Studies presented in this thesis demonstrated that EETs delay the collapse of mitochondrial membrane potential and attenuate mitochondrial fragmentation following the oxidative stress induced by photodynamic therapy. Also, EETs preserved mitochondrial functions during prolonged serum starvation. In addition to the previously reported EETs' protective effects on cardiac mitochondria following ischemia and reperfusion in mice[10] and against doxorubicin induced toxicity[74], these data strongly suggest that EET signaling promotes mitochondrial resistance to injury induced by cellular stress.

However, the mechanism of such mitochondrial protection remains debatable. In acute cellular stress such as the reperfusion stress in cardiomyocytes or the photodynamic therapy in WI-38 cells, EETs' mitochondrial protection is most probably due to their inhibitory effect on the mitochondrial permeability transition pore (mPTP)[10]. This can be secondary by the stimulatory effect of EETs on PI3K/Akt prosurvival pathway that has

been reported in cardiomyocytes and endothelial cells[50, 95]. Activation of the PI3K/Akt pathway leads to the inhibition of hexokinase II, a component of the mPTP channel causing a suppressed activity of the channel[342]. Akt also inhibit several pro-apoptotic factors such as Bax, Bad, and Bim leading to suppression of mitochondrial outer membrane permeabilization (MOMP) as well[343-345]. Indeed, pharmacological inhibition of PI3K blocked the cardio-protective effect of EETs against ischemic injury in an *ex vivo* isolated heart model[106], and the use of an mPTP opener deleted the effect of EETs on the channel[10]. Therefore, current evidence suggest that EET protect mitochondria through inhibition of their permeability transition channels and possibly by inhibiting the permeabilization of their outer membranes during acute cellular stress. However, such a theory requires further specific investigation in relevant experimental models to confirm these effector mediators.

EETs and mitochondrial dynamics

Mitochondrial fusion and fission dynamics are closely related to mitochondrial quality control and to the cellular stress and metabolic demand. Some models of cellular stress, especially those of acute nature, induce mitochondrial fragmentation as seen in photodynamic (PD) stress in this thesis as well as following ischemia and reperfusion (IR) events reported earlier[10]. However, milder and more chronic stress models such as serum or amino acid starvation induce mitochondrial hyperfusion[135, 192]. Interestingly, EETs attenuated the PD and IR induced mitochondrial

fragmentation (anti-fission effect) while limited the mitochondrial hyperfusion induced by prolonged starvation (anti-fusion effect). Thus the effect of EETs on mitochondrial dynamics is context-specific rather than a direct pro-fusion or pro-fission effect. Although inhibition of DRP1 by EET-activated PKA can serve as a direct link between EET signaling and mitochondrial fission, we did not detect a significant influence of such link on mitochondrial dynamic balance. Therefore, studies presented here suggest that EETs might be affecting mitochondrial dynamics in an indirect way as a part of the cellular response to the particular stress.

EETs and mitochondrial quality control

The efficiency and the quality of cardiac mitochondria is a critical factor for cardiac health and disease[125]. The quality of mitochondria is controlled, at the organelle level, by the autophagic removal of defective mitochondria and the generation of new mitochondrial proteins by mitochondrial biogenesis. These two opposing processes are in balance to maintain adequate mitochondrial activity at all times[346]. Interestingly, both processes are interlinked and can be activated simultaneously[334]. Studies presented in this thesis demonstrated that EETs significantly induce mitochondrial biogenesis in addition to the previously reported activation of autophagy[11]. This effect was mediated by activation of AMPK and SIRT1 which are known activators for both autophagy[347-349] and mitochondrial biogenesis[323, 350-352]. This led to a marked improvement in mitochondrial quality during challenging conditions such as sustained starvation. Such

findings can have a significant therapeutic potential for EET mimetics in combating several diseases that are marked with degraded mitochondrial quality control, typically seen in age-related cardiac and neuronal diseases. However, further research is required to validate EET-induced improvement in mitochondrial quality in *in vivo* models. For example, assessing mitochondrial efficiency in young and old mice models that overexpress the cardiac CYP2J2 or the models lacking the sEH can offer more insight. Also, whether EET promote mitochondrial quality during normal non-stressful condition is yet to be determined.

5.2. MITOCHONDRIA AND CELLULAR STRESS

Cellular resistance to stress conditions depends largely on cellular energy levels. ATP level is a significant determinant for whether the cell will survive or initiate programmed cell death[326]. Therefore, mitochondria are particularly critical during cellular stress. Studies presented here demonstrated the cellular strategy to invest in mitochondrial quality during the early stages of starvation stress. This was evident by the increased mitochondrial biogenesis despite the restricted availability of amino acids. Further, other studies reported higher rate of mitochondrial consumption of amino acids as respiratory substrates during starvation[353]. Such priority is given to the mitochondria as they are necessary to provide ATP for cell survival. This survival strategy aims to postpone the cellular death as long as possible, and to secure enough energy for programmed cell death as a last resort.

During starvation, autophagy is activated to degrade cytosolic components recycling their amino acids. To spare the mitochondria from autophagic degradation, mitochondrial fission is inhibited and mitochondria hyperfuse[135, 192]. This saves the mitochondrial network from mitophagy[135, 225], however it has a negative effect on mitochondrial quality on the long term[229]. It is reasonable to think that this is also a part of the cellular strategy to withstand stress even if it is on the expense of long term benefits.

The results presented in this thesis support this survival program and suggest that EETs prolong the survival phase of the cellular strategy against

starvation stress. This was mediated by improved mitochondrial quality secondary to induced mitochondrial biogenesis and enhanced OPA1-dependent stress response in addition to the previously reported enhancement of autophagy[11]. However, as the starvation continues, the cell will eventually initiate apoptotic cascade to avoid the un-programed necrosis.

This understanding of the cellular survival program gives an important insight on why mild stress is beneficial. Temporary cellular stress that initiates the early stages of this survival program would lead to higher mitochondrial efficiency without the negative effects seen later during stress. Indeed, several studies have reported that short periods of starvation boost mitochondrial energy production[135, 192]. Also, exposing the heart to intermittent episodes of ischemia, known as ischemic preconditioning, significantly improves the cardiac resistance to longer ischemic attacks[124, 354]. The same concept can help explain the significant health benefits of caloric restriction and intermittent fasting. In fact, these relatively simple dietary interventions are currently under serious scientific investigation as promising cardioprotective approaches[355, 356] with several health benefits against diabetes, cancer, Alzheimer's disease and other age-related diseases[357-361].

Accumulating evidence demonstrated the role of mitochondria in diseases associated with advanced age. In fact, a leading theory in the aging research blames mitochondrial dysfunction for the age-related

decline in organ functions (summarized in our review article[7]). Therefore, interventions that attenuate mitochondrial dysfunction or improve their quality control system are promising approaches in combating aging diseases[357, 362]. Interestingly, non-pharmacological interventions such as physical exercise and caloric restriction have shown significant benefits for such diseases. For example, physical exercise improves insulin sensitivity[295], a major factor in many age-related diseases such as diabetes and heart failure. Also, caloric restriction and losing body weight improved cardiac functions in a mouse model of heart failure[355]. Furthermore, intermittent fasting significantly delayed the onset of Alzheimer's disease in mice models[363, 364]. Indeed, caloric restriction increases the lifespan of all tested organism from yeast to mammals via delaying aging-associated diseases[360, 365]. As exercise, caloric restriction, and intermittent fasting are all forms of metabolic demands, it is not surprising that enhancement of mitochondrial quality is involved in the profound health benefits obtained from these relatively simple interventions[366-368]. Our results support the beneficial effects of mild or transient starvation on the mitochondrial quality on the cellular level and encourage more research to utilize these benefits on the physiological level. This notion emphasizes the need for better understating of the mechanisms that promote mitochondrial health which can have a significant impact on current therapeutic strategies to treat these diseases in our aging population.

REFERENCES

1. Capdevila, J.H., Falck, J.R. & Estabrook, R.W. Cytochrome P450 and the arachidonate cascade. *FASEB J* **6**, 731-736 (1992).
2. Roman, R.J. P-450 metabolites of arachidonic acid in the control of cardiovascular function. *Physiol Rev* **82**, 131-185 (2002).
3. Capdevila, J.H., Falck, J.R. & Harris, R.C. Cytochrome P450 and arachidonic acid bioactivation. Molecular and functional properties of the arachidonate monooxygenase. *J Lipid Res* **41**, 163-181 (2000).
4. Spector, A.A. & Norris, A.W. Action of epoxyeicosatrienoic acids on cellular function. *Am J Physiol Cell Physiol* **292**, C996-1012 (2007).
5. Oni-Orisan, A., Alsaleh, N., Lee, C.R. & Seubert, J.M. Epoxyeicosatrienoic acids and cardioprotection: the road to translation. *J Mol Cell Cardiol* **74**, 199-208 (2014).
6. Crow, M.T., Mani, K., Nam, Y.J. & Kitsis, R.N. The mitochondrial death pathway and cardiac myocyte apoptosis. *Circ Res* **95**, 957-970 (2004).
7. Chaudhary, K.R., El-Sikhry, H. & Seubert, J.M. Mitochondria and the aging heart. *J Geriatr Cardiol* **8**, 159-167 (2011).
8. Ni, H.M., Williams, J.A. & Ding, W.X. Mitochondrial dynamics and mitochondrial quality control. *Redox Biol* **4**, 6-13 (2015).

9. Ong, S.B., Hall, A.R. & Hausenloy, D.J. Mitochondrial dynamics in cardiovascular health and disease. *Antioxid Redox Signal* **19**, 400-414 (2013).

10. Katragadda, D. *et al.* Epoxyeicosatrienoic acids limit damage to mitochondrial function following stress in cardiac cells. *J Mol Cell Cardiol* **46**, 867-875 (2009).

11. Samokhvalov, V. *et al.* Epoxyeicosatrienoic acids protect cardiac cells during starvation by modulating an autophagic response. *Cell Death Dis* **4**, e885 (2013).

12. Soberman, R.J. & Christmas, P. The organization and consequences of eicosanoid signaling. *J Clin Invest* **111**, 1107-1113 (2003).

13. Warner, T.D. & Mitchell, J.A. Cyclooxygenases: new forms, new inhibitors, and lessons from the clinic. *FASEB J* **18**, 790-804 (2004).

14. Samuelsson, B., Dahlen, S.E., Lindgren, J.A., Rouzer, C.A. & Serhan, C.N. Leukotrienes and lipoxins: structures, biosynthesis, and biological effects. *Science* **237**, 1171-1176 (1987).

15. Spector, A.A. Arachidonic acid cytochrome P450 epoxygenase pathway. *J Lipid Res* **50 Suppl**, S52-56 (2009).

16. Campbell, W.B., Gebremedhin, D., Pratt, P.F. & Harder, D.R. Identification of epoxyeicosatrienoic acids as endothelium-derived hyperpolarizing factors. *Circ Res* **78**, 415-423 (1996).

17. Delozier, T.C. *et al.* Detection of human CYP2C8, CYP2C9, and CYP2J2 in cardiovascular tissues. *Drug Metab Dispos* **35**, 682-688 (2007).

18. Bieche, I. *et al.* Reverse transcriptase-PCR quantification of mRNA levels from cytochrome (CYP)1, CYP2 and CYP3 families in 22 different human tissues. *Pharmacogenet Genomics* **17**, 731-742 (2007).

19. Imig, J.D. Epoxides and soluble epoxide hydrolase in cardiovascular physiology. *Physiol Rev* **92**, 101-130 (2012).

20. Yu, Z. *et al.* Soluble epoxide hydrolase regulates hydrolysis of vasoactive epoxyeicosatrienoic acids. *Circ Res* **87**, 992-998 (2000).

21. Iliff, J.J. *et al.* Epoxyeicosanoid signaling in CNS function and disease. *Prostaglandins Other Lipid Mediat* **91**, 68-84 (2010).

22. Wu, S., Moomaw, C.R., Tomer, K.B., Falck, J.R. & Zeldin, D.C. Molecular cloning and expression of CYP2J2, a human cytochrome P450 arachidonic acid epoxygenase highly expressed in heart. *J Biol Chem* **271**, 3460-3468 (1996).

23. Xiao, Y.F. *et al.* Enhancement of cardiac L-type Ca2+ currents in transgenic mice with cardiac-specific overexpression of CYP2J2. *Mol Pharmacol* **66**, 1607-1616 (2004).

24. Hutchens, M.P. *et al.* Soluble epoxide hydrolase gene deletion reduces survival after cardiac arrest and cardiopulmonary resuscitation. *Resuscitation* **76**, 89-94 (2008).

25. Zhang, W. *et al.* Soluble epoxide hydrolase gene deletion is protective against experimental cerebral ischemia. *Stroke* **39**, 2073-2078 (2008).

26. Bettaieb, A. *et al.* Effects of soluble epoxide hydrolase deficiency on acute pancreatitis in mice. *PLoS One* **9**, e113019 (2014).

27. Imig, J.D., Zhao, X., Capdevila, J.H., Morisseau, C. & Hammock, B.D. Soluble epoxide hydrolase inhibition lowers arterial blood pressure in angiotensin II hypertension. *Hypertension* **39**, 690-694 (2002).

28. Fang, X. *et al.* Effect of soluble epoxide hydrolase inhibition on epoxyeicosatrienoic acid metabolism in human blood vessels. *Am J Physiol Heart Circ Physiol* **287**, H2412-2420 (2004).

29. Ulu, A. *et al.* Soluble epoxide hydrolase inhibitors reduce the development of atherosclerosis in apolipoprotein e-knockout mouse model. *J Cardiovasc Pharmacol* **52**, 314-323 (2008).

30. Fleming, I. & Busse, R. Endothelium-derived epoxyeicosatrienoic acids and vascular function. *Hypertension* **47**, 629-633 (2006).

31. Jung, O. *et al.* Soluble epoxide hydrolase is a main effector of angiotensin II-induced hypertension. *Hypertension* **45**, 759-765 (2005).

32. Merabet, N. *et al.* Soluble epoxide hydrolase inhibition improves myocardial perfusion and function in experimental heart failure. *J Mol Cell Cardiol* **52**, 660-666 (2012).

33. Muller, D.N. *et al.* A peroxisome proliferator-activated receptor-alpha activator induces renal CYP2C23 activity and protects from angiotensin II-induced renal injury. *Am J Pathol* **164**, 521-532 (2004).

34. Imig, J.D. & Hammock, B.D. Soluble epoxide hydrolase as a therapeutic target for cardiovascular diseases. *Nat Rev Drug Discov* **8**, 794-805 (2009).

35. Morisseau, C. & Hammock, B.D. Impact of soluble epoxide hydrolase and epoxyeicosanoids on human health. *Annu Rev Pharmacol Toxicol* **53**, 37-58 (2013).

36. Larsen, B.T. *et al.* Epoxyeicosatrienoic and dihydroxyeicosatrienoic acids dilate human coronary arterioles via BK(Ca) channels: implications for soluble epoxide hydrolase inhibition. *Am J Physiol Heart Circ Physiol* **290**, H491-499 (2006).

37. Lu, T., Hoshi, T., Weintraub, N.L., Spector, A.A. & Lee, H.C. Activation of ATP-sensitive K(+) channels by epoxyeicosatrienoic acids in rat cardiac ventricular myocytes. *J Physiol* **537**, 811-827 (2001).

38. Ye, D., Zhou, W. & Lee, H.C. Activation of rat mesenteric arterial KATP channels by 11,12-epoxyeicosatrienoic acid. *Am J Physiol Heart Circ Physiol* **288**, H358-364 (2005).

39. Node, K. *et al.* Activation of Galpha s mediates induction of tissue-type plasminogen activator gene transcription by epoxyeicosatrienoic acids. *J Biol Chem* **276**, 15983-15989 (2001).

40. Wong, P.Y., Lai, P.S., Shen, S.Y., Belosludtsev, Y.Y. & Falck, J.R. Post-receptor signal transduction and regulation of 14(R),15(S)-epoxyeicosatrienoic acid (14,15-EET) binding in U-937 cells. *J Lipid Mediat Cell Signal* **16**, 155-169 (1997).

41. Wong, P.Y., Lai, P.S. & Falck, J.R. Mechanism and signal transduction of 14 (R), 15 (S)-epoxyeicosatrienoic acid (14,15-EET) binding in guinea pig monocytes. *Prostaglandins Other Lipid Mediat* **62**, 321-333 (2000).

42. Abukhashim, M., Wiebe, G.J. & Seubert, J.M. Regulation of forskolin-induced cAMP production by cytochrome P450 epoxygenase metabolites of arachidonic acid in HEK293 cells. *Cell Biol Toxicol* **27**, 321-332 (2011).

43. Chen, Y., Falck, J.R., Tuniki, V.R. & Campbell, W.B. 20-125Iodo-14,15-epoxyeicosa-5(Z)-enoic acid: a high-affinity radioligand used to characterize the epoxyeicosatrienoic acid antagonist binding site. *J Pharmacol Exp Ther* **331**, 1137-1145 (2009).

44. Lu, T., Hong, M.P. & Lee, H.C. Molecular determinants of cardiac K(ATP) channel activation by epoxyeicosatrienoic acids. *J Biol Chem* **280**, 19097-19104 (2005).

45. Lu, T. *et al.* Cardiac and vascular KATP channels in rats are activated by endogenous epoxyeicosatrienoic acids through different mechanisms. *J Physiol* **575**, 627-644 (2006).

46. Fleming, I. *et al.* The coronary endothelium-derived hyperpolarizing factor (EDHF) stimulates multiple signalling pathways and proliferation in vascular cells. *Pflugers Arch* **442**, 511-518 (2001).

47. Michaelis, U.R. *et al.* Cytochrome P450 epoxygenases 2C8 and 2C9 are implicated in hypoxia-induced endothelial cell migration and angiogenesis. *J Cell Sci* **118**, 5489-5498 (2005).

48. Yan, G., Chen, S., You, B. & Sun, J. Activation of sphingosine kinase-1 mediates induction of endothelial cell proliferation and angiogenesis by epoxyeicosatrienoic acids. *Cardiovasc Res* **78**, 308-314 (2008).

49. Wang, Y. *et al.* Arachidonic acid epoxygenase metabolites stimulate endothelial cell growth and angiogenesis via mitogen-activated protein kinase and phosphatidylinositol 3-kinase/Akt signaling pathways. *J Pharmacol Exp Ther* **314**, 522-532 (2005).

50. Pozzi, A. *et al.* Characterization of 5,6- and 8,9-epoxyeicosatrienoic acids (5,6- and 8,9-EET) as potent in vivo angiogenic lipids. *J Biol Chem* **280**, 27138-27146 (2005).

51. Potente, M., Fisslthaler, B., Busse, R. & Fleming, I. 11,12-Epoxyeicosatrienoic acid-induced inhibition of FOXO factors

promotes endothelial proliferation by down-regulating p27Kip1. *J Biol Chem* **278**, 29619-29625 (2003).

52. Zhang, B., Cao, H. & Rao, G.N. Fibroblast growth factor-2 is a downstream mediator of phosphatidylinositol 3-kinase-Akt signaling in 14,15-epoxyeicosatrienoic acid-induced angiogenesis. *J Biol Chem* **281**, 905-914 (2006).

53. Michaelis, U.R. *et al.* Cytochrome P450 2C9-derived epoxyeicosatrienoic acids induce angiogenesis via cross-talk with the epidermal growth factor receptor (EGFR). *FASEB J* **17**, 770-772 (2003).

54. Sun, J. *et al.* Inhibition of vascular smooth muscle cell migration by cytochrome p450 epoxygenase-derived eicosanoids. *Circ Res* **90**, 1020-1027 (2002).

55. Michaelis, U.R., Falck, J.R., Schmidt, R., Busse, R. & Fleming, I. Cytochrome P4502C9-derived epoxyeicosatrienoic acids induce the expression of cyclooxygenase-2 in endothelial cells. *Arterioscler Thromb Vasc Biol* **25**, 321-326 (2005).

56. Node, K. *et al.* Anti-inflammatory properties of cytochrome P450 epoxygenase-derived eicosanoids. *Science* **285**, 1276-1279 (1999).

57. Deng, Y. *et al.* Endothelial CYP epoxygenase overexpression and soluble epoxide hydrolase disruption attenuate acute vascular inflammatory responses in mice. *FASEB J* **25**, 703-713 (2011).

58. Schmelzer, K.R. *et al.* Soluble epoxide hydrolase is a therapeutic target for acute inflammation. *Proc Natl Acad Sci U S A* **102**, 9772-9777 (2005).

59. Zhao, X. *et al.* Soluble epoxide hydrolase inhibition protects the kidney from hypertension-induced damage. *J Am Soc Nephrol* **15**, 1244-1253 (2004).

60. Manhiani, M. *et al.* Soluble epoxide hydrolase gene deletion attenuates renal injury and inflammation with DOCA-salt hypertension. *Am J Physiol Renal Physiol* **297**, F740-748 (2009).

61. Morin, C., Sirois, M., Echave, V., Gomes, M.M. & Rousseau, E. EET displays anti-inflammatory effects in TNF-alpha stimulated human bronchi: putative role of CPI-17. *Am J Respir Cell Mol Biol* **38**, 192-201 (2008).

62. Ng, V. Cytochrome P450 eicosanoids regulate fatty acid metabolism via PPARα. *Clinical Pharmacology & Therapeutics* **75**, P45 (2004).

63. Liu, Y. *et al.* The antiinflammatory effect of laminar flow: the role of PPARgamma, epoxyeicosatrienoic acids, and soluble epoxide hydrolase. *Proc Natl Acad Sci U S A* **102**, 16747-16752 (2005).

64. Ng, V.Y. *et al.* Cytochrome P450 eicosanoids are activators of peroxisome proliferator-activated receptor alpha. *Drug Metab Dispos* **35**, 1126-1134 (2007).

65. Fitzpatrick, F.A. *et al.* Inhibition of cyclooxygenase activity and platelet aggregation by epoxyeicosatrienoic acids. Influence of stereochemistry. *J Biol Chem* **261**, 15334-15338 (1986).

66. Heizer, M.L., McKinney, J.S. & Ellis, E.F. 14,15-Epoxyeicosatrienoic acid inhibits platelet aggregation in mouse cerebral arterioles. *Stroke* **22**, 1389-1393 (1991).

67. Malcolm, K.C. & Fitzpatrick, F.A. Epoxyeicosatrienoic acids inhibit Ca2+ entry into platelets stimulated by thapsigargin and thrombin. *J Biol Chem* **267**, 19854-19858 (1992).

68. Larsen, B.T., Gutterman, D.D. & Hatoum, O.A. Emerging role of epoxyeicosatrienoic acids in coronary vascular function. *Eur J Clin Invest* **36**, 293-300 (2006).

69. Gauthier, K.M., Yang, W., Gross, G.J. & Campbell, W.B. Roles of epoxyeicosatrienoic acids in vascular regulation and cardiac preconditioning. *J Cardiovasc Pharmacol* **50**, 601-608 (2007).

70. Simpkins, A.N. *et al.* Soluble epoxide inhibition is protective against cerebral ischemia via vascular and neural protection. *Am J Pathol* **174**, 2086-2095 (2009).

71. Dorrance, A.M. *et al.* An epoxide hydrolase inhibitor, 12-(3-adamantan-1-yl-ureido)dodecanoic acid (AUDA), reduces ischemic cerebral infarct size in stroke-prone spontaneously hypertensive rats. *J Cardiovasc Pharmacol* **46**, 842-848 (2005).

72. Yang, S. *et al.* Cytochrome P-450 epoxygenases protect endothelial cells from apoptosis induced by tumor necrosis factor-alpha via MAPK and PI3K/Akt signaling pathways. *Am J Physiol Heart Circ Physiol* **293**, H142-151 (2007).

73. Chen, W. *et al.* CYP2J2 and EETs Protect against Oxidative Stress and Apoptosis in Vivo and in Vitro Following Lung Ischemia/Reperfusion. *Cellular physiology and biochemistry : international journal of experimental cellular physiology, biochemistry, and pharmacology* **33**, 1663-1680 (2014).

74. Zhang, Y. *et al.* Overexpression of CYP2J2 provides protection against doxorubicin-induced cardiotoxicity. *Am J Physiol Heart Circ Physiol* **297**, H37-46 (2009).

75. Dhanasekaran, A. *et al.* Multiple antiapoptotic targets of the PI3K/Akt survival pathway are activated by epoxyeicosatrienoic acids to protect cardiomyocytes from hypoxia/anoxia. *Am J Physiol Heart Circ Physiol* **294**, H724-735 (2008).

76. Ma, J. *et al.* 8,9-Epoxyeicosatrienoic acid analog protects pulmonary artery smooth muscle cells from apoptosis via ROCK pathway. *Exp Cell Res* **316**, 2340-2353 (2010).

77. Bodiga, S. *et al.* Protective actions of epoxyeicosatrienoic acid: dual targeting of cardiovascular PI3K and KATP channels. *J Mol Cell Cardiol* **46**, 978-988 (2009).

78. Jiang, J.G., Shen, G.F., Chen, C., Fu, X.N. & Wang, D.W. Effects of cytochrome P450 arachidonic acid epoxygenases on the proliferation of tumor cells. *Ai Zheng* **28**, 14-19 (2009).

79. Jiang, J.G. *et al.* Cytochrome p450 epoxygenase promotes human cancer metastasis. *Cancer Res* **67**, 6665-6674 (2007).

80. Panigrahy, D. *et al.* Epoxyeicosanoids promote organ and tissue regeneration. *Proc Natl Acad Sci U S A* **110**, 13528-13533 (2013).

81. Panigrahy, D. *et al.* Epoxyeicosanoids stimulate multiorgan metastasis and tumor dormancy escape in mice. *J Clin Invest* **122**, 178-191 (2012).

82. Chen, C. *et al.* Cytochrome P450 2J2 is highly expressed in hematologic malignant diseases and promotes tumor cell growth. *J Pharmacol Exp Ther* **336**, 344-355 (2011).

83. Jiang, J.G. *et al.* Cytochrome P450 2J2 promotes the neoplastic phenotype of carcinoma cells and is up-regulated in human tumors. *Cancer Res* **65**, 4707-4715 (2005).

84. Jiang, J.G., Fu, X.N., Chen, C.L. & Wang, D.W. Expression of cytochrome P450 arachidonic acid epoxygenase 2J2 in human tumor tissues and cell lines. *Ai Zheng* **28**, 93-96 (2009).

85. Chen, C. *et al.* Selective inhibitors of CYP2J2 related to terfenadine exhibit strong activity against human cancers in vitro and in vivo. *J Pharmacol Exp Ther* **329**, 908-918 (2009).

86. Nithipatikom, K. *et al.* Inhibition of carcinoma cell motility by epoxyeicosatrienoic acid (EET) antagonists. *Cancer Sci* **101**, 2629-2636 (2010).

87. Wang, D. & Dubois, R.N. Epoxyeicosatrienoic acids: a double-edged sword in cardiovascular diseases and cancer. *J Clin Invest* **122**, 19-22 (2012).

88. Park, S.W., Heo, D.S. & Sung, M.W. The shunting of arachidonic acid metabolism to 5-lipoxygenase and cytochrome p450 epoxygenase antagonizes the anti-cancer effect of cyclooxygenase-2 inhibition in head and neck cancer cells. *Cell Oncol (Dordr)* **35**, 1-8 (2012).

89. Liu, L. *et al.* Epoxyeicosatrienoic acids attenuate reactive oxygen species level, mitochondrial dysfunction, caspase activation, and apoptosis in carcinoma cells treated with arsenic trioxide. *J Pharmacol Exp Ther* **339**, 451-463 (2011).

90. Spiecker, M. *et al.* Risk of coronary artery disease associated with polymorphism of the cytochrome P450 epoxygenase CYP2J2. *Circulation* **110**, 2132-2136 (2004).

91. Liu, P.Y. *et al.* Synergistic effect of cytochrome P450 epoxygenase CYP2J2*7 polymorphism with smoking on the onset of premature myocardial infarction. *Atherosclerosis* **195**, 199-206 (2007).

92. Dreisbach, A.W. *et al.* The Prevalence of CYP2C8, 2C9, 2J2, and soluble epoxide hydrolase polymorphisms in African Americans with hypertension. *Am J Hypertens* **18**, 1276-1281 (2005).

93. Wu, S.N. *et al.* Evidence for association of polymorphisms in CYP2J2 and susceptibility to essential hypertension. *Ann Hum Genet* **71**, 519-525 (2007).

94. Seubert, J. *et al.* Enhanced postischemic functional recovery in CYP2J2 transgenic hearts involves mitochondrial ATP-sensitive K+ channels and p42/p44 MAPK pathway. *Circ Res* **95**, 506-514 (2004).

95. Seubert, J.M. *et al.* Role of soluble epoxide hydrolase in postischemic recovery of heart contractile function. *Circ Res* **99**, 442-450 (2006).

96. Gross, G.J., Hsu, A., Falck, J.R. & Nithipatikom, K. Mechanisms by which epoxyeicosatrienoic acids (EETs) elicit cardioprotection in rat hearts. *J Mol Cell Cardiol* **42**, 687-691 (2007).

97. Batchu, S.N. *et al.* Cardioprotective effect of a dual acting epoxyeicosatrienoic acid analogue towards ischaemia reperfusion injury. *Br J Pharmacol* **162**, 897-907 (2011).

98. Chaudhary, K.R., Abukhashim, M., Hwang, S.H., Hammock, B.D. & Seubert, J.M. Inhibition of soluble epoxide hydrolase by trans-4- [4-(3-adamantan-1-yl-ureido)-cyclohexyloxy]-benzoic acid is protective

against ischemia-reperfusion injury. *J Cardiovasc Pharmacol* **55**, 67-73 (2010).

99. Gross, G.J. *et al.* Effects of the selective EET antagonist, 14,15-EEZE, on cardioprotection produced by exogenous or endogenous EETs in the canine heart. *Am J Physiol Heart Circ Physiol* **294**, H2838-2844 (2008).

100. Li, N. *et al.* Beneficial effects of soluble epoxide hydrolase inhibitors in myocardial infarction model: Insight gained using metabolomic approaches. *J Mol Cell Cardiol* **47**, 835-845 (2009).

101. Kompa, A.R. *et al.* Soluble epoxide hydrolase inhibition exerts beneficial anti-remodeling actions post-myocardial infarction. *Int J Cardiol* **167**, 210-219 (2013).

102. Xu, D. *et al.* Prevention and reversal of cardiac hypertrophy by soluble epoxide hydrolase inhibitors. *Proc Natl Acad Sci U S A* **103**, 18733-18738 (2006).

103. Ai, D. *et al.* Soluble epoxide hydrolase plays an essential role in angiotensin II-induced cardiac hypertrophy. *Proc Natl Acad Sci U S A* **106**, 564-569 (2009).

104. Monti, J. *et al.* Soluble epoxide hydrolase is a susceptibility factor for heart failure in a rat model of human disease. *Nat Genet* **40**, 529-537 (2008).

105. Sirish, P. *et al.* Unique mechanistic insights into the beneficial effects of soluble epoxide hydrolase inhibitors in the prevention of cardiac fibrosis. *Proc Natl Acad Sci U S A* **110**, 5618-5623 (2013).

106. Batchu, S.N. *et al.* Role of PI3Kalpha and sarcolemmal ATP-sensitive potassium channels in epoxyeicosatrienoic acid mediated cardioprotection. *J Mol Cell Cardiol* **53**, 43-52 (2012).

107. Chaudhary, K.R. *et al.* Role of B-type natriuretic peptide in epoxyeicosatrienoic acid-mediated improved post-ischaemic recovery of heart contractile function. *Cardiovasc Res* **83**, 362-370 (2009).

108. Marino, G., Niso-Santano, M., Baehrecke, E.H. & Kroemer, G. Self-consumption: the interplay of autophagy and apoptosis. *Nat Rev Mol Cell Biol* **15**, 81-94 (2014).

109. Kanamori, H. *et al.* The role of autophagy emerging in postinfarction cardiac remodelling. *Cardiovasc Res* **91**, 330-339 (2011).

110. Marín-García, J., Akhmedov, A., Rybin, V. & Moe, G.W. *Mitochondria and their role in cardiovascular disease*. (2013).

111. Green, D.R., Galluzzi, L. & Kroemer, G. Cell biology. Metabolic control of cell death. *Science* **345**, 1250256 (2014).

112. Bergmann, O. *et al.* Evidence for cardiomyocyte renewal in humans. *Science* **324**, 98-102 (2009).

113. Aon, M.A., Cortassa, S., Akar, F.G. & O'Rourke, B. Mitochondrial criticality: a new concept at the turning point of life or death. *Biochim Biophys Acta* **1762**, 232-240 (2006).

114. Bell, R.M. & Yellon, D.M. There is more to life than revascularization: therapeutic targeting of myocardial ischemia/reperfusion injury. *Cardiovasc Ther* **29**, e67-79 (2011).

115. Yellon, D.M. & Hausenloy, D.J. Myocardial reperfusion injury. *N Engl J Med* **357**, 1121-1135 (2007).

116. Kroemer, G., Galluzzi, L. & Brenner, C. Mitochondrial membrane permeabilization in cell death. *Physiol Rev* **87**, 99-163 (2007).

117. Honda, H.M., Korge, P. & Weiss, J.N. Mitochondria and ischemia/reperfusion injury. *Ann N Y Acad Sci* **1047**, 248-258 (2005).

118. Halestrap, A.P. What is the mitochondrial permeability transition pore? *J Mol Cell Cardiol* **46**, 821-831 (2009).

119. Halestrap, A.P., Clarke, S.J. & Khalilin, I. The Mitochondrial Permeability Transition Pore – from Molecular Mechanism to Reperfusion Injury and Cardioprotection, in *Mitochondria*. (eds. S.W. Schaffer & M.-S. Suleiman) 241-269 (Springer New York, 2007).

120. Halestrap, A.P., Clarke, S.J. & Javadov, S.A. Mitochondrial permeability transition pore opening during myocardial reperfusion--a target for cardioprotection. *Cardiovasc Res* **61**, 372-385 (2004).

121. Shanmuganathan, S., Hausenloy, D.J., Duchen, M.R. & Yellon, D.M. Mitochondrial permeability transition pore as a target for cardioprotection in the human heart. *Am J Physiol Heart Circ Physiol* **289**, H237-242 (2005).

122. He, Q., Harris, N., Ren, J. & Han, X. Mitochondria-targeted antioxidant prevents cardiac dysfunction induced by tafazzin gene knockdown in cardiac myocytes. *Oxid Med Cell Longev* **2014**, 654198 (2014).

123. Toogood, P.L. Mitochondrial drugs. *Curr Opin Chem Biol* **12**, 457-463 (2008).

124. Huang, C. *et al.* Preconditioning involves selective mitophagy mediated by Parkin and p62/SQSTM1. *PLoS One* **6**, e20975 (2011).

125. Gottlieb, R.A. & Gustafsson, A.B. Mitochondrial turnover in the heart. *Biochim Biophys Acta* **1813**, 1295-1301 (2011).

126. Schwartz Longacre, L. *et al.* New horizons in cardioprotection: recommendations from the 2010 National Heart, Lung, and Blood Institute Workshop. *Circulation* **124**, 1172-1179 (2011).

127. Walters, A.M., Porter, G.A., Jr. & Brookes, P.S. Mitochondria as a drug target in ischemic heart disease and cardiomyopathy. *Circ Res* **111**, 1222-1236 (2012).

128. Jezek, P. & Plecita-Hlavata, L. Mitochondrial reticulum network dynamics in relation to oxidative stress, redox regulation, and hypoxia. *Int J Biochem Cell Biol* **41**, 1790-1804 (2009).

129. Park, J., Lee, J. & Choi, C. Mitochondrial network determines intracellular ROS dynamics and sensitivity to oxidative stress through switching inter-mitochondrial messengers. *PLoS One* **6**, e23211 (2011).

130. Wu, S., Zhou, F., Zhang, Z. & Xing, D. Mitochondrial oxidative stress causes mitochondrial fragmentation via differential modulation of mitochondrial fission-fusion proteins. *FEBS J* **278**, 941-954 (2011).

131. Chen, L., Gong, Q., Stice, J.P. & Knowlton, A.A. Mitochondrial OPA1, apoptosis, and heart failure. *Cardiovasc Res* **84**, 91-99 (2009).

132. Marín-García, J. Mitochondrial Structure, Composition, and Dynamics, in *Mitochondria and Their Role in Cardiovascular Disease* 29-57 (Springer US, 2013).

133. Liesa, M., Palacin, M. & Zorzano, A. Mitochondrial dynamics in mammalian health and disease. *Physiol Rev* **89**, 799-845 (2009).

134. Taguchi, N., Ishihara, N., Jofuku, A., Oka, T. & Mihara, K. Mitotic phosphorylation of dynamin-related GTPase Drp1 participates in mitochondrial fission. *J Biol Chem* **282**, 11521-11529 (2007).

135. Gomes, L.C., Di Benedetto, G. & Scorrano, L. During autophagy mitochondria elongate, are spared from degradation and sustain cell viability. *Nat Cell Biol* **13**, 589-598 (2011).

136. Chen, Y., Liu, Y. & Dorn, G.W., 2nd Mitochondrial fusion is essential for organelle function and cardiac homeostasis. *Circ Res* **109**, 1327-1331 (2011).

137. Archer, S.L. Mitochondrial dynamics--mitochondrial fission and fusion in human diseases. *N Engl J Med* **369**, 2236-2251 (2013).

138. McNew, J.A., Sondermann, H., Lee, T., Stern, M. & Brandizzi, F. GTP-dependent membrane fusion. *Annu Rev Cell Dev Biol* **29**, 529-550 (2013).

139. Wilkens, V., Kohl, W. & Busch, K. Restricted diffusion of OXPHOS complexes in dynamic mitochondria delays their exchange between cristae and engenders a transitory mosaic distribution. *J Cell Sci* **126**, 103-116 (2013).

140. Chen, H. *et al.* Mitochondrial fusion is required for mtDNA stability in skeletal muscle and tolerance of mtDNA mutations. *Cell* **141**, 280-289 (2010).

141. Duvezin-Caubet, S. *et al.* Proteolytic processing of OPA1 links mitochondrial dysfunction to alterations in mitochondrial morphology. *J Biol Chem* **281**, 37972-37979 (2006).

142. Twig, G. *et al.* Fission and selective fusion govern mitochondrial segregation and elimination by autophagy. *EMBO J* **27**, 433-446 (2008).

143. Kasahara, A., Cipolat, S., Chen, Y., Dorn, G.W., 2nd & Scorrano, L. Mitochondrial fusion directs cardiomyocyte differentiation via calcineurin and Notch signaling. *Science* **342**, 734-737 (2013).

144. Chen, H. *et al.* Mitofusins Mfn1 and Mfn2 coordinately regulate mitochondrial fusion and are essential for embryonic development. *J Cell Biol* **160**, 189-200 (2003).

145. Davies, V.J. *et al.* Opa1 deficiency in a mouse model of autosomal dominant optic atrophy impairs mitochondrial morphology, optic nerve structure and visual function. *Hum Mol Genet* **16**, 1307-1318 (2007).

146. Frank, S. *et al.* The role of dynamin-related protein 1, a mediator of mitochondrial fission, in apoptosis. *Dev Cell* **1**, 515-525 (2001).

147. Karbowski, M. *et al.* Spatial and temporal association of Bax with mitochondrial fission sites, Drp1, and Mfn2 during apoptosis. *J Cell Biol* **159**, 931-938 (2002).

148. Mozdy, A.D., McCaffery, J.M. & Shaw, J.M. Dnm1p GTPase-mediated mitochondrial fission is a multi-step process requiring the novel integral membrane component Fis1p. *J Cell Biol* **151**, 367-380 (2000).

149. Otera, H. *et al.* Mff is an essential factor for mitochondrial recruitment of Drp1 during mitochondrial fission in mammalian cells. *J Cell Biol* **191**, 1141-1158 (2010).

150. Friedman, J.R. *et al.* ER tubules mark sites of mitochondrial division. *Science* **334**, 358-362 (2011).

151. Shim, S.H. *et al.* Super-resolution fluorescence imaging of organelles in live cells with photoswitchable membrane probes. *Proc Natl Acad Sci U S A* **109**, 13978-13983 (2012).

152. Ingerman, E. *et al.* Dnm1 forms spirals that are structurally tailored to fit mitochondria. *J Cell Biol* **170**, 1021-1027 (2005).

153. Mears, J.A. *et al.* Conformational changes in Dnm1 support a contractile mechanism for mitochondrial fission. *Nat Struct Mol Biol* **18**, 20-26 (2011).

154. Sweitzer, S.M. & Hinshaw, J.E. Dynamin undergoes a GTP-dependent conformational change causing vesiculation. *Cell* **93**, 1021-1029 (1998).

155. Yoon, Y., Pitts, K.R. & McNiven, M.A. Mammalian dynamin-like protein DLP1 tubulates membranes. *Mol Biol Cell* **12**, 2894-2905 (2001).

156. Youle, R.J. & Karbowski, M. Mitochondrial fission in apoptosis. *Nat Rev Mol Cell Biol* **6**, 657-663 (2005).

157. Hom, J. & Sheu, S.S. Morphological dynamics of mitochondria--a special emphasis on cardiac muscle cells. *J Mol Cell Cardiol* **46**, 811-820 (2009).

158. Frank, M. *et al.* Mitophagy is triggered by mild oxidative stress in a mitochondrial fission dependent manner. *Biochim Biophys Acta* **1823**, 2297-2310 (2012).

159. Hyde, B.B., Twig, G. & Shirihai, O.S. Organellar vs cellular control of mitochondrial dynamics. *Semin Cell Dev Biol* **21**, 575-581 (2010).

160. Palmer, C.S., Osellame, L.D., Stojanovski, D. & Ryan, M.T. The regulation of mitochondrial morphology: intricate mechanisms and dynamic machinery. *Cell Signal* **23**, 1534-1545 (2011).

161. Wilson, T.J., Slupe, A.M. & Strack, S. Cell signaling and mitochondrial dynamics: Implications for neuronal function and neurodegenerative disease. *Neurobiol Dis* **51**, 13-26 (2013).

162. Anne Stetler, R., Leak, R.K., Gao, Y. & Chen, J. The dynamics of the mitochondrial organelle as a potential therapeutic target. *J Cereb Blood Flow Metab* **33**, 22-32 (2013).

163. Olichon, A. *et al.* The human dynamin-related protein OPA1 is anchored to the mitochondrial inner membrane facing the inter-membrane space. *FEBS Letters* **523**, 171-176 (2002).

164. Satoh, M., Hamamoto, T., Seo, N., Kagawa, Y. & Endo, H. Differential sublocalization of the dynamin-related protein OPA1

isoforms in mitochondria. *Biochem Biophys Res Commun* **300**, 482-493 (2003).

165. Misaka, T., Miyashita, T. & Kubo, Y. Primary structure of a dynamin-related mouse mitochondrial GTPase and its distribution in brain, subcellular localization, and effect on mitochondrial morphology. *J Biol Chem* **277**, 15834-15842 (2002).

166. Alexander, C. *et al.* OPA1, encoding a dynamin-related GTPase, is mutated in autosomal dominant optic atrophy linked to chromosome 3q28. *Nat Genet* **26**, 211-215 (2000).

167. Alavi, M.V. *et al.* A splice site mutation in the murine Opa1 gene features pathology of autosomal dominant optic atrophy. *Brain* **130**, 1029-1042 (2007).

168. Hudson, G. *et al.* Mutation of OPA1 causes dominant optic atrophy with external ophthalmoplegia, ataxia, deafness and multiple mitochondrial DNA deletions: a novel disorder of mtDNA maintenance. *Brain* **131**, 329-337 (2008).

169. Amati-Bonneau, P. *et al.* OPA1-associated disorders: phenotypes and pathophysiology. *Int J Biochem Cell Biol* **41**, 1855-1865 (2009).

170. Akepati, V.R. *et al.* Characterization of OPA1 isoforms isolated from mouse tissues. *J Neurochem* **106**, 372-383 (2008).

171. Song, Z., Chen, H., Fiket, M., Alexander, C. & Chan, D.C. OPA1 processing controls mitochondrial fusion and is regulated by mRNA

splicing, membrane potential, and Yme1L. *J Cell Biol* **178**, 749-755 (2007).

172. Cipolat, S., Martins de Brito, O., Dal Zilio, B. & Scorrano, L. OPA1 requires mitofusin 1 to promote mitochondrial fusion. *Proc Natl Acad Sci U S A* **101**, 15927-15932 (2004).

173. Escobar-Henriques, M. & Anton, F. Mechanistic perspective of mitochondrial fusion: tubulation vs. fragmentation. *Biochim Biophys Acta* **1833**, 162-175 (2013).

174. Patten, D.A. *et al.* OPA1-dependent cristae modulation is essential for cellular adaptation to metabolic demand. *EMBO J* **33**, 2676-2691 (2014).

175. Head, B., Griparic, L., Amiri, M., Gandre-Babbe, S. & van der Bliek, A.M. Inducible proteolytic inactivation of OPA1 mediated by the OMA1 protease in mammalian cells. *J Cell Biol* **187**, 959-966 (2009).

176. Alavi, M.V. & Fuhrmann, N. Dominant optic atrophy, OPA1, and mitochondrial quality control: understanding mitochondrial network dynamics. *Mol Neurodegener* **8**, 32 (2013).

177. DeVay, R.M. *et al.* Coassembly of Mgm1 isoforms requires cardiolipin and mediates mitochondrial inner membrane fusion. *J Cell Biol* **186**, 793-803 (2009).

178. Frezza, C. *et al.* OPA1 controls apoptotic cristae remodeling independently from mitochondrial fusion. *Cell* **126**, 177-189 (2006).

179. Pellegrini, L. & Scorrano, L. A cut short to death: Parl and Opa1 in the regulation of mitochondrial morphology and apoptosis. *Cell Death Differ* **14**, 1275-1284 (2007).

180. Yamaguchi, R. *et al.* Opa1-mediated cristae opening is Bax/Bak and BH3 dependent, required for apoptosis, and independent of Bak oligomerization. *Mol Cell* **31**, 557-569 (2008).

181. Rujiviphat, J., Meglei, G., Rubinstein, J.L. & McQuibban, G.A. Phospholipid association is essential for dynamin-related protein Mgm1 to function in mitochondrial membrane fusion. *J Biol Chem* **284**, 28682-28686 (2009).

182. Ban, T., Heymann, J.A., Song, Z., Hinshaw, J.E. & Chan, D.C. OPA1 disease alleles causing dominant optic atrophy have defects in cardiolipin-stimulated GTP hydrolysis and membrane tubulation. *Hum Mol Genet* **19**, 2113-2122 (2010).

183. Gilkerson, R.W., Selker, J.M. & Capaldi, R.A. The cristal membrane of mitochondria is the principal site of oxidative phosphorylation. *FEBS Lett* **546**, 355-358 (2003).

184. Zick, M., Rabl, R. & Reichert, A.S. Cristae formation-linking ultrastructure and function of mitochondria. *Biochim Biophys Acta* **1793**, 5-19 (2009).

185. Kushnareva, Y.E. *et al.* Loss of OPA1 disturbs cellular calcium homeostasis and sensitizes for excitotoxicity. *Cell Death Differ* **20**, 353-365 (2013).

186. Cipolat, S. *et al.* Mitochondrial rhomboid PARL regulates cytochrome c release during apoptosis via OPA1-dependent cristae remodeling. *Cell* **126**, 163-175 (2006).

187. Cogliati, S. (2011).

188. Amutha, B., Gordon, D.M., Gu, Y. & Pain, D. A novel role of Mgm1p, a dynamin-related GTPase, in ATP synthase assembly and cristae formation/maintenance. *Biochem J* **381**, 19-23 (2004).

189. Olichon, A. *et al.* Loss of OPA1 perturbates the mitochondrial inner membrane structure and integrity, leading to cytochrome c release and apoptosis. *J Biol Chem* **278**, 7743-7746 (2003).

190. Sood, A. *et al.* A Mitofusin-2-dependent inactivating cleavage of Opa1 links changes in mitochondria cristae and ER contacts in the postprandial liver. *Proc Natl Acad Sci U S A* **111**, 16017-16022 (2014).

191. Sanjuan Szklarz, L.K. & Scorrano, L. The antiapoptotic OPA1/Parl couple participates in mitochondrial adaptation to heat shock. *Biochim Biophys Acta* **1817**, 1886-1893 (2012).

192. Tondera, D. *et al.* SLP-2 is required for stress-induced mitochondrial hyperfusion. *EMBO J* **28**, 1589-1600 (2009).

193. Galluzzi, L. & Kroemer, G. Necroptosis: a specialized pathway of programmed necrosis. *Cell* **135**, 1161-1163 (2008).

194. Jourdain, A. & Martinou, J.C. Mitochondrial outer-membrane permeabilization and remodelling in apoptosis. *Int J Biochem Cell Biol* **41**, 1884-1889 (2009).

195. Rehm, M. *et al.* Dynamics of outer mitochondrial membrane permeabilization during apoptosis. *Cell Death Differ* **16**, 613-623 (2009).

196. Gottlieb, E. OPA1 and PARL keep a lid on apoptosis. *Cell* **126**, 27-29 (2006).

197. Landes, T. *et al.* The BH3-only Bnip3 binds to the dynamin Opa1 to promote mitochondrial fragmentation and apoptosis by distinct mechanisms. *EMBO Rep* **11**, 459-465 (2010).

198. Ramonet, D. *et al.* Optic atrophy 1 mediates mitochondria remodeling and dopaminergic neurodegeneration linked to complex I deficiency. *Cell Death Differ* **20**, 77-85 (2013).

199. Civiletto, G. *et al.* Opa1 overexpression ameliorates the phenotype of two mitochondrial disease mouse models. *Cell Metab* **21**, 845-854 (2015).

200. Fulop, L., Szanda, G., Enyedi, B., Varnai, P. & Spat, A. The effect of OPA1 on mitochondrial Ca(2)(+) signaling. *PLoS One* **6**, e25199 (2011).

201. Garedew, A., Andreassi, C. & Moncada, S. Mitochondrial dynamics, biogenesis, and function are coordinated with the cell cycle by APC/C CDH1. *Cell Metab* **15**, 466-479 (2012).

202. Griparic, L., Kanazawa, T. & van der Bliek, A.M. Regulation of the mitochondrial dynamin-like protein Opa1 by proteolytic cleavage. *J Cell Biol* **178**, 757-764 (2007).

203. Ishihara, N., Fujita, Y., Oka, T. & Mihara, K. Regulation of mitochondrial morphology through proteolytic cleavage of OPA1. *EMBO J* **25**, 2966-2977 (2006).

204. Ehses, S. *et al.* Regulation of OPA1 processing and mitochondrial fusion by m-AAA protease isoenzymes and OMA1. *J Cell Biol* **187**, 1023-1036 (2009).

205. Mishra, P., Carelli, V., Manfredi, G. & Chan, D.C. Proteolytic cleavage of Opa1 stimulates mitochondrial inner membrane fusion and couples fusion to oxidative phosphorylation. *Cell Metab* **19**, 630-641 (2014).

206. Guillery, O. *et al.* Metalloprotease-mediated OPA1 processing is modulated by the mitochondrial membrane potential. *Biol Cell* **100**, 315-325 (2008).

207. Quinsay, M.N. *et al.* Bnip3 mediates permeabilization of mitochondria and release of cytochrome c via a novel mechanism. *J Mol Cell Cardiol* **48**, 1146-1156 (2010).

208. Samant, S.A. *et al.* SIRT3 deacetylates and activates OPA1 to regulate mitochondrial dynamics during stress. *Mol Cell Biol* **34**, 807-819 (2014).

209. Yoon, Y.S. *et al.* Formation of elongated giant mitochondria in DFO-induced cellular senescence: involvement of enhanced fusion process through modulation of Fis1. *J Cell Physiol* **209**, 468-480 (2006).

210. Shutt, T., Geoffrion, M., Milne, R. & McBride, H.M. The intracellular redox state is a core determinant of mitochondrial fusion. *EMBO Rep* **13**, 909-915 (2012).

211. Norton, M. *et al.* ROMO1 is an essential redox-dependent regulator of mitochondrial dynamics. *Sci Signal* **7**, ra10 (2014).

212. Zhu, P.P. *et al.* Intra- and intermolecular domain interactions of the C-terminal GTPase effector domain of the multimeric dynamin-like GTPase Drp1. *J Biol Chem* **279**, 35967-35974 (2004).

213. Bleazard, W. *et al.* The dynamin-related GTPase Dnm1 regulates mitochondrial fission in yeast. *Nat Cell Biol* **1**, 298-304 (1999).

214. Reddy, P.H. *et al.* Dynamin-related protein 1 and mitochondrial fragmentation in neurodegenerative diseases. *Brain Res Rev* **67**, 103-118 (2011).

215. Chang, C.R. & Blackstone, C. Dynamic regulation of mitochondrial fission through modification of the dynamin-related protein Drp1. *Ann N Y Acad Sci* **1201**, 34-39 (2010).

216. Jahani-Asl, A. & Slack, R.S. The phosphorylation state of Drp1 determines cell fate. *EMBO Rep* **8**, 912-913 (2007).

217. Ugarte-Uribe, B. & Garcia-Saez, A.J. Membranes in motion: mitochondrial dynamics and their role in apoptosis. *Biol Chem* **395**, 297-311 (2014).

218. van der Bliek, A.M. A mitochondrial division apparatus takes shape. *J Cell Biol* **151**, F1-4 (2000).

219. Arnoult, D. Mitochondrial fragmentation in apoptosis. *Trends Cell Biol* **17**, 6-12 (2007).

220. Hall, A.R., Burke, N., Dongworth, R.K. & Hausenloy, D.J. Mitochondrial fusion and fission proteins: novel therapeutic targets for combating cardiovascular disease. *Br J Pharmacol* **171**, 1890-1906 (2014).

221. Sharp, W.W. Dynamin-related protein 1 as a therapeutic target in cardiac arrest. *Journal of molecular medicine* **93**, 243-252 (2015).

222. Cassidy-Stone, A. *et al.* Chemical inhibition of the mitochondrial division dynamin reveals its role in Bax/Bak-dependent mitochondrial outer membrane permeabilization. *Dev Cell* **14**, 193-204 (2008).

223. Ong, S.B. *et al.* Inhibiting mitochondrial fission protects the heart against ischemia/reperfusion injury. *Circulation* **121**, 2012-2022 (2010).

224. Gomes, L.C., Di Benedetto, G. & Scorrano, L. Essential amino acids and glutamine regulate induction of mitochondrial elongation during autophagy. *Cell Cycle* **10**, 2635-2639 (2011).

225. Rambold, A.S., Kostelecky, B., Elia, N. & Lippincott-Schwartz, J. Tubular network formation protects mitochondria from autophagosomal degradation during nutrient starvation. *Proc Natl Acad Sci U S A* **108**, 10190-10195 (2011).

226. Ikeda, Y. *et al.* Endogenous Drp1 mediates mitochondrial autophagy and protects the heart against energy stress. *Circ Res* **116**, 264-278 (2015).

227. Kageyama, Y. *et al.* Parkin-independent mitophagy requires Drp1 and maintains the integrity of mammalian heart and brain. *EMBO J* **33**, 2798-2813 (2014).

228. Song, M., Mihara, K., Chen, Y., Scorrano, L. & Dorn, G.W., 2nd Mitochondrial fission and fusion factors reciprocally orchestrate mitophagic culling in mouse hearts and cultured fibroblasts. *Cell Metab* **21**, 273-285 (2015).

229. Dorn, G.W., 2nd Gone fission...: diverse consequences of cardiac Drp1 deficiency. *Circ Res* **116**, 225-228 (2015).

230. Qi, X., Disatnik, M.H., Shen, N., Sobel, R.A. & Mochly-Rosen, D. Aberrant mitochondrial fission in neurons induced by protein kinase C{delta} under oxidative stress conditions in vivo. *Mol Biol Cell* **22**, 256-265 (2011).

231. Chang, C.R. & Blackstone, C. Cyclic AMP-dependent protein kinase phosphorylation of Drp1 regulates its GTPase activity and mitochondrial morphology. *J Biol Chem* **282**, 21583-21587 (2007).

232. Cribbs, J.T. & Strack, S. Reversible phosphorylation of Drp1 by cyclic AMP-dependent protein kinase and calcineurin regulates mitochondrial fission and cell death. *EMBO Rep* **8**, 939-944 (2007).

233. Cereghetti, G.M. *et al.* Dephosphorylation by calcineurin regulates translocation of Drp1 to mitochondria. *Proc Natl Acad Sci U S A* **105**, 15803-15808 (2008).

234. Cereghetti, G.M., Costa, V. & Scorrano, L. Inhibition of Drp1-dependent mitochondrial fragmentation and apoptosis by a polypeptide antagonist of calcineurin. *Cell Death Differ* **17**, 1785-1794 (2010).

235. Batchu, S.N., Law, E., Brocks, D.R., Falck, J.R. & Seubert, J.M. Epoxyeicosatrienoic acid prevents postischemic electrocardiogram abnormalities in an isolated heart model. *J Mol Cell Cardiol* **46**, 67-74 (2009).

236. Han, X.J. *et al.* CaM kinase I alpha-induced phosphorylation of Drp1 regulates mitochondrial morphology. *J Cell Biol* **182**, 573-585 (2008).

237. Strack, S., Wilson, T.J. & Cribbs, J.T. Cyclin-dependent kinases regulate splice-specific targeting of dynamin-related protein 1 to microtubules. *J Cell Biol* **201**, 1037-1051 (2013).

238. De Palma, C. *et al.* Nitric oxide inhibition of Drp1-mediated mitochondrial fission is critical for myogenic differentiation. *Cell Death Differ* **17**, 1684-1696 (2010).

239. Karbowski, M., Neutzner, A. & Youle, R.J. The mitochondrial E3 ubiquitin ligase MARCH5 is required for Drp1 dependent mitochondrial division. *J Cell Biol* **178**, 71-84 (2007).

240. Braschi, E., Zunino, R. & McBride, H.M. MAPL is a new mitochondrial SUMO E3 ligase that regulates mitochondrial fission. *EMBO Rep* **10**, 748-754 (2009).

241. Zunino, R., Braschi, E., Xu, L. & McBride, H.M. Translocation of SenP5 from the nucleoli to the mitochondria modulates DRP1-dependent fission during mitosis. *J Biol Chem* **284**, 17783-17795 (2009).

242. Wasiak, S., Zunino, R. & McBride, H.M. Bax/Bak promote sumoylation of DRP1 and its stable association with mitochondria during apoptotic cell death. *J Cell Biol* **177**, 439-450 (2007).

243. Santel, A. & Fuller, M.T. Control of mitochondrial morphology by a human mitofusin. *J Cell Sci* **114**, 867-874 (2001).

244. Eura, Y., Ishihara, N., Yokota, S. & Mihara, K. Two mitofusin proteins, mammalian homologues of FZO, with distinct functions are both required for mitochondrial fusion. *J Biochem* **134**, 333-344 (2003).

245. de Brito, O.M. & Scorrano, L. Mitofusin 2 tethers endoplasmic reticulum to mitochondria. *Nature* **456**, 605-610 (2008).

246. Chen, Y. & Dorn, G.W., 2nd PINK1-phosphorylated mitofusin 2 is a Parkin receptor for culling damaged mitochondria. *Science* **340**, 471-475 (2013).

247. Misko, A., Jiang, S., Wegorzewska, I., Milbrandt, J. & Baloh, R.H. Mitofusin 2 is necessary for transport of axonal mitochondria and interacts with the Miro/Milton complex. *J Neurosci* **30**, 4232-4240 (2010).

248. Zuchner, S. *et al.* Mutations in the mitochondrial GTPase mitofusin 2 cause Charcot-Marie-Tooth neuropathy type 2A. *Nat Genet* **36**, 449-451 (2004).

249. Loson, O.C., Song, Z., Chen, H. & Chan, D.C. Fis1, Mff, MiD49, and MiD51 mediate Drp1 recruitment in mitochondrial fission. *Mol Biol Cell* **24**, 659-667 (2013).

250. Lee, Y.J., Jeong, S.Y., Karbowski, M., Smith, C.L. & Youle, R.J. Roles of the mammalian mitochondrial fission and fusion mediators Fis1, Drp1, and Opa1 in apoptosis. *Mol Biol Cell* **15**, 5001-5011 (2004).

251. Otera, H., Ishihara, N. & Mihara, K. New insights into the function and regulation of mitochondrial fission. *Biochim Biophys Acta* **1833**, 1256-1268 (2013).

252. El-Sikhry, H.E., Miller, G.G., Madiyalakan, M.R. & Seubert, J.M. Sonodynamic and photodynamic mechanisms of action of the novel hypocrellin sonosensitizer, SL017: mitochondrial cell death is

attenuated by 11, 12-epoxyeicosatrienoic acid. *Invest New Drugs* **29**, 1328-1336 (2011).

253. Martinet, W., De Meyer, G.R., Herman, A.G. & Kockx, M.M. Amino acid deprivation induces both apoptosis and autophagy in murine C2C12 muscle cells. *Biotechnol Lett* **27**, 1157-1163 (2005).

254. Codogno, P. & Meijer, A.J. Autophagy and signaling: their role in cell survival and cell death. *Cell Death Differ* **12 Suppl 2**, 1509-1518 (2005).

255. Rockson, S.G., Lorenz, D.P., Cheong, W.F. & Woodburn, K.W. Photoangioplasty: An emerging clinical cardiovascular role for photodynamic therapy. *Circulation* **102**, 591-596 (2000).

256. Tachibana, K., Feril, L.B., Jr. & Ikeda-Dantsuji, Y. Sonodynamic therapy. *Ultrasonics* **48**, 253-259 (2008).

257. Tang, W. *et al.* Potential mechanism in sonodynamic therapy and focused ultrasound induced apoptosis in sarcoma 180 cells in vitro. *Ultrasonics* **49**, 786-793 (2009).

258. Hiraoka, W., Honda, H., Feril, L.B., Jr., Kudo, N. & Kondo, T. Comparison between sonodynamic effect and photodynamic effect with photosensitizers on free radical formation and cell killing. *Ultrason Sonochem* **13**, 535-542 (2006).

259. Rosenthal, I., Sostaric, J.Z. & Riesz, P. Sonodynamic therapy--a review of the synergistic effects of drugs and ultrasound. *Ultrason Sonochem* **11**, 349-363 (2004).

260. Ali, S.M., Chee, S.K., Yuen, G.Y. & Olivo, M. Hypericin and hypocrellin induced apoptosis in human mucosal carcinoma cells. *J Photochem Photobiol B* **65**, 59-73 (2001).

261. Miller, G.G. *et al.* Preclinical assessment of hypocrellin B and hypocrellin B derivatives as sensitizers for photodynamic therapy of cancer: progress update. *Photochem Photobiol* **65**, 714-722 (1997).

262. Jakus, J. & Farkas, O. Photosensitizers and antioxidants: a way to new drugs? *Photochemical & photobiological sciences : Official journal of the European Photochemistry Association and the European Society for Photobiology* **4**, 694-698 (2005).

263. Estey, E.P. *et al.* Hypocrellins as photosensitizers for photodynamic therapy: a screening evaluation and pharmacokinetic study. *Cancer Chemother Pharmacol* **37**, 343-350 (1996).

264. Yumita, N., Umemura, S., Magario, N., Umemura, K. & Nishigaki, R. Membrane lipid peroxidation as a mechanism of sonodynamically induced erythrocyte lysis. *Int J Radiat Biol* **69**, 397-404 (1996).

265. Yumita, N. *et al.* Sonochemical activation of hematoporphyrin: an ESR study. *Radiat Res* **138**, 171-176 (1994).

266. Yumita, N., Nishigaki, R., Umemura, K. & Umemura, S. Hematoporphyrin as a sensitizer of cell-damaging effect of ultrasound. *Jpn J Cancer Res* **80**, 219-222 (1989).

267. El Maalouf, J., Bera, J.C., Alberti, L., Cathignol, D. & Mestas, J.L. In vitro sonodynamic cytotoxicity in regulated cavitation conditions. *Ultrasonics* **49**, 238-243 (2009).

268. Furt, F. & Moreau, P. Importance of lipid metabolism for intracellular and mitochondrial membrane fusion/fission processes. *Int J Biochem Cell Biol* **41**, 1828-1836 (2009).

269. Chan, D.C. Mitochondria: dynamic organelles in disease, aging, and development. *Cell* **125**, 1241-1252 (2006).

270. Maack, C. & O'Rourke, B. Excitation-contraction coupling and mitochondrial energetics. *Basic Res Cardiol* **102**, 369-392 (2007).

271. Stanley, W.C. *et al.* Malonyl-CoA decarboxylase inhibition suppresses fatty acid oxidation and reduces lactate production during demand-induced ischemia. *Am J Physiol Heart Circ Physiol* **289**, H2304-2309 (2005).

272. Ussher, J.R. & Lopaschuk, G.D. The malonyl CoA axis as a potential target for treating ischaemic heart disease. *Cardiovasc Res* **79**, 259-268 (2008).

273. Wang, W. *et al.* Superoxide flashes in single mitochondria. *Cell* **134**, 279-290 (2008).

274. Hanley, P.J. & Daut, J. K(ATP) channels and preconditioning: a re-examination of the role of mitochondrial K(ATP) channels and an overview of alternative mechanisms. *J Mol Cell Cardiol* **39**, 17-50 (2005).

275. Hausenloy, D.J. & Yellon, D.M. New directions for protecting the heart against ischaemia-reperfusion injury: targeting the Reperfusion Injury Salvage Kinase (RISK)-pathway. *Cardiovasc Res* **61**, 448-460 (2004).

276. Benard, G. *et al.* Mitochondrial bioenergetics and structural network organization. *J Cell Sci* **120**, 838-848 (2007).

277. Hayflick, L. The Limited in Vitro Lifetime of Human Diploid Cell Strains. *Exp Cell Res* **37**, 614-636 (1965).

278. McDonald, J.H. & Dunn, K.W. Statistical tests for measures of colocalization in biological microscopy. *J Microsc* **252**, 295-302 (2013).

279. Choudhary, S., Nouri, K. & Elsaie, M.L. Photodynamic therapy in dermatology: a review. *Lasers Med Sci* **24**, 971-980 (2009).

280. Lu, Z. *et al.* Mitochondrial reactive oxygen species and nitric oxide-mediated cancer cell apoptosis in 2-butylamino-2-demethoxyhypocrellin B photodynamic treatment. *Free Radic Biol Med* **41**, 1590-1605 (2006).

281. Karbowski, M. & Youle, R.J. Dynamics of mitochondrial morphology in healthy cells and during apoptosis. *Cell Death Differ* **10**, 870-880 (2003).

282. Zhang, P. & Hinshaw, J.E. Three-dimensional reconstruction of dynamin in the constricted state. *Nat Cell Biol* **3**, 922-926 (2001).

283. Montessuit, S. *et al.* Membrane remodeling induced by the dynamin-related protein Drp1 stimulates Bax oligomerization. *Cell* **142**, 889-901 (2010).

284. Tanaka, A. & Youle, R.J. A chemical inhibitor of DRP1 uncouples mitochondrial fission and apoptosis. *Mol Cell* **29**, 409-410 (2008).

285. Cho, S.G., Du, Q., Huang, S. & Dong, Z. Drp1 dephosphorylation in ATP depletion-induced mitochondrial injury and tubular cell apoptosis. *Am J Physiol Renal Physiol* **299**, F199-206 (2010).

286. Gomes, L.C. & Scorrano, L. Mitochondrial elongation during autophagy: a stereotypical response to survive in difficult times. *Autophagy* **7**, 1251-1253 (2011).

287. Dickey, A.S. & Strack, S. PKA/AKAP1 and PP2A/Bbeta2 regulate neuronal morphogenesis via Drp1 phosphorylation and mitochondrial bioenergetics. *J Neurosci* **31**, 15716-15726 (2011).

288. Merkwirth, C. *et al.* Prohibitins control cell proliferation and apoptosis by regulating OPA1-dependent cristae morphogenesis in mitochondria. *Genes Dev* **22**, 476-488 (2008).

289. Piquereau, J. *et al.* Down-regulation of OPA1 alters mouse mitochondrial morphology, PTP function, and cardiac adaptation to pressure overload. *Cardiovasc Res* **94**, 408-417 (2012).

290. Mosmann, T. Rapid colorimetric assay for cellular growth and survival: application to proliferation and cytotoxicity assays. *J Immunol Methods* **65**, 55-63 (1983).

291. Strober, W. Trypan blue exclusion test of cell viability. *Curr Protoc Immunol* **Appendix 3**, Appendix 3B (2001).

292. Berridge, M.V., Herst, P.M. & Tan, A.S. Tetrazolium dyes as tools in cell biology: New insights into their cellular reduction. *Biotechnology annual review* **11**, 127-152 (2005).

293. Aras, M.A., Hartnett, K.A. & Aizenman, E. Assessment of cell viability in primary neuronal cultures. *Curr Protoc Neurosci* **Chapter 7**, Unit 7 18 (2008).

294. Wang, S., Yu, H. & Wickliffe, J.K. Limitation of the MTT and XTT assays for measuring cell viability due to superoxide formation induced by nano-scale TiO2. *Toxicol In Vitro* **25**, 2147-2151 (2011).

295. Lanza, I.R. *et al.* Endurance exercise as a countermeasure for aging. *Diabetes* **57**, 2933-2942 (2008).

296. Yu, T., Jhun, B.S. & Yoon, Y. High-glucose stimulation increases reactive oxygen species production through the calcium and mitogen-activated protein kinase-mediated activation of mitochondrial fission. *Antioxid Redox Signal* **14**, 425-437 (2011).

297. McBride, H. & Soubannier, V. Mitochondrial function: OMA1 and OPA1, the grandmasters of mitochondrial health. *Curr Biol* **20**, R274-276 (2010).

298. Baricault, L. *et al.* OPA1 cleavage depends on decreased mitochondrial ATP level and bivalent metals. *Exp Cell Res* **313**, 3800-3808 (2007).

299. Lopaschuk, G.D., Belke, D.D., Gamble, J., Itoi, T. & Schonekess, B.O. Regulation of fatty acid oxidation in the mammalian heart in health and disease. *Biochim Biophys Acta* **1213**, 263-276 (1994).

300. Meyers, D.E., Basha, H.I. & Koenig, M.K. Mitochondrial cardiomyopathy: pathophysiology, diagnosis, and management. *Tex Heart Inst J* **40**, 385-394 (2013).

301. Bayeva, M., Gheorghiade, M. & Ardehali, H. Mitochondria as a therapeutic target in heart failure. *J Am Coll Cardiol* **61**, 599-610 (2013).

302. Ashrafi, G. & Schwarz, T.L. The pathways of mitophagy for quality control and clearance of mitochondria. *Cell Death Differ* **20**, 31-42 (2013).

303. Griffiths, E.J. Mitochondria and heart disease. *Adv Exp Med Biol* **942**, 249-267 (2012).

304. Ballweg, K., Mutze, K., Konigshoff, M., Eickelberg, O. & Meiners, S. Cigarette smoke extract affects mitochondrial function in alveolar epithelial cells. *Am J Physiol Lung Cell Mol Physiol* **307**, L895-907 (2014).

305. Gomes, L.C. & Scorrano, L. Mitochondrial morphology in mitophagy and macroautophagy. *Biochim Biophys Acta* **1833**, 205-212 (2013).

306. Zemirli, N. *et al.* Mitochondrial hyperfusion promotes NF-kappaB activation via the mitochondrial E3 ligase MULAN. *FEBS J* **281**, 3095-3112 (2014).

307. Westrate, L.M., Sayfie, A.D., Burgenske, D.M. & MacKeigan, J.P. Persistent mitochondrial hyperfusion promotes G2/M accumulation and caspase-dependent cell death. *PLoS One* **9**, e91911 (2014).

308. MacVicar, T.D. & Lane, J.D. Impaired OMA1-dependent cleavage of OPA1 and reduced DRP1 fission activity combine to prevent mitophagy in cells that are dependent on oxidative phosphorylation. *J Cell Sci* **127**, 2313-2325 (2014).

309. Batchu, S.N. *et al.* Novel soluble epoxide hydrolase inhibitor protects mitochondrial function following stress. *Can J Physiol Pharmacol* **90**, 811-823 (2012).

310. Brady, N.R., Hamacher-Brady, A., Yuan, H. & Gottlieb, R.A. The autophagic response to nutrient deprivation in the hl-1 cardiac myocyte is modulated by Bcl-2 and sarco/endoplasmic reticulum calcium stores. *FEBS J* **274**, 3184-3197 (2007).

311. Celotto, A.M., Chiu, W.K., Van Voorhies, W. & Palladino, M.J. Modes of metabolic compensation during mitochondrial disease using the Drosophila model of ATP6 dysfunction. *PLoS One* **6**, e25823 (2011).

312. Kuznetsov, A.V. *et al.* Analysis of mitochondrial function in situ in permeabilized muscle fibers, tissues and cells. *Nat Protoc* **3**, 965-976 (2008).

313. Samokhvalov, V. *et al.* PPARgamma signaling is required for mediating EETs protective effects in neonatal cardiomyocytes exposed to LPS. *Front Pharmacol* **5**, 242 (2014).

314. Chevrollier, A. *et al.* Standardized mitochondrial analysis gives new insights into mitochondrial dynamics and OPA1 function. *Int J Biochem Cell Biol* **44**, 980-988 (2012).

315. Talbot, D.A. & Brand, M.D. Uncoupling protein 3 protects aconitase against inactivation in isolated skeletal muscle mitochondria. *Biochim Biophys Acta* **1709**, 150-156 (2005).

316. Bota, D.A., Van Remmen, H. & Davies, K.J. Modulation of Lon protease activity and aconitase turnover during aging and oxidative stress. *FEBS Lett* **532**, 103-106 (2002).

317. Blackstone, C. & Chang, C.R. Mitochondria unite to survive. *Nat Cell Biol* **13**, 521-522 (2011).

318. Cogliati, S. *et al.* Mitochondrial cristae shape determines respiratory chain supercomplexes assembly and respiratory efficiency. *Cell* **155**, 160-171 (2013).

319. Wang, D., Hirase, T., Nitto, T., Soma, M. & Node, K. Eicosapentaenoic acid increases cytochrome P-450 2J2 gene expression and epoxyeicosatrienoic acid production via peroxisome proliferator-activated receptor gamma in endothelial cells. *J Cardiol* **54**, 368-374 (2009).

320. Fan, W. & Evans, R. PPARs and ERRs: molecular mediators of mitochondrial metabolism. *Curr Opin Cell Biol* **33**, 49-54 (2015).

321. Miglio, G. *et al.* PPARgamma stimulation promotes mitochondrial biogenesis and prevents glucose deprivation-induced neuronal cell loss. *Neurochem Int* **55**, 496-504 (2009).

322. Wang, L. *et al.* 14,15-EET promotes mitochondrial biogenesis and protects cortical neurons against oxygen/glucose deprivation-induced apoptosis. *Biochem Biophys Res Commun* **450**, 604-609 (2014).

323. Menzies, K.J. & Hood, D.A. The role of SirT1 in muscle mitochondrial turnover. *Mitochondrion* **12**, 5-13 (2012).

324. Kelly, D.P. & Scarpulla, R.C. Transcriptional regulatory circuits controlling mitochondrial biogenesis and function. *Genes Dev* **18**, 357-368 (2004).

325. Zamaraeva, M.V. *et al.* Cells die with increased cytosolic ATP during apoptosis: a bioluminescence study with intracellular luciferase. *Cell Death Differ* **12**, 1390-1397 (2005).

326. Tsujimoto, Y. Apoptosis and necrosis: intracellular ATP level as a determinant for cell death modes. *Cell Death Differ* **4**, 429-434 (1997).

327. Kim, I. & Lemasters, J.J. Mitochondrial degradation by autophagy (mitophagy) in GFP-LC3 transgenic hepatocytes during nutrient deprivation. *Am J Physiol Cell Physiol* **300**, C308-317 (2011).

328. Kim, I. & Lemasters, J.J. Mitophagy selectively degrades individual damaged mitochondria after photoirradiation. *Antioxid Redox Signal* **14**, 1919-1928 (2011).

329. Parone, P.A. *et al.* Preventing mitochondrial fission impairs mitochondrial function and leads to loss of mitochondrial DNA. *PLoS One* **3**, e3257 (2008).

330. Ikeda, Y. *et al.* Molecular mechanisms mediating mitochondrial dynamics and mitophagy and their functional roles in the cardiovascular system. *J Mol Cell Cardiol* **78**, 116-122 (2015).

331. Navratil, M., Terman, A. & Arriaga, E.A. Giant mitochondria do not fuse and exchange their contents with normal mitochondria. *Exp Cell Res* **314**, 164-172 (2008).

332. Landes, T. *et al.* OPA1 (dys)functions. *Semin Cell Dev Biol* **21**, 593-598 (2010).

333. Ardehali, H. *et al.* Targeting myocardial substrate metabolism in heart failure: potential for new therapies. *Eur J Heart Fail* **14**, 120-129 (2012).

334. Andres, A.M., Stotland, A., Queliconi, B.B. & Gottlieb, R.A. A time to reap, a time to sow: mitophagy and biogenesis in cardiac pathophysiology. *J Mol Cell Cardiol* **78**, 62-72 (2015).

335. White, S.M., Constantin, P.E. & Claycomb, W.C. Cardiac physiology at the cellular level: use of cultured HL-1

cardiomyocytes for studies of cardiac muscle cell structure and function. *Am J Physiol Heart Circ Physiol* **286**, H823-829 (2004).

336. Claycomb, W.C. *et al.* HL-1 cells: a cardiac muscle cell line that contracts and retains phenotypic characteristics of the adult cardiomyocyte. *Proc Natl Acad Sci U S A* **95**, 2979-2984 (1998).

337. Eimre, M. *et al.* Distinct organization of energy metabolism in HL-1 cardiac cell line and cardiomyocytes. *Biochim Biophys Acta* **1777**, 514-524 (2008).

338. Lopaschuk, G. Regulation of carbohydrate metabolism in ischemia and reperfusion. *Am Heart J* **139**, S115-119 (2000).

339. Anmann, T. *et al.* Different kinetics of the regulation of respiration in permeabilized cardiomyocytes and in HL-1 cardiac cells. Importance of cell structure/organization for respiration regulation. *Biochim Biophys Acta* **1757**, 1597-1606 (2006).

340. Seppet, E.K. *et al.* Structure-function relationships in the regulation of energy transfer between mitochondria and ATPases in cardiac cells. *Exp Clin Cardiol* **11**, 189-194 (2006).

341. Elshenawy, O.H., Anwar-Mohamed, A., Abdelhamid, G. & El-Kadi, A.O. Murine atrial HL-1 cell line is a reliable model to study drug metabolizing enzymes in the heart. *Vascul Pharmacol* **58**, 326-333 (2013).

342. Bopassa, J.C., Ferrera, R., Gateau-Roesch, O., Couture-Lepetit, E. & Ovize, M. PI 3-kinase regulates the mitochondrial transition pore

in controlled reperfusion and postconditioning. *Cardiovasc Res* **69**, 178-185 (2006).

343. Yamaguchi, H. & Wang, H.G. The protein kinase PKB/Akt regulates cell survival and apoptosis by inhibiting Bax conformational change. *Oncogene* **20**, 7779-7786 (2001).

344. Tsuruta, F., Masuyama, N. & Gotoh, Y. The phosphatidylinositol 3-kinase (PI3K)-Akt pathway suppresses Bax translocation to mitochondria. *J Biol Chem* **277**, 14040-14047 (2002).

345. Gardai, S.J. *et al.* Phosphorylation of Bax Ser184 by Akt regulates its activity and apoptosis in neutrophils. *J Biol Chem* **279**, 21085-21095 (2004).

346. Stotland, A. & Gottlieb, R.A. Mitochondrial quality control: Easy come, easy go. *Biochim Biophys Acta* **1853**, 2802-2811 (2015).

347. Lee, J.W., Park, S., Takahashi, Y. & Wang, H.G. The association of AMPK with ULK1 regulates autophagy. *PLoS One* **5**, e15394 (2010).

348. Kim, J., Kundu, M., Viollet, B. & Guan, K.L. AMPK and mTOR regulate autophagy through direct phosphorylation of Ulk1. *Nat Cell Biol* **13**, 132-141 (2011).

349. Lee, I.H. *et al.* A role for the NAD-dependent deacetylase Sirt1 in the regulation of autophagy. *Proc Natl Acad Sci U S A* **105**, 3374-3379 (2008).

350. Jager, S., Handschin, C., St-Pierre, J. & Spiegelman, B.M. AMP-activated protein kinase (AMPK) action in skeletal muscle via direct phosphorylation of PGC-1alpha. *Proc Natl Acad Sci U S A* **104**, 12017-12022 (2007).

351. Canto, C. & Auwerx, J. PGC-1alpha, SIRT1 and AMPK, an energy sensing network that controls energy expenditure. *Curr Opin Lipidol* **20**, 98-105 (2009).

352. Jornayvaz, F.R. & Shulman, G.I. Regulation of mitochondrial biogenesis. *Essays Biochem* **47**, 69-84 (2010).

353. Johnson, M.A. *et al.* Amino acid starvation has opposite effects on mitochondrial and cytosolic protein synthesis. *PLoS One* **9**, e93597 (2014).

354. Murry, C.E., Jennings, R.B. & Reimer, K.A. Preconditioning with ischemia: a delay of lethal cell injury in ischemic myocardium. *Circulation* **74**, 1124-1136 (1986).

355. Sankaralingam, S. *et al.* Lowering body weight in obese mice with diastolic heart failure improves cardiac insulin sensitivity and function: implications for the obesity paradox. *Diabetes* **64**, 1643-1657 (2015).

356. Ahmet, I., Tae, H.J., de Cabo, R., Lakatta, E.G. & Talan, M.I. Effects of calorie restriction on cardioprotection and cardiovascular health. *J Mol Cell Cardiol* **51**, 263-271 (2011).

357. Chistiakov, D.A., Sobenin, I.A., Revin, V.V., Orekhov, A.N. & Bobryshev, Y.V. Mitochondrial aging and age-related dysfunction of mitochondria. *Biomed Res Int* **2014**, 238463 (2014).

358. Lv, M., Zhu, X., Wang, H., Wang, F. & Guan, W. Roles of caloric restriction, ketogenic diet and intermittent fasting during initiation, progression and metastasis of cancer in animal models: a systematic review and meta-analysis. *PLoS One* **9**, e115147 (2014).

359. Quarles, E.K. *et al.* Quality control systems in cardiac aging. *Ageing Res Rev* **23**, 101-115 (2015).

360. Longo, V.D. & Mattson, M.P. Fasting: molecular mechanisms and clinical applications. *Cell Metab* **19**, 181-192 (2014).

361. Dirks-Naylor, A.J. *et al.* Can short-term fasting protect against doxorubicin-induced cardiotoxicity? *World J Biol Chem* **5**, 269-274 (2014).

362. Cuervo, A.M. *et al.* Autophagy and aging: the importance of maintaining "clean" cells. *Autophagy* **1**, 131-140 (2005).

363. Halagappa, V.K. *et al.* Intermittent fasting and caloric restriction ameliorate age-related behavioral deficits in the triple-transgenic mouse model of Alzheimer's disease. *Neurobiol Dis* **26**, 212-220 (2007).

364. Martin, B., Mattson, M.P. & Maudsley, S. Caloric restriction and intermittent fasting: two potential diets for successful brain aging. *Ageing Res Rev* **5**, 332-353 (2006).

365. Curtis, J. & de Cabo, R. Utilizing calorie restriction to evaluate the role of sirtuins in healthspan and lifespan of mice. *Methods in molecular biology* **1077**, 303-311 (2013).

366. Civitarese, A.E. *et al.* Calorie restriction increases muscle mitochondrial biogenesis in healthy humans. *PLoS Med* **4**, e76 (2007).

367. Lanza, I.R. *et al.* Chronic caloric restriction preserves mitochondrial function in senescence without increasing mitochondrial biogenesis. *Cell Metab* **16**, 777-788 (2012).

368. Niemann, B., Chen, Y., Issa, H., Silber, R.E. & Rohrbach, S. Caloric restriction delays cardiac ageing in rats: role of mitochondria. *Cardiovasc Res* **88**, 267-276 (2010).